ABSTRACT

STUDIES OF THE MOLECULAR STRUCTURE OF ETHYL CHLORIDE, CHLOROMETHYLSILANE, AND CYCLOPROPYL CHLORIDE BY MICROWAVE SPECTROSCOPY

by Gerald Daniel Jacobs

A brief outline of the history of microwave spectroscopy is presented. The theory of rotational spectra as it pertains to the determination of molecular structure, barriers to internal rotation, and quadrupole effects is discussed. A description of the microwave spectrometer is also included.

The microwave spectra of $C^{13}H_3CH_2Cl^{35}$, $CH_3C^{13}H_2Cl^{35}$, $CH_3CD_2Cl^{35}$, and $CH_2DCH_2Cl^{35}$ have been examined and rotational constants assigned. Both a-type and b-type spectra have been observed. From these spectra and those previously reported for $CH_3CH_2Cl^{35}$, $CH_3CH_2Cl^{37}$, and $CH_2DCH_2Cl^{35}$ a complete structure has been obtained by means of the substitution method. The bond distances and bond angles obtained are as follows: CC = 1.520A, CCl = 1.788 A, CH (methyl) = 1.091 A, CH (methylene) = 1.089 A, CCCl = 111.0°, HCH (methyl) = 108.5°, HCH (methylene) = 109.2°, CCH (methylene) = 111.6°. The quadrupole coupling parameters and barriers to internal rotation have been re-evaluated in terms of the above structure. The quadrupole coupling parameters are χ_{bond} = -68.80 Mc and η_{bond} = 0.035, if the angle between the a axis and the CCl bond is determined from the structure; or χ_{bond} = -71.24 Mc, if a cylindrical charge distribution is assumed near the chlorine nucleus. The barrier to internal rotation is found to be 3685 cal/mole.

Observations of the microwave spectra of seven ground-state species and three first excited torsional state species of CH_2ClSiH_3 are reported. From an analysis of the moments of inertia of the various species structural parameters are deduced as follows: bond distances; CCl = 1.788 A, CSi = 1.889 A, CH = 1.096 A, SiH = 1.477 A, and bond angles; SiCCl = 109.3°, SiCH = 109.3°, HSiH = 110.6°, and HCH = 107.5°. An analysis of the hyperfine splitting leads to quadrupole coupling parameters χ_{bond} = -68.7 Mc, η_{bond} = 0.048, if it is assumed that the CCl bond direction forms one principal axis of the quadrupole tensor; and χ_{bond} = -72.0 Mc if it is assumed that the quadrupole tensor is cylindrically symmetric. Analysis of splittings in the first excited torsional state indicate that the height of the potential barrier hindering internal rotation of the silyl group is 2.55 kcal/mole.

The microwave spectra of the Cl-35 and Cl-37 species of cyclopropyl chloride have been examined and R-branch a-type, R-branch c-type, and Q-branch c-type transitions assigned.

STUDIES OF THE MOLECULAR STRUCTURE OF ETHYL CHLORIDE, CHLOROMETHYLSILANE, AND CYCLOPROPYL CHLORIDE BY MICROWAVE SPECTROSCOPY

By

Gerald Daniel Jacobs

A THESIS

Submitted to
Michigan State University
in partial fulfillment of the requirements
for the degree of

DOCTOR OF PHILOSOPHY

Department of Chemistry

1961

To My Wife Linda

ACKNOWLEDGMENTS

The author wishes to express his sincere appreciation to Dr. Richard H. Schwendeman for his assistance, encouragement, and guidance which he so generously gave during the course of this investigation and preparation of this thesis.

Financial aid in the form of Fellowships from the National Science Foundation and Petroleum Research Foundation are gratefully acknowledged.

****

TABLE OF CONTENTS

TABLE OF CONTENTS - Continued

LIST OF TABLES

LIST OF TABLES - Continued

LIST OF TABLES - Continued

LIST OF FIGURES

I. HISTORICAL BACKGROUND

Apart from the pioneering work of Cleeton and Williams (1) in 1933 on the absorption of centimeter radiation by ammonia, microwave spectroscopy must be regarded as a post-World War II development. The unique combination of graduate students with previous electronic training and the availability of discarded 1.25 centimeter radar equipment contributed strongly to the early development.

Additional stimulation for the early development of microwave spectroscopy was the high resolution obtainable as demonstrated in the early experiments of Bleaney and Penrose (2, 3) and Coles and Good (4). Furthermore it soon became obvious that the pure rotation spectra of a large number of molecules would appear in this spectral region.

Most of the early work in microwave spectroscopy was concerned with the development of more sensitive instruments for detecting the absorption of the microwave radiation, with the investigation of the pure rotation spectra of linear and symmetric top molecules, with the extension of the frequency range available for spectroscopy, with the characterization of the inversion of ammonia, and with a number of measurements of physical quantities (e.g. the magnetic moment of H_2O). An extremely important development was the suggestion by Hughes and Wilson (5) that a periodic Stark effect field be applied to the sample gas to modulate the absorption. The relatively high sensitivity obtained with such Stark effect microwave spectrometers has made them the most important instruments in this region.

The preoccupation of the early workers with the spectra of linear and symmetric top molecules was due to the simplicity of the spectra and to the availability of simple, precise quantum mechanical expressions for their energy levels and absorption frequencies. The study of

asymmetric rotor molecules did not become widespread until after several years when good approximate methods for the calculation of the energy levels of asymmetric top molecules and the development of computers to use the methods became available.

Theory predicted that the Stark effect shift and splitting for a linear molecule should be proportional to the square of the electric field strength and to the square of the dipole moment. Measurements on the molecule OCS (6) confirmed the theory and now dipole moments are measured quite routinely by microwave spectroscopy.

The examination of a rotational transition under high resolution very often reveals a complex structure of many lines. Such splitting of the rotational transitions can occur if internal rotation is possible in the molecule or if a nucleus with a quadrupole moment is present. The first work on the calculation of barriers to internal rotation by microwave spectroscopy was performed by Burkhard and Dennison (7) on the molecule methyl alcohol. Later, extensive work on this problem was carried out by E. B. Wilson, Jr., and co-workers (see section 2.5, this thesis).

A development of great interest to chemists is the interpretation of nuclear quadrupole coupling constants in relation to chemical bond type. These constants are obtained directly from microwave spectra and measure the variation of electrostatic energy with orientation of the nucleus. From the coupling constants and an approximate treatment developed by Townes and Dailey (8) it is possible to obtain information about the hybridization and the covalent or ionic character of chemical bonds.

The determination of bond distances and bond angles is the most common application of microwave spectroscopy. The rotational constants obtained from the microwave spectra are essentially reciprocal moments of inertia and are determined by the location of the atoms in a

molecule and their masses. Bond distances and bond angles were first determined by fitting the moments of inertia of several isotopic species. This procedure was later refined to include a fit by the method of least squares of differences between observed and calculated moments. A method was presented by Kraitchman (9) which provided for fitting differences in moments of inertia of two isotopically different molecules to determine the position coordinates of the substituted atom. The large number of isotopic species required discouraged the use of Kraitchman's equations until it became apparent that essentially the same number of species was required for the least squares method owing to the insensitivity of the moments of inertia of some of the species to the locations of some of the atoms. Furthermore it was pointed out by Costain (10) that for theoretical and practical reasons the structures obtained by means of Kraitchman's equations were more reliable than those obtained by fitting the moments of inertia directly.

II. THEORY OF ROTATIONAL SPECTRA

2.1 Introduction

In the microwave region of the electromagnetic spectrum (0.06-30 cm wavelength) we are concerned mainly with transitions between rotational energy levels of molecules in their ground vibrational and electronic states. Occasionally, however, ground state to first excited state vibrational transitions are found in this region (e.g. the ammonia inversion spectrum) and, in addition, rotational transitions in excited vibrational states often contribute to the spectrum.

Due to quantization of the rotational energy levels a discrete rather than a continuous spectrum is observed. The frequency of a given transition is obtained from the Bohr frequency relation $h\nu = W_2 - W_1$, where W_2 represents the final and W_1 the initial energy state.

The problem resolves itself into one of finding suitable relationships for the evaluation of these energy levels from molecular parameters.

From the theory of Born and Oppenheimer, we may break the complete wave equation for a molecule into two main parts, one being the electronic wave equation and the other the wave equation for nuclear motion. The wave equation for nuclear motion may be further separated into two parts, one expressing the vibrational motion and one dealing with the rotational motion of the nuclei. In the separation of the nuclear wave equation it is customary as a first approximation to consider the vibrational motion of a non-rotating molecule followed by the rotational motion of a rigid body, and neglect interaction between these two parts. The theory of interaction, however, has been well characterized.

The classical quantum mechanical problem of the rotation of diatomic and symmetric top molecules has been described by many

authors (11). The solution for the case of an asymmetric top molecule is considerably more difficult but has been worked out in detail (12).

Since microwave spectroscopy affords values of the so-called rotational constants, which are essentially reciprocal moments of inertia, it seems appropriate to first consider the subject of moments of inertia.

2.2 Moments of Inertia

For a rigid molecule, the moment of inertia about any axis passing through the center of mass is defined by

$$I = \Sigma_i m_i r_i^2 \qquad (2\text{-}1)$$

where r_i is the perpendicular distance from the axis and m_i is the mass of the i^{th} nucleus. A theorem of mechanics states that the locus of points formed by plotting $I^{-\frac{1}{2}}$ along axes through the center of mass is the surface of a triaxial ellipsoid, known as the momental ellipsoid. Moments of inertia about the three mutually perpendicular principal axes of the ellipsoid are called principal moments of inertia. It is customary to label the axes of the ellipsoid $a > b > c$ so that for the principal moments of inertia $I_a < I_b < I_c$. Molecules are then described as linear if one of their principal moments of inertia is zero, as symmetrical rotors if two of the moments are equal, and as asymmetrical rotors if all three moments are different.

The direction of one or more of the principal axes of a molecule may often be determined from the symmetry of the molecule. If a molecule possesses a plane of symmetry, the plane will be a principal section of the ellipsoid. The principal section will contain two of the principal axes and in addition be perpendicular to the third axis. This is the case in the molecules ethyl chloride, chloromethylsilane, and cyclopropyl chloride with which we will be particularly concerned in this thesis.

In the usual case where symmetry does not permit the location of all the principal axes, they may be found by means of angular momentum calculations.

Angular momentum may be defined as

$$\underset{\sim}{P} = I\,\underset{\sim}{\omega} \tag{2-2}$$

where $\underset{\sim}{P}$ = vector of angular momentum

$\underset{\sim}{\omega}$ = vector of angular velocity

I = moment of inertia (a tensor of second rank or a dyadic)

In general $\underset{\sim}{P}$ and $\underset{\sim}{\omega}$ will be column matrices of the same rank and therefore I will have square dimensions. The inertia dyadic may be written (13):

$$I = \Sigma_i m_i(r_i^2\, 1 \; - \underset{\sim}{r}_i \cdot \underset{\sim}{r}_i) \tag{2-3}$$

where m_i = mass of i^{th} atom

$\underset{\sim}{r}_i$ = distance of i^{th} atom from the center of mass

1 = unit dyadic

In matrix form:

$$I = \begin{pmatrix} I_{xx} & I_{xy} & I_{xz} \\ I_{yx} & I_{yy} & I_{yz} \\ I_{zx} & I_{zy} & I_{zz} \end{pmatrix} \tag{2-4}$$

where: $I_{xx} = \Sigma_i m_i(y_i^2 + z_i^2)$ $\quad I_{xy} = I_{yx} = -\Sigma_i m_i x_i y_i$

$I_{yy} = \Sigma_i m_i(x_i^2 + z_i^2)$ $\quad I_{xz} = I_{zx} = -\Sigma_i m_i x_i z_i$

$I_{zz} = \Sigma_i m_i(x_i^2 + y_i^2)$ $\quad I_{yz} = I_{zy} = -\Sigma_i m_i y_i z_i$

and x_i, y_i, z_i are the coordinates of the i^{th} atom measured from the center of mass. The quantities I_{xx}, I_{yy}, and I_{zz} are often called the axial moments of inertia or simply moments of inertia, and I_{xy}, I_{xz}, etc.,

the product moments of inertia or simply products of inertia. Diagonalization of the inertia tensor will give the principal moments of inertia.

The discussion of the moments of inertia of an asymmetric top is simplified by defining a matrix of the second moments, the P matrix. We define P as

$$P = i_0 \, 1 - I \tag{2-6}$$

where

$$i_0 = \Sigma_i m_i (x_i^2 + y_i^2 + z_i^2), \tag{2-7}$$

a scalar quantity, and 1 is the unit or identity matrix. This new matrix has the form

$$P = \begin{pmatrix} P_{xx} & P_{xy} & P_{xz} \\ P_{yx} & P_{yy} & P_{yz} \\ P_{zx} & P_{zy} & P_{zz} \end{pmatrix} \tag{2-8}$$

where in general $P_{uv} = \Sigma_i m_i u_i v_i$[1], and u, v = x, y, or z. This matrix is diagonalized by the same coordinate transformation which diagonalizes the I matrix as may be seen by the following:

$$S^{-1} I S = i_0 \, 1 - S^{-1} P S \tag{2-9}$$

Since $i_0 1$ is diagonal $S^{-1}PS$ will be diagonal when $S^{-1}IS$ is and vice versa.

Due to trace invariance under a similarity transformation we have

$$P_{xx} + P_{yy} + P_{zz} = P_{aa} + P_{bb} + P_{cc} = i_0, \tag{2-10}$$

where P_{aa}, P_{bb}, and P_{cc} are the diagonal values of $S^{-1}PS$. Finally we may relate P_{aa}, P_{bb}, and P_{cc} to I_a, I_b, and I_c, the principal moments of the molecule as follows:

$$\begin{aligned} P_{aa} + P_{bb} &= i_0 - P_{cc} = I_c \\ P_{aa} + P_{cc} &= i_0 - P_{bb} = I_b \\ P_{bb} + P_{cc} &= i_0 - P_{aa} = I_a \end{aligned} \tag{2-11}$$

---

[1]The components of the P matrix, P_{uv}, are written with two subscripts and should not be confused with the components of angular momentum which will be written with only one subscript.

If a coordinate system x', y', z', parallel to the x, y, z system is used, whose origin is not at the center of mass of the molecule, then the second moments in the x, y, z system are related to those in the x', y', z' system by the equation

$$P_{uv} = P_{u'v'} - Mu_0v_0 \qquad (2\text{-}12)$$

where $Mu_0 = \Sigma_i m_i u_i$, $M = \Sigma_i m_i$ and u_i, v_i are x_i, y_i, z_i. If the mass of one of the atoms, m_s, is increased by an amount Δm (as would occur in isotopic substitution) the second moment tensor becomes

$$P' = \begin{pmatrix} P_{aa} + \mu a_s^2 & \mu a_s b_s & \mu a_s c_s \\ \mu b_s a_s & P_{bb} + \mu b_s^2 & \mu b_s c_s \\ \mu c_s a_s & \mu c_s b_s & P_{cc} + \mu c_s^2 \end{pmatrix} \qquad (2\text{-}13)$$

where P_{aa}, P_{bb}, P_{cc} are the principal second moments of the original molecule, a_s, b_s, c_s are the coordinates of the augmented mass and $\mu = (M' - M)M/M'$. Here M and M' are the masses of the original and substituted molecules respectively.

Kraitchman (9) has shown that the diagonal values of P and P' may be used to determine the values of a_s, b_s, and c_s. The expression for a_s is

$$|a_s| = \left\{\mu^{-1}\left[(P_{aa'}-P_{aa})\left(1 + \frac{P_{bb'}-P_{bb}}{P_{bb}-P_{aa}}\right)\left(1 + \frac{P_{cc'}-P_{cc}}{P_{cc}-P_{aa}}\right)\right]\right\}^{\frac{1}{2}} \qquad (2\text{-}14)$$

and similar expressions for b_s and c_s may be obtained by cyclic permutation of the subscripts.

Using arguments similar to those used by Kraitchman (9) the following equation and one similar to it for $|b_s|$ may be derived for the in-plane coordinates of a pair of atoms which straddle a plane of symmetry (the ab plane in this case):

$$|a_s| = \left\{\mu^{-1}\left[\frac{(P_{bb'} - P_{aa})(P_{aa} - P_{aa'})}{(P_{aa} - P_{bb})}\right]\right\}^{\frac{1}{2}}. \qquad (2\text{-}15)$$

The out-of-plane coordinates of these atoms which straddle the plane of symmetry are found from an expression of the form:

$$| c_s | = \left\{ \frac{1}{2m_0} (P_{cc}' - P_{cc}) \right\}^{\frac{1}{2}} \qquad (2\text{-}16)$$

where m_0 is the difference in mass between the substituted and unsubstituted atoms. Again, arguments similar to those used by Kraitchman (9) were used in the derivation (14).

Measurements with the spectrometer yield values of I_a, I_b, I_c, principal moments for the unsubstituted or "parent" molecule and I_a', I_b', I_c', principal moments of the isotopically substituted molecule. These may be related to the second moments by the equations

$$\begin{aligned} 2P_{aa} &= I_c + I_b - I_a \\ 2P_{bb} &= I_a + I_c - I_b \\ 2P_{cc} &= I_a + I_b - I_c \end{aligned} \qquad (2\text{-}17)$$

The coordinates of the substituted atom (a_s, b_s, c_s) are then computed using Equations (2-14), (2-15), or (2-16) depending on the position of substitution.

2.3 Energy of Rotation

The total energy of a rigid rotator can be expressed in terms of its principal moments of inertia I_a, I_b, and I_c and angular momenta $\underset{\sim}{P}_a$, $\underset{\sim}{P}_b$, $\underset{\sim}{P}_c$ as:

$$W_R = \frac{\underset{\sim}{P}_a^2}{2I_a} + \frac{\underset{\sim}{P}_b^2}{2I_b} + \frac{\underset{\sim}{P}_c^2}{2I_c} \; . \qquad (2\text{-}18)$$

The total angular momentum is given by:

$$\underset{\sim}{P}^2 = \underset{\sim}{P}_a^2 + \underset{\sim}{P}_b^2 + \underset{\sim}{P}_c^2 \qquad (2\text{-}19)$$

The total angular momentum $\underset{\sim}{P}$ is quantized taking only the values

$$\underset{\sim}{P} = [J(J+1)]^{\frac{1}{2}} \; h/2\pi \quad , \tag{2-20}$$

where J is a quantum number limited to positive integers or zero. The component of $\underset{\sim}{P}$ along a direction fixed in space obeys the quantum condition

$$P_z = M \; h/2\pi \tag{2-21}$$

where M can assume the 2J + 1 values

$$M = 0, \pm 1, \pm 2, \cdots \pm J \; .$$

If there is a fixed component of J along an internal molecular axis then it is quantized according to the relation

$$P_K = K \; h/2\pi, \tag{2-22}$$

where K may assume the values

$$K = 0, \pm 1, \pm 2, \cdots \pm J.$$

The quantized rotational energy levels of a rigid linear or symmetric top molecule may now be easily computed. For a linear molecule, $I_a = 0$, $I_b = I_c = I$ and therefore

$$W_R = \frac{h^2}{8\pi^2 I} J(J+1) = hBJ(J+1) \tag{2-23}$$

where $B = h/8\pi^2 I$ is called a rotational constant. The selection rule for absorption is $\Delta J = +1$ so that the Bohr frequency condition gives

$$\nu = 2B(J+1) \tag{2-24}$$

A symmetric top molecule is one for which two moments of inertia are equal. Symmetric rotors are further classified as oblate or prolate rotors. The oblate type has $I_a = I_b < I_c$ and the prolate $I_a < I_b = I_c$. This means that for the prolate rotor B = C, and for the oblate rotor A = B, where

$$A = \frac{h}{8\pi^2 I_a} \; , \quad B = \frac{h}{8\pi^2 I_b} \; , \quad C = \frac{h}{8\pi^2 I_c} \tag{2-25}$$

The energy levels of a prolate symmetric top are given by

$$W_R = \frac{h^2}{8\pi^2 I_b} J(J+1) + \frac{h^2}{8\pi^2}\left(\frac{1}{I_a} - \frac{1}{I_b}\right) K^2$$

$$= h\left[BJ(J+1) + (A-B)K^2\right]. \qquad (2\text{-}26)$$

The selection rules for absorption are $\Delta J = +1$, $\Delta K = 0$ so that the transition frequencies are

$$\nu = 2B(J+1), \qquad (2\text{-}27)$$

the same as for linear molecules.

In the above treatment we have neglected the effects of centrifugal distortion (or non-rigidity) which are quite pronounced for high values of J. In the linear molecule the expression for the frequency becomes

$$\nu = 2B(J+1) - 4D_J(J+1)^3, \qquad (2\text{-}28)$$

while in the symmetric top case

$$\nu = 2B(J+1) - 4D_J(J+1)^3 - 2D_{JK}(J+1)K^2. \qquad (2\text{-}29)$$

The D's represent distortion constants which depend on the various molecular force constants and the moments of inertia and are usually small compared to the rotational constants. The theory of centrifugal distortion for symmetric rotors was first described by Slawsky and Dennison (15).

For asymmetric rotors it is not possible to write down an explicit energy expression as in the linear and symmetric top cases. It is possible, however, to calculate precise values for the energy through the use of published tables. In one particularly useful approach introduced by Ray (16) and developed by King, Hainer, and Cross (17) the rotational energy is written as

$$W_R = \left(\frac{A + C}{2}\right)J(J + 1) + \left(\frac{A - C}{2}\right) E_\tau^J(\kappa) \qquad (2\text{-}30)$$

where J and τ are quantum numbers and κ is an asymmetry parameter defined by

$$\kappa = \frac{2B-A-C}{A - C} \quad . \qquad (2\text{-}31)$$

The reduced energy function $E_\tau^J(\kappa)$ has been tabulated at intervals of 0.01 in κ between $\kappa = -1$, the prolate top limit, and $\kappa = +1$, the oblate top limit (18).

Another method of calculation is available for molecules which are nearly symmetrical rotors. For a nearly prolate rotor ($B \sim C$), $\kappa \sim -1$, and

$$W_R = \frac{B + C}{2} J(J + 1) + \left(A - \frac{B + C}{2}\right) \omega_\tau^J (b_p). \qquad (2\text{-}32)$$

Here b_p is an asymmetry parameter given by

$$b_p = \frac{C - B}{2A - B - C} = \frac{\kappa + 1}{\kappa - 3} \qquad (2\text{-}33)$$

The reduced energy function $\omega_\tau^J (b_p)$ may be obtained from systematic application of perturbation theory as a power series in b_p,

$$\omega_\tau^J (b_p) = K^2 + C_1 b_p + C_2 b_p^{\,2} + C_3 b_p^{\,3} + \cdots \qquad (2\text{-}34)$$

The values of K^2 and C_1 through C_5 have been tabulated for all energy levels with $J \leq 40$ (19).

The similar expression for the case of a nearly oblate rotor ($A \sim B$), $\kappa \sim +1$, is

$$W_R = \frac{A + B}{2} J(J + 1) + \left(C - \frac{A + B}{2}\right) \omega_\tau^J (b_o) \ , \qquad (2\text{-}35)$$

where

$$b_o = \frac{A - B}{2C - A - B} = \frac{\kappa - 1}{\kappa + 3} \ . \qquad (2\text{-}36)$$

The rotation absorption frequencies are computed from the Bohr frequency condition

$$h\nu_R = W_{R'} - W_R \qquad (2\text{-}37)$$

The index τ is normally replaced by the index $K_{-1}K_{+1}$ ($\tau = K_{-1}\text{-}K_{+1}$) where K_{-1} ($\frac{h}{2\pi}$) would be the angular momentum of the molecule about the a axis in the case of a limiting prolate symmetric top, and K_{+1} ($\frac{h}{2\pi}$) would be the angular momentum about the c axis in the case of a limiting oblate symmetric top. The subscripts -1 and +1 refer to the value of the asymmetry parameter κ in the two limiting symmetric top cases. The quantities K_{-1} and K_{+1} assume the values zero or positive integers less than or equal to J.

The selection rule for J is $\Delta J = 0$, or ± 1 and as an aid to classifying transitions the designations P, Q, and R- branches are used for $\Delta J = -1$, 0, and +1 respectively. In addition transitions are classified as a, b, and c-type transitions according to the direction of the component of the dipole moment which interacts with the incident radiation. Selection rules for a, b, and c-type transitions are as follows:

a-type:	ΔK_{-1} = even	ΔK_{+1} = odd	
b-type:	ΔK_{-1} = odd	ΔK_{+1} = odd	(2-38)
c-type:	ΔK_{-1} = odd	ΔK_{+1} = even	

Before continuing to the "finer aspects" of rotational spectra a short digression is necessary concerning the rotational constants. The moments of inertia and hence rotational constants which are normally measured are for the lowest vibrational state. The relation between the measured rotational constant and the equilibrium value is given by

$$A_{v_1 v_2 \ldots} = A_e - \Sigma_i \alpha_i (v_i + \frac{d_i}{2}) , \qquad (2\text{-}39)$$

where A_e is the equilibrium value. The α's are small constants and v_i represents the vibrational quantum number of the i^{th} mode and d_i its

degeneracy. Similar expressions can be written for B and C. To determine the equilibrium value it is necessary to know the rotational constants for each singly excited vibrational state in addition to the ground state. Herein lies the center of the difficulty in the determination of structures since equilibrium rotational constants have been obtainable only for a few very simple polyatomic molecules (e.g. H_2O).

2.4 Nuclear Quadrupole Hyperfine Structure

In microwave spectroscopy one of the richest sources of interest and information is the hyperfine structure exhibited by many pure rotation lines due to the coupling of nuclear spin and molecular rotation (20). The presence of extra lines constituting a hyperfine structure in molecular rotational spectra was first reported by Good (21) for the inversion spectrum of ammonia. The observed hyperfine structure patterns have been interpreted as resulting from a splitting of the molecular levels caused by an interaction between nuclear electric quadrupole moments and the gradient of the molecular electric field at the position of the nucleus. This interaction depends on the orientation of the nucleus with respect to the rest of the molecule and therefore causes a given level to split into a series of levels corresponding to the different possible values of the total (nuclear plus rotational) angular momentum (22). The splitting of rotational levels resulting from interaction (or coupling) of nuclear spin and molecular rotation is called the nuclear quadrupole hyperfine structure. The other type of nuclear effect which would be expected to lead to a splitting of molecular rotational lines is nuclear magnetic dipole interactions. However, these magnetic dipole interactions are generally very small in most molecules since the molecules are in $^1\Sigma$ states.

Of great importance to chemists is the interpretation of this nuclear quadrupole coupling in terms of chemical bond type. Townes and

Dailey (8) have shown that the gradient of the electric field at the quadrupolar nucleus arises mainly from the valence electrons associated with the given atom. According to their interpretation the electrons in closed shells about the nucleus contribute essentially nothing to the electric field gradient due to their spherical symmetry. Distortion of this symmetry due to other atoms in the molecule is of minor importance. Furthermore, nuclei and electrons of other atoms are not assumed to contribute due to their distance from the nucleus being considered. Thus we are left with only the valence electrons as principal contributors to the field gradient. The spherical symmetry of s orbitals and low penetrating power of d or higher orbitals rules out any major contribution from these sources. We are left then with the interpretation that the hyperfine splitting is due mainly to the amount of p-orbital character of the valence electrons associated with the quadrupolar nucleus. Thus it is possible to obtain information on the nature of the hybridization and the covalent or ionic character of the bond.

The quantum mechanical treatment of the splitting due to a single nucleus coupled to the molecular rotation of a linear molecule through electric quadrupole effects was first worked out by Casimir (23). This work was later expanded to include linear molecules with one or two quadrupolar nuclei (24), symmetric tops with one quadrupolar nucleus (25), (26), (27), (28), symmetric tops with two quadrupolar nuclei (28), symmetric tops with three symmetrically located nuclei (29), and asymmetric rotors with one or two quadrupolar nuclei (30), (31), (32).

The Hamiltonian which was found to describe the nuclear quadrupole interactions to first order has the form:

$$H_Q = \Sigma_i eQ_i \left\langle \frac{\partial^2 V}{\partial z^2} \right\rangle_{A_V} \left[\frac{3(\underset{\sim}{J}\cdot\underset{\sim}{I}_i)^2 + 3/2(\underset{\sim}{J}\cdot\underset{\sim}{I}_i) - \underset{\sim}{J}^2\underset{\sim}{I}_i^2}{2J(2J-1)I_i(2I_i-1)} \right] \qquad (2\text{-}40)$$

where: e is the electronic charge

J represents the total angular momentum of the molecule exclusive of nuclear spins

I_i represents the angular momentum of the i^{th} nucleus.

Q_i is the electric quadrupole moment of the i^{th} nucleus, a property of the nucleus and its energy state.

and $\left\langle \frac{\partial^2 v}{\partial z^2} \right\rangle_{A_v}$ is the average electric field gradient at the i^{th} nucleus. Here v is the potential at the i^{th} nucleus which results from all the extranuclear charges, and z is a space-fixed axis.

For molecules with a single quadrupolar nucleus the Hamiltonian given above leads to a quadrupole perturbation energy of the form

$$W_Q = eQ \left\langle \frac{\partial^2 v}{\partial z^2} \right\rangle_{A_v} \left[\frac{3/4C(C+1) - I(I+1)J(J+1)}{2J(2J-1)I(2I-1)} \right], \qquad (2\text{-}41)$$

where $C = F(F+1) - I(I+1) - J(J+1)$

and $F = J+I,\ J+I-1,\ \cdots\ |J-I|.$

Since W_Q is different for each value of F, the total rotational energy

$$W = W_R + W_Q \qquad (2\text{-}41)$$

will depend on F also (normally however, $W_R >> W_Q$).

The average field gradient is evaluated along a space-fixed direction and hence depends upon the electronic and molecular states of the particular molecule. Classically

$$\left\langle \frac{\partial^2 v}{\partial z^2} \right\rangle_{A_v} = \left\langle \Sigma_j e \left[\frac{3\cos^2\theta_j - 1}{r_j^3} \right] \right\rangle_{A_v}, \qquad (2\text{-}43)$$

where r_j is the radius vector between the nucleus and the k^{th} charge and θ_j is the angle r_j makes with the space-fixed Z axis.

Concise expressions for $\left\langle \frac{\partial^2 v}{\partial z^2} \right\rangle_{A_v}$ may be obtained for the cases of the linear and symmetric top molecules. However, for the case of

an asymmetric top this is no longer possible. Bragg (30), (31) has evaluated $\left\langle \frac{\partial^2 v}{\partial z^2} \right\rangle_{A_v}$ by first order perturbation theory and finds it to be:

$$q_J \equiv \left\langle \frac{\partial^2 v}{\partial z^2} \right\rangle_{A_v} = \frac{2}{(J+1)(2J+3)} \left[\frac{\partial^2 v}{\partial a^2} \frac{\partial W_R}{\partial A} + \frac{\partial^2 v}{\partial b^2} \frac{\partial W_R}{\partial B} + \frac{\partial^2 v}{\partial c^2} \frac{\partial W_R}{\partial C} \right], \tag{2-44}$$

where A, B, and C are the rotational constants and W_R is the energy of the rigid rotator. Thus q_J represents a molecular property which depends both on the geometry of the molecule and the distribution of charges within the molecule. It is then possible to combine the equation for q_J with Laplace's equation ($\nabla^2 V = 0$) and obtain several useful expressions for the quadrupole energy W_Q. If Laplace's equation is assumed to hold then only two of the partial derivatives of the potential are independent. It is customary to choose one of these as unique and use a linear combination of the other two as the second parameter.

One expression which is useful for near symmetric rotors is

$$q_J = \frac{2}{(J+1))2J+3)} \left\{ \left[3K^2 - J(J+1) + 3\sum_{n=o} (1-n) C_n b^n \right] q_m - \left[\sum_{n=o} (n+1) C_{n+1} b^n \right] q_m \eta \right\} \tag{2-45}$$

where K, b, and the C's are given by Equation (2-34).

Also $$q_m = \frac{\partial^2 v}{\partial z_m^2} \tag{2-46}$$

= second derivative of the potential along the molecule-fixed principal axis which most nearly represents a symmetry axis of the momental ellipsoid,

and $$\eta = (\partial^2 v / \partial x_m^2 - \partial^2 v / \partial y_m^2) / q_m . \tag{2-47}$$

The energy is written (stopping the sums at n = 2)

$$W_Q = \frac{1}{J(J+1)} [(3K^2 - J(J+1) - 3C_2b^2)q_m + (C_1 + 2C_2b + 3C_3b^2)q_m\eta]Y(F) \quad (2\text{-}48)$$

where

$$(Y(F) \equiv f(IJF) = \frac{\frac{3}{4}C(C+1) - J(J+1)I(I+1)}{2(2J-1)(2J+3)I(2I-1)} \quad . \quad (2\text{-}49)$$

The quantity Y(F), known as Casimir's function, has been tabulated for values of rotational angular momentum J between 0 and 10, for the nuclear spins I = 1, 3/2, 2, 5/2, 3, 7/2, 4, 9/2, or 11/2, and all possible values of F (33). This table also includes relative intensities of the hyperfine structure components.

Using values of q_m and $q_m \eta$ which may be approximated by reference to known similar molecules, energy values for the hyperfine structure components may be calculated. Using the table mentioned in the previous paragraph, energy differences of the appropriate hyperfine components may be computed to give the frequency displacements from the hypothetical unsplit frequency. Obviously once the transitions have been identified and the frequencies accurately measured a reverse calculation affords accurate values of the coupling parameters q_m and $q_m \eta$.

Another approach is to express the average field gradient in terms of the asymmetric top reduced energy function $E_\tau^J(\kappa)$ and $\frac{dE(\kappa)}{d\kappa}$ (34):

$$W_Q = \frac{1}{J(J+1)} \left\{ (\chi_{aa} + \chi_{cc})[J(J+1) - 3\frac{dE(\kappa)}{d\kappa}] + (\chi_{aa} - \chi_{cc})[E(\kappa) - \kappa\frac{dE(\kappa)}{d\kappa}] \right\} Y(F) \quad (2\text{-}50)$$

where $E(\kappa)$ is defined in Equation (2-30) and κ by Equation (2-31). The quantities χ_{aa}, etc. are given by

$$\chi_{aa} = eQ\frac{\partial^2 V}{\partial a^2} \quad . \quad (2\text{-}51)$$

In asymmetric top molecules the principal inertial axes seldom coincide with any of the bonds in the molecule. In these cases the coupling

constants (χ's) must first be referred to bond axes before they can be used for a discussion of the bonds. If the off-diagonal elements χ_{ab}, χ_{ac}, and χ_{bc} of the coupling tensor were known the procedure would be both simple and rigorous. Since in first order the off-diagonal elements do not contribute and hence are not determined, the most common procedure is to assume that these off-diagonal elements go to zero for axes corresponding to bond axes.

If a and b represent axes in the principal axis system of a molecule possessing a plane of symmetry (the ab plane), and z and x represent the in-plane axes of the principal axis system of the quadrupole coupling tensor, then immediately we may write down the expressions (all multiplied by a scale constant eQ)

$$\frac{\partial^2 V}{\partial a^2} = \chi_{aa} \quad \frac{\partial^2 V}{\partial b^2} = \chi_{bb} \quad \frac{\partial^2 V}{\partial c^2} = \chi_{cc}$$

$$\frac{\partial^2 V}{\partial a\, \partial b} = \chi_{ab} \quad \frac{\partial^2 V}{\partial a\, \partial c} = \frac{\partial^2 V}{\partial b\, \partial c} = 0 \qquad (2\text{-}52)$$

$$\frac{\partial^2 V}{\partial x^2} = \chi_{xx} \quad \frac{\partial^2 V}{\partial y^2} = \chi_{yy} \quad \frac{\partial^2 V}{\partial z^2} = \chi_{zz}$$

$$\frac{\partial^2 V}{\partial x\, \partial y} = \frac{\partial^2 V}{\partial x\, \partial z} = \frac{\partial^2 V}{\partial y\, \partial z} = 0 \qquad (2\text{-}53)$$

The two sets of second derivatives are related by an axis transformation in the plane of symmetry. The equations for this transformation are

$$\chi_{aa} = \chi_{zz} \cos^2\theta_z + \chi_{xx} \sin^2\theta_z$$

$$\chi_{bb} = \chi_{zz} \sin^2\theta_z + \chi_{xx} \cos^2\theta_z \,, \qquad (2\text{-}54)$$

where θ_z is the angle between the a and z axes. Alternatively

$$\chi_{zz} = \frac{\chi_{aa}\cos^2\theta_z - \chi_{bb}\sin^2\theta_z}{\cos^2\theta_z - \sin^2\theta_z} \quad , \text{ and}$$

$$\chi_{xx} = \frac{\chi_{aa}\sin^2\theta_z - \chi_{bb}\cos^2\theta_z}{\sin^2\theta_z - \cos^2\theta_z} \quad . \tag{2-55}$$

The value of the angle θ_z may be determined in several ways. If it is assumed that the bond connecting the quadrupolar nucleus to an adjacent atom (e.g. C-Cl) lies along the z axis of the quadrupole tensor, then θ_z may be computed from the structure of the molecule. On the other hand if it is assumed that the quadrupole tensor represents a cylindrical charge distribution about the z axis then

$$\chi_{yy} = \chi_{xx} = -1/2\ \chi_{zz}$$

$$\chi_{xy} = \chi_{xz} = \chi_{yz} = 0 \ . \tag{2-56}$$

In this case

$$\chi_{aa} = \chi_{zz}\ \left(\frac{3\cos^2\theta_z - 1}{2}\right) \tag{2-57}$$

and the values of χ_{zz} and θ_z may be determined.

Still a third way to obtain θ_z is from quadrupole coupling constants for two isotopic species. In this case it is assumed that the potential in the neighborhood of the quadrupolar nucleus is the same for the two species. Combination of the coupling constants for the two isotopic species enables the determination of χ_{ab}, the non-zero off-diagonal element in the a, b, c axis system. The equations are

$$\chi_{ab} = \frac{\chi'_{aa} - (\chi_{aa}\cos^2\theta_z + \chi_{bb}\sin^2\theta_z)}{2\ \sin\theta_z\cos\theta_z}$$

or

$$\chi_{ab} = \frac{\chi'_{bb} - (\chi_{aa}\sin^2\theta_z + \chi_{bb}\cos^2\theta_z)}{-2\ \sin\theta_z\cos\theta_z} \tag{2-58}$$

where the primes refer to the isotopically substituted species. This value of χ_{ab} along with values of χ_{aa} and χ_{bb} allows calculation of the angle θ_z from

$$\tan 2\theta_z = \frac{2\chi_{ab}}{\chi_{aa}-\chi_{bb}} \qquad (2\text{-}59)$$

It has been shown (35) that the quadrupole coupling constant in the bond direction of a chlorine atom is related to the ionic character of the bond (I), to the s and d character (s^2 and d^2) of the chlorine bond orbital, and to a quantity II which is determined by the double bond character of the bond. The relation is as follows:

$$I = (1 - s^2 - d^2 + II) - (\chi_{zz} / eQq_{atom}) . \qquad (2\text{-}60)$$

Here $eQq_{atom} = -107.74$ Mc is the quadrupole coupling constant of a free chlorine atom.

2.5 Internal Rotation

Another type of motion which provides effects visible in the microwave region is the rotation of one part of a molecule with respect to the remainder, the so-called internal rotation. The fine structure observable in the spectrum as a result of this type of motion is a very sensitive measure of the potential barrier hindering the internal rotation.

The quantum mechanics of this problem was first treated by Nielson (36) and later extensively by Dennison and his students (37) in their study of methyl alcohol. Further extensive theoretical work was carried out at Harvard University under Professor E. Bright Wilson, Jr. This work, for the general case of molecules with a relatively high barrier, has been presented by Herschbach (38, 39). A recent review article covering the application of microwave spectroscopy to the study of internal

rotation has also been published (40). The following brief treatment of this problem will be based largely on the paper by Herschbach (39).

The model comprises a rigid symmetric rotor attached to a rigid asymmetric frame. The hindered motion involves rotation of the symmetric rotor about its axis (a). The kinetic energy of this system may be expressed in the form

$$2T = \Sigma_g I_g \omega_g^2 + 2I_a \dot{\alpha} \Sigma_g \lambda_g \omega_g + I_a \dot{\alpha}^2 \qquad (2\text{-}61)$$

where g = a, b, c refers to principal axes of inertia fixed in the framework part of the molecule

I_g represents the principal moments of inertia of the entire molecule

I_a is the moment of inertia of the internal top about its symmetry axis

λ_g is the direction cosine between the top axis and the g^{th} principal axes

ω_g is the component of angular velocity of the framework along the g^{th} principal axes

$\dot{\alpha}$ is the angular velocity of the top relative to the framework.

The first term on the right-hand side of Equation (2-61) may be recognized as that used when there is no internal rotation present, while the last term represents the kinetic energy of the top and the middle term is a coupling between these two types of motion.

We now redefine the total angular momentum about the principal axes

$$P_g = \frac{\partial T}{\partial \omega_g} = I_g \omega_g + I_a \dot{\alpha} \lambda_g \qquad (2\text{-}62)$$

so as to include a contribution from the internal rotation, and the total angular momentum of the internal top about its symmetry axis

$$p = \frac{\partial T}{\partial \dot{\alpha}} = I_\alpha \Sigma_g \lambda_g \omega_g + I_\alpha \dot{\alpha} \qquad (2\text{-}63)$$

to include a contribution from overall rotation.

The kinetic energy may now be expressed as

$$2T = \Sigma_g \frac{P_g^2}{I_g} + \frac{(p - \mathcal{P})^2}{rI_\alpha} , \qquad (2\text{-}64)$$

where $(p - \mathcal{P})$ is defined as the relative angular momentum of the internal top and the framework ($\mathcal{P} = \Sigma_g P_g \lambda_g I_\alpha / I_g$) and rI_α is a reduced moment of inertia given by

$$rI_\alpha = I_\alpha \left[1 - \Sigma_g \frac{\lambda_g^2 I_\alpha}{I_g}\right] = I_{\text{reduced}} . \qquad (2\text{-}65)$$

The form of the potential barrier hindering the internal rotation of rotors of threefold symmetry is taken to be

$$2V = V_3 (1 - \cos 3\alpha) , \qquad (2\text{-}66)$$

where α is the angle which gives the relative orientation of the rotor and framework.

The classical Hamiltonian becomes

$$H = \Sigma_g \frac{P_g^2}{2I_g} + \frac{(p - \mathcal{P})^2}{2rI_\alpha} + \frac{V_3}{2} (1 - \cos 3\alpha), \qquad (2\text{-}67)$$

or upon defining an inverse of the reduced moment of inertia

$$F = \frac{\hbar^2}{2 r I_\alpha} , \qquad (2\text{-}68)$$

$$H = H_R + F (p - \mathcal{P})^2 + \frac{V_3}{2} (1 - \cos 3\alpha) \qquad (2\text{-}69)$$

where H_R is the Hamiltonian for the ordinary rigid rotator problem.

In the treatment by Herschbach (39), the $F\mathcal{P}^2$ term is absorbed into H_R since it is a quadratic form in P_g. The $F^2p^2 + \frac{V_3}{2} (1 - \cos 3\alpha)$ terms are treated as torsional terms, the eigenvalue problem of which leads to a form of the Mathieu equation, and the cross term $-2Fp\mathcal{P}$ is considered as a perturbation.

If the barrier to internal rotation is very large, then each torsional state v is essentially triply degenerate and the torsional motion is simply an oscillation in one of the three equivalent potential wells. The spectrum will be that of a rigid rotator. However, as the barrier is lowered it can be shown that the torsional levels of a symmetric rotor such as the methyl group are split into two components by the quantum mechanical tunneling effect and further that these levels have slightly different moments of inertia for over-all rotation. As a result the rotational lines are doubled. The separation is small for high barriers but increases with J, torsional quantum state, and decreasing barrier height.

The two components are labeled by the letters A and E indicating the period ($2\pi/3$ and 2π respectively) and transformation characteristics under the symmetry group C_3. Thus each torsional level v splits into two sublevels, a nondegenerate level, $v_A(\sigma = o)$, and a doubly degenerate level, v_E $(\sigma = \pm 1)$.

Herschbach (39) has shown that each torsional state may be treated singly by perturbation theory after a Van Vleck transformation has been applied to the Hamiltonian in matrix form. This reduces the $-2Fp\,\wp$ terms which are nondiagonal in v to higher order so that they may be neglected. The transformed Hamiltonian is written

$$H_{v\sigma} = H_R + F \Sigma_n W_{v\sigma}^{(n)} \wp^n \quad , \qquad (2\text{-}70)$$

and is termed the effective rotational Hamiltonian for the torsional state specified by the quantum numbers v and σ. The terms $W_{v\sigma}^{(n)}$ are dimensionless perturbation coefficients which depend only on the ratio V_3/F. The index n signifies the order to which the perturbation calculation is carried. The perturbation coefficients have been tabulated as a function of a dimensionless parameter s

$$s = 4/9\ (V_3/F) \quad , \qquad (2\text{-}71)$$

to fourth order for the v = 0, 1, and 2 torsional states. These perturbation coefficients will differ in sign and magnitude for the A and E levels of a given torsional level v. Since the selection rule is $\Delta\sigma = 0$, each rotational transition will be a doublet consisting of a transition between E levels (of frequency ν_E) and a transition between A levels (of frequency ν_A).

The remainder of the theory of internal rotational splitting will be carried through in combination with an example--the determination (to second order) of the barrier in chloromethylsilane. A preliminary study indicated that the barrier lay in the range 2.4 - 2.6 kcal./mole so that s values of 110, 113, and 116 were carried through in the calculations. A plot of the calculated splittings, $\nu_E - \nu_A$, for these values of s allows the determination of the exact value of s from the location of the experimentally measured $\nu_E - \nu_A$. The barrier height is then determined from Equation (2-71). Each split line allows an independent evaluation of the barrier height.

The transitions $10_{29} \longrightarrow 9_{36}$, $10_{28} \longrightarrow 9_{37}$, $11_{29} \longrightarrow 10_{38}$ and $11_{2,10} \longrightarrow 10_{37}$ of the first excited torsional state showed resolvable internal rotation splittings. The first two will be carried through the sample calculations.

If the calculation is to be carried to second order then from Equation (2-70)

$$H_{v\sigma} = H_R + FW_{v\sigma}^{(1)} \rho + FW_{v\sigma}^{(2)} \rho^2 \quad . \qquad (2\text{-}72)$$

Herschbach (39) has shown that the odd order terms in ρ vanish for the A levels while those for the E levels are either negligible or can be treated as perturbations. Substituting in Equation (2-72) expressions for ρ it may be shown that the energies of the A and E levels are

$$W_A = W_R + \frac{\partial W_R}{\partial A} \Delta A_A + \frac{\partial W_R}{\partial B} \Delta B_A + \frac{\partial W_R}{\partial C} \Delta C_A \qquad (2\text{-}73)$$

$$W_E = W_R + \frac{\partial W_R}{\partial A} \Delta A_E + \frac{\partial W_R}{\partial B} \Delta B_E + \frac{\partial W_R}{\partial C} \Delta C_E + \Delta W^{(1)}, \qquad (2\text{-}74)$$

where $\Delta W^{(1)}$ represents the contribution to the E level from the term first order in γ and the terms in ΔA_A, ΔB_A, etc. represent the contributions from the terms second order in γ. The difference in energy of the A and E levels for chloromethylsilane becomes

$$W_A - W_E = \frac{\partial W_R}{\partial A} (\Delta A_A - \Delta A_E) + \frac{\partial W_R}{\partial B} (\Delta B_A - \Delta B_E) - \Delta W^{(1)}. \qquad (2\text{-}75)$$

The quantities ΔC_A and ΔC_E are zero because the c axis of chloromethylsilane is perpendicular to a plane of symmetry. The partial derivatives are obtained from Equation (2-32) or (2-35) while the Δ terms are replaced by

$$\Delta A_A - \Delta A_E = F a^2 [W_{1A}^{(2)} - W_{1E}^{(2)}] \qquad (2\text{-}76)$$

$$\Delta B_A - \Delta B_E = F \beta^2 [W_{1A}^{(2)} - W_{1E}^{(2)}] = \frac{\beta^2}{a^2} [\Delta A_A - \Delta A_E] \qquad (2\text{-}77)$$

The energy difference then becomes

$$W_A - W_E = \left(\frac{\partial W_R}{\partial A} + \frac{\beta^2}{a^2} \frac{\partial W_R}{\partial B} \right) \frac{3}{2} F a^2 W_{1A}^{(2)} - \Delta W^{(1)}, \qquad (2\text{-}78)$$

using $W_{1E}^{(2)} = -1/2\, W_{1A}^{(2)}$ from Herschbach's table (39) for high s in the first excited torsional state.

For the case of a near symmetric prolate rotor like chloromethylsilane the first order correction to the E levels of the upper level of a so-called asymmetry doublet becomes

$$\Delta W^{(1)} = F W_{1E}^{(1)} \gamma = \frac{(K_{-1} F a W_{1E}^{(1)})^2}{W - W'} \qquad (2\text{-}79)$$

where $\alpha = \lambda_a I_\alpha / I_a$

W = rotational energy of upper level of asymmetry doublet

W' = rotational energy of lower level of asymmetry doublet

The value of $\Delta W^{(1)}$ for the lower level of the asymmetry doublet is the negative of Equation (2-79).

The experimental parameters used for the barrier calculation in chloromethylsilane are shown in Table I. The first and second order corrections to the energy levels are shown tabulated in Table II while Figure 1 is a schematic representation of the splittings for the case of $s = 113$ of the $10 \longrightarrow 9$ transitions. A table of calculated versus observed splittings for the four observed transitions is shown in Chapter IV, Section 5.6. The average value of the barrier height found was 2.55 kcal/mole.

2.6 Stark Effect

A microwave spectrometer employing Stark modulation was first described by Hughes and Wilson (5). The basic principle is modulation of the microwave absorption using a periodic (100 kc) Stark effect field.

The theory of the Stark effect of asymmetric rotators has been described by Golden and Wilson (41). Only a brief introduction to the theory will be presented here followed by a short discussion of its use in identification of spectra and in determining dipole moments.

Rotational levels are ordinarily (2J+1)-fold degenerate corresponding to the (2J+1) orientations of the total angular momentum with respect to a space-fixed axis. The fundamental property of the Stark effect is that it lifts this spatial (M) degeneracy. In the usual case the electric field will produce an effect which is small compared to the rotational energy so that the Stark splitting may be treated as a perturbation on the total energy. As a result

Table I. Parameters Used in the Analysis of Internal Rotation in Chloromethylsilane.

A	=	21666.99 Mc[(a)]/sec
B	=	3186.19
C	=	2928.36
I_a	=	23.331852 amu A^2
I_b	=	158.663168
I_α	=	5.957 amu A^2
λ_a[(b)]	=	0.8287 λ_b = 0.5597 λ_c = 0
r	=	0.81290
rI_α	=	4.8424 amu A^2
F	=	104.397 kMc[(c)]
α^2	=	0.044766
β^2		0.000441

(a) Mc = megacycles = $10^6 sec^{-1}$

(b) from ground state

(c) kMc = kilomegacycles

TABLE II. Calculation of Corrections to A and E Levels of Chloromethylsilane.

First Order Correction to E Levels

		$(K_{-1}F\,a W_{1E}^{(1)})^2/(W - W')$		
Asymmetry doublet	$(W-W')Mc$	s = 110	113	116
9_{36}-9_{37}	16.045	0.317	0.192	0.118
10_{29}-10_{28}	1304.767	0.002	0.001	0.000

Second Order Correction to A and E Levels

$$-\tfrac{3}{2}\left\{\left[\frac{\partial W_R}{\partial A}+\left(\frac{\beta^2}{a^2}\right)\frac{\partial W_R}{\partial B}\right]F\,a^2 W_{1A}^{(2)}\right\}$$

Level	$\frac{\partial W_R}{\partial A}$	$\frac{\beta^2}{a^2}\left(\frac{\partial W_R}{\partial B}\right)$	s = 110	113	116
9_{36}	8.9921	0.4161	2.715	2.116	1.654
9_{37}	8.9939	0.4142	2.715	2.116	1.654
10_{28}	3.9423	0.6185	1.316	1.026	0.802
10_{29}	4.0102	0.5152	1.353	1.054	0.824

Level	W(E) - W(A)			$\nu_E - \nu_A$		
	s = 110	113	116	110	113	116
9_{36}	3.032	2.308	1.772	1.728	1.291	0.976
10_{29}	1.304	1.017	0.796			
9_{37}	2.398	1.924	1.536	1.080	0.897	0.734
10_{28}	1.318	1.027	0.802			

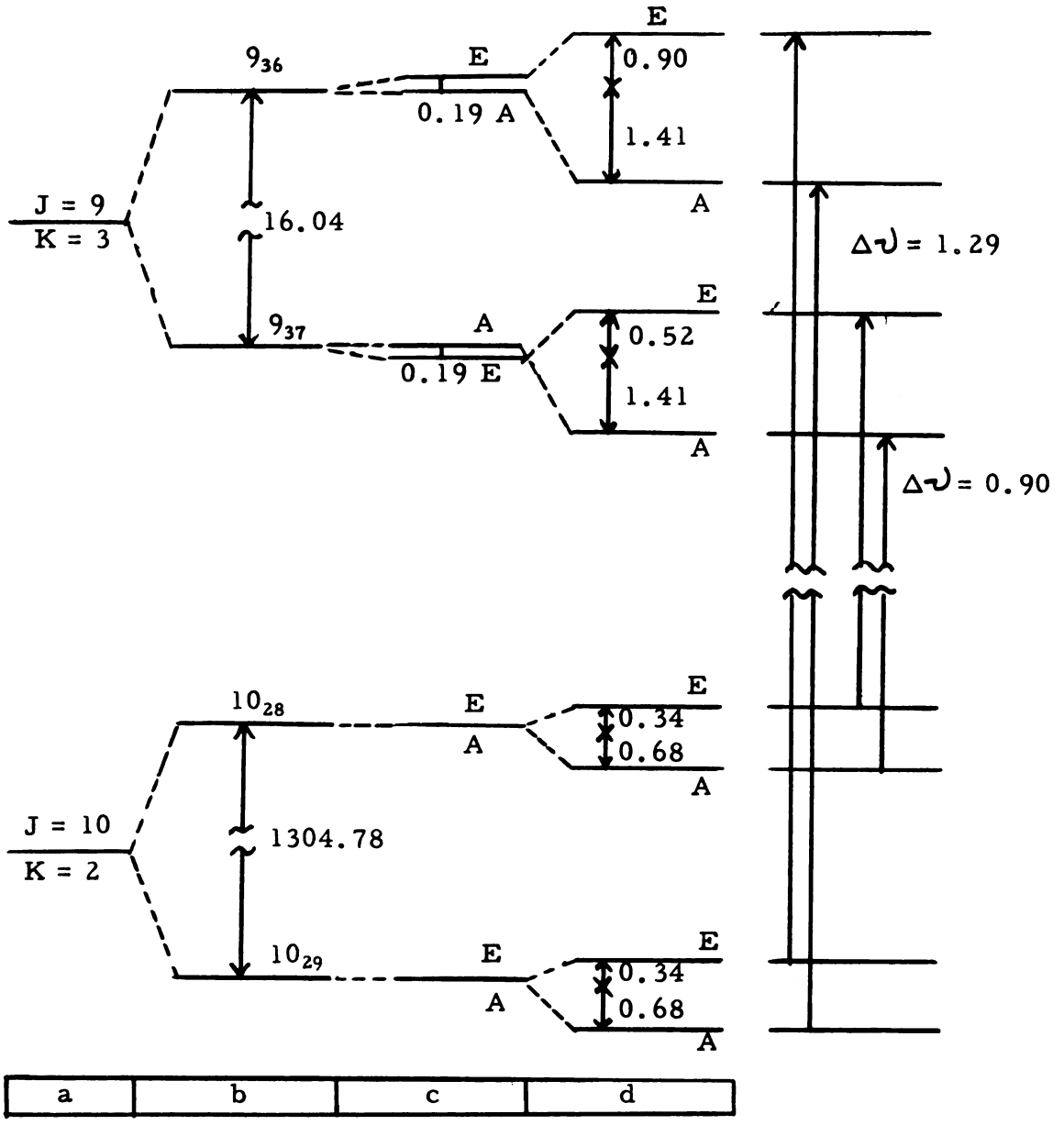

a - Symmetric Rotor
b - Slightly Asymmetric Rotor (no internal rotation)
c - With Internal Rotation: First Order Correction } for s = 113
d - With Internal Rotation: Second Order Correction }

Figure 1. Schematic Representation of Splittings (Mc) in 10 ⟶ 9 Transitions of Chloromethylsilane.

$$W = W_R + W_Q + W_{IR} + W_S \qquad (2\text{-}80)$$

where W_R is the energy of a rigid rotator, W_Q is the nuclear quadrupole contribution, W_{IR} is the contribution from internal rotation, and W_S the correction due to the electric field.

A uniform electric field is applied so that the field direction is the space-fixed direction. The Stark effect then arises from the interaction of this field with the permanent electric dipole oriented within the molecule and with a dipole induced in the molecule by the field. For practical purposes the latter may be neglected.

From the theory of Golden and Wilson (41) a shift in the energy levels is predicted which is proportional to the square of the component of the dipole moment along a given axis and to the square of the field strength. The direction cosines between the space-fixed axis and rotating molecule-fixed principal axes also enter into the calculation. These have been shown to be directly related to line strengths so that existing tables may be conveniently used. Therefore, by using a plot of the frequency of a Stark component versus square-of-the-electric field for several transitions, the components of the dipole moment along the principal axes of the molecule can be computed. Certain transitions and Stark components are more favorable depending upon the particular molecule.

The identification of certain classes of absorption lines may be carried out by observing the Stark effect. For low J transitions of molecules with no quadrupolar nucleus the Stark effect is very characteristic. The presence of a quadrupolar nucleus within the molecule, as is true of the cases studied here, leads to many more lines and tends to smear out the Stark effect. However, if the molecule is a near symmetric top then a characteristic Stark effect is still observable for certain transitions, e.g. the Q-branch transitions in the molecules discussed in this thesis.

III. DESCRIPTION OF THE MICROWAVE SPECTROMETER

3.1 Introduction

In common with instruments used in other frequency regions a microwave spectrometer consists basically of the following: 1) a source of electromagnetic radiation of variable frequency, 2) a frequency measuring device, 3) a sample absorption cell, 4) a detector of the microwave radiation, and 5) a means of displaying the signal from the detector, i.e. power output versus frequency. In addition the conventional microwave spectrometer includes a square wave generator to apply a radiofrequency Stark-effect field which modulates the absorption by the sample.

Although the above lists the essential components a number of variations are possible. The microwave spectrometer currently in use at Michigan State University is shown in the schematic diagram of Figure 2. An explanation of the components is given below.

3.2 Reflex Klystron Oscillators

Figure 3 is a schematic diagram of a reflex klystron oscillator of the type commonly used for the production of microwave radiation. A beam voltage (up to 2500 V) is applied to the cathode. Electrons are emitted which pass by the anode and through a deformable metal cavity whose dimensions can be adjusted externally. A bunching of the electrons occurs as the result of an alternating electric field existing within the cavity. Just beyond the cavity there appears a highly negative electrode called the repeller or reflector which reverses the direction of the electrons, sending them back through the cavity. These bunches of electrons upon passing back through the cavity give up some of their

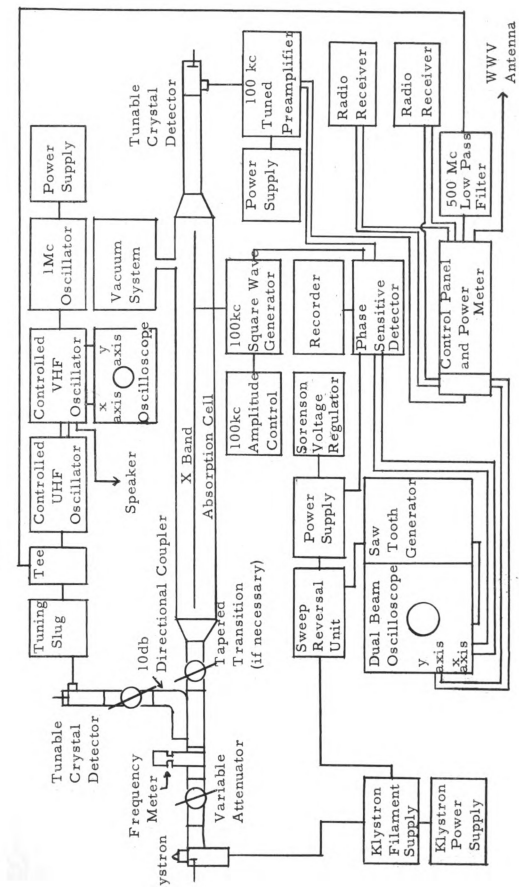

Figure 2. Block Diagram of the Microwave Spectrometer.

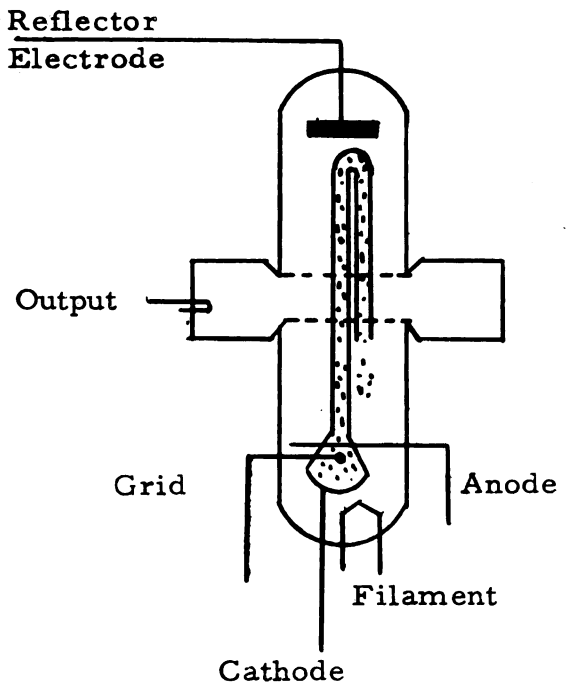

Figure 3. Schematic Diagram of a Reflex Klystron Oscillator.

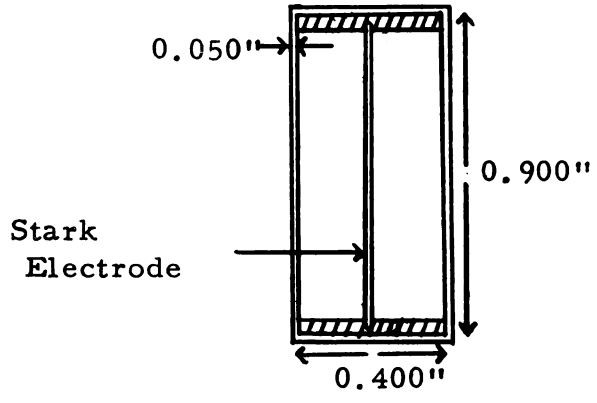

Teflon Tape: 0.062' x 0.400" with 0.032" groove 0.010" deep
Coin Silver Septum: 0.032" x 0.796"
Length of Waveguide: 10'

Figure 4. Stark-Waveguide Cross Section.

energy in the form of pulses provided they return with the proper phase. The phase upon return and hence the oscillations in the cavity are reinforced by adjustment of the reflector voltage and cavity dimensions.

The cavity is coupled out of the klystron into the waveguide through a mica window. The result is practically monochromatic radiation which is sent through the waveguide absorption cell.

Table III is a list of the klystrons presently available in this laboratory with the frequency ranges covered. The frequency of each individual klystron is variable over 40-60 Mc by adjustment of the reflector voltage or over 3-5 kMc by variation of the size of the cavity.

The power supply for the klystrons is an FXR Type Z815B[1] and is designed specifically to provide the necessary voltages for powering reflex klystron oscillators. The specifications include 200 to 3600 V in two ranges for the beam voltage, 0 to -1000 V (relative to the beam) reflector voltage, 0 to -300 V (relative to the beam) to the grid and 6.3 V A.C. for the heater. A separate regulated D. C. filament supply insures stable heating for the klystron cathode.

3.3 Waveguide Absorption Cell

The waveguide absorption cell consists of a ten foot piece of X-band[2] waveguide made of brass and having a silvered inside surface. Figure 4 (page 34) is a cross section of the guide showing the dimensions. Along the top and bottom of the guide is placed a strip of Teflon tape containing slots for holding and insulating the Stark electrode. Further details on the Stark electrode system may be found in the section on the square wave generator. This X-band waveguide will conduct electromagnetic radiation

---

[1]Manufactured by Electronics and X-Ray Division, F. R. Machine Works Inc., Woodside 77, New Jersey.

[2]X-band: 8.2-12.4 kMc; P-band: 12.4 - 18.0 kMc; K-band: 18.0 - 26.5 kMc; R-band: 26.5 - 40.0 kMc.

Table III. Klystrons Presently Available at Michigan State University.

Klystron	Manufacturer	Frequency Range (kMc)
X-13	Varian Associates[a]	8.2-12.4
X-12[d]	Varian Associates	12.4-18.0
QK306	Raytheon[b]	18.0-22.0
2K33	Raytheon	22.0-25.0
QK289	Raytheon	27.3-30.0
R9518	EMI/US[c]	27.2-32.3
R9546	EMI/US	32.3-37.5

[a] Varian Associates, Palo Alto, California

[b] Raytheon Manufacturing Company, Watham, Massachusetts

[c] EMI/US Ltd., 50 Swalm St., Westbury, Long Island, New York

[d] Purchased after work on ethyl chloride and chloromethylsilane was completed.

of frequency from 8.2 to 40 kMc. Tapered transitions are used to connect the K- and R-band klystrons to the waveguide. The absorption cell is sealed off from the rest of the system and made vacuum tight by means of mica windows. Originally the mica windows were sealed to the waveguide by means of Apiezon W wax, but due to the low temperature hardening of this wax the present system employs O-ring seals. Most of the length of the guide is contained in an aluminum-lined insulated box so that the sample may be cooled to Dry-Ice temperature. A second waveguide is now available which employs a liquid coolant and thus allows for a wider range of temperature variation.

3.4 Sample Introduction System

The absorption cell is coupled to the sample introduction system through a tube soldered to the side of the waveguide. The vacuum system is shown in Figure 5. Samples which are condensible at -190°C may be recovered unchanged after obtaining the spectra by freezing them back into the sample bulb. The pressures used in microwave spectroscopy vary from 10 mm to 10^{-4} mm Hg but normally the sample is observed at from 0.1 mm to 0.01 mm Hg. Pressures are measured by means of thermocouple gauges, one attached to the absorption cell and another to the sampling system.

3.5 Detection

After passage through the region of low pressure gas in the waveguide absorption cell, the microwave power is measured by a detector. "Crystal rectifiers are used almost exclusively for detectors of microwave power in spectroscopy, although thermal detectors have been applied in some special cases. The crystal detector consists of a fine wire in contact with a block of semiconducting material (most often silicon but

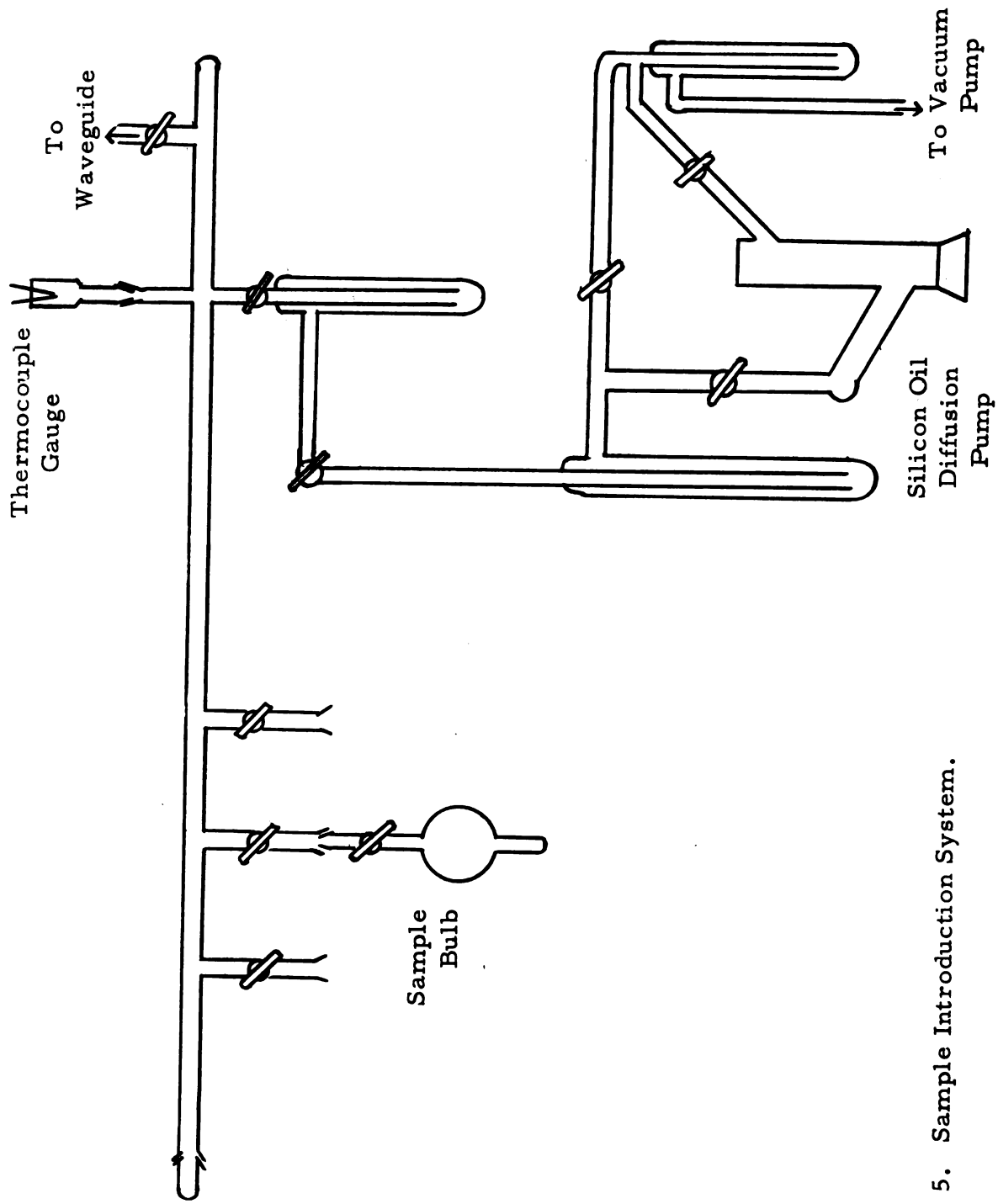

Figure 5. Sample Introduction System.

sometimes germanium). The contact resistance is greater in one direction than in the reverse, and the current-voltage characteristic is very nonlinear near the origin so that rectification occurs when an alternating voltage is applied" (42). The crystal types used were IN23 for X-band, IN26 for K-band and R-band.[1] The D.C. portion of the output from the crystal is sent through a current meter for indicating the power level at the crystal. The A.C. portion of the output from the crystal is amplified from its microvolt level by means of a high-gain tuned preamplifier. From the preamplifier the signal is further amplified and sent to the phase-sensitive detector. The reference signal for the phase detector is the 100 kc signal from the square wave generator.

The output of the phase-sensitive detector is then sent either to the oscilloscope or to the recorder. Signals from the detector, i.e. absorption lines and Stark components, appear in the output with opposite D.C. polarity. The signal is applied to the y-axis of one trace of a dual-beam Tektronix oscilloscope.[2] On the x-axis of this trace is placed a slowly varying sawtooth voltage. This same sawtooth voltage is applied to the reflector electrode of the klystron, so that the horizontal axis of the oscilloscope is a frequency scale, i.e. the oscillator frequency and oscilloscope are being swept synchronously. The sawtooth voltage sweeps the klystron uniformly over a mode which varies in general from 5 Mc to 20 Mc in width. On the oscilloscope will appear a plot of microwave absorption versus oscillator frequency.

An alternative way of displaying the spectrum is to send the output of the phase-sensitive detector to a recorder. The klystron is driven mechanically over the frequency range desired and now a permanent

---

[1]Obtainable from Microwave Associates Inc., Burlington, Massachusetts.

[2]Tektronix Inc., Portland, Oregon.

record of microwave absorption versus frequency is obtained. Examples of recorded spectra are shown in Figures 6 and 7.

3.6 Square Wave Generator

The square wave generator was designed by L. C. Hedrick (43). The specifications include 0-1250V zero-based square wave at 100 kc/sec. However, the base of the square wave may be adjusted to other D.C. levels if desired. The output of the generator is connected to the Stark electrode shown in place in the waveguide cross section of Figure 4. At one end of the sample cell a spring loaded contact presses against the top edge of the septum through a hole in the Teflon tape. The electrical contact to the outside is through a sealed N-type connector which is joined with an O-ring seal.

The basic principle used is the modulation of the absorption of the sample at a low radio-frequency (here 100 kc) by the application of a square wave voltage to the electrode in the waveguide, thus creating an alternating Stark effect.[1] This introduces a modulation of the microwave energy at the low radio-frequency in the vicinity of absorption lines.

The function of the square wave generator then is to expose the sample to this electric field for alternate five microsecond periods, thus switching the absorption on and off 100,000 times per second. Therefore, when the frequency of the klystron corresponds to an absorption frequency of the sample, a portion of the microwave energy will be modulated due to the varying absorption of the sample as the Stark-effect components are moved back and forth in frequency. This type of spectrometer was first described by Hughes and Wilson (5).

---

[1]The Stark effect is discussed in Section 2.6.

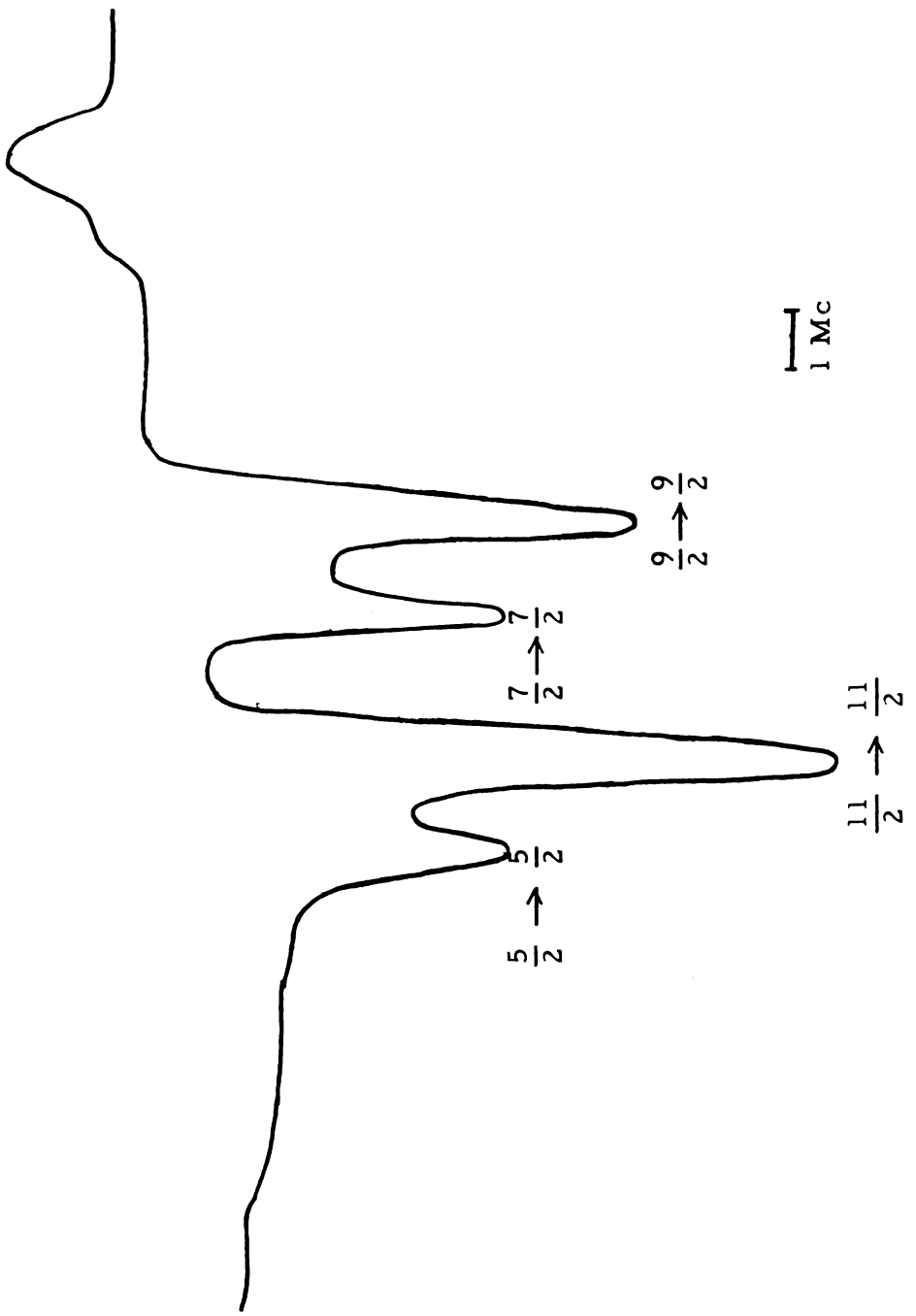

Figure 6. Recorded Spectrum of the $4_{04} \rightarrow 4_{13}$ Transition in $CH_2DCH_2Cl^{35}$ (trans) Showing Quadrupole Hyperfine Structure. (For further details see Chapter IV)

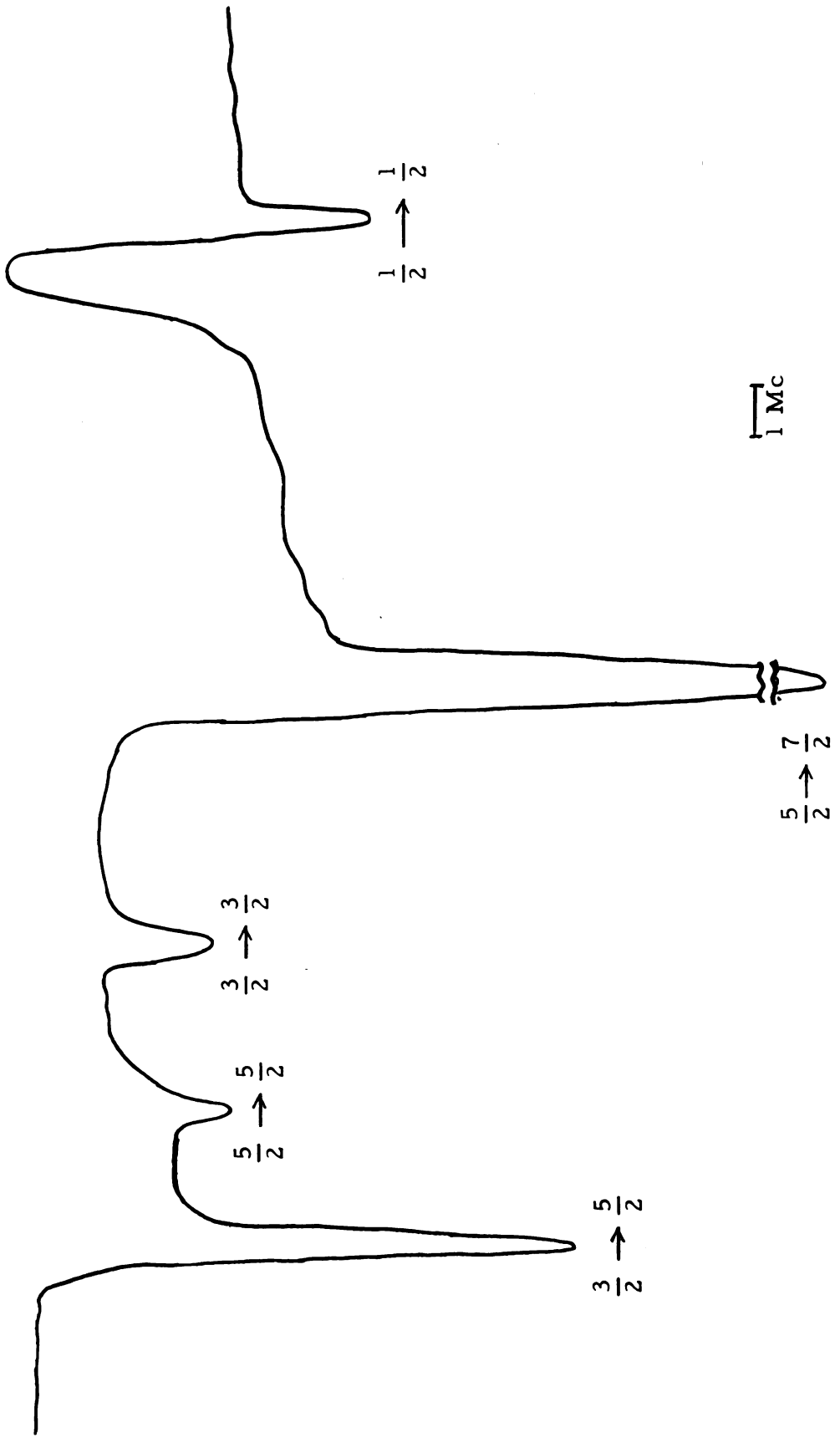

Figure 7. Recorded Spectrum of the $1_{11} \longrightarrow 2_{12}$ Transition in $CH_2D\text{-}CH_2Cl^{35}$ (gauche) Showing Quadrupole Hyperfine Structure. (For further details see Chapter IV)

3.7 Frequency Measurements

The measurement of the frequency of an absorption line is usually done in two steps. The steps consist of an approximate measurement with a wavemeter followed by an "exact" measurement using a frequency standard.

The absorption or cavity type wavemeters used throughout these investigations are coupled to the waveguide by means of small holes. As the klystron frequency sweeps through the frequency to which a wavemeter is tuned, the wavemeter absorbs some of the energy. The resonance curve of the wavemeter is traced out on the second beam of the dual-beam oscilloscope and has the appearance of a weak absorption line. The wavemeter is tuned by means of a micrometer screw and plunger arrangement in the cavity.

There are four wavemeters currently available in this laboratory and the one used will depend on the region of the spectrum being scanned. The types and frequency range covered are shown in Table IV. Calibrations were supplied by the manufacturer.

The arrangement for making precise frequency measurements is shown in Figure 8. The Manson RD-140[1] is a proportional oven and crystal oscillator which supplies a one megacycle sinusoidal output frequency of high stability. The frequency stability is of the order of one part in 10^8 per day. The Gertsch AM-1A VHF interpolator[2] is designed to measure and generate frequencies from 20 Mc to 1000 Mc using an external 1 Mc standard. Accuracy of one part in 10^7 is reported and has been verified in this laboratory. The frequency of the LFO (see Figure 8), ω_L, is determined by using only those values of ω_L which give stable

---

[1]Manson Laboratories Inc., 375 Fairfield Ave., Stamford, Connecticut.

[2]Gertsch Products Inc., 3211 S. LaCienega Blvd., Los Angeles 16, California.

Table IV. Wavemeters in Use at Michigan State University.

Manufacturer	Model	Serial Number	Frequency Range (kMc)
Narda[a]	810	128	8.2 - 12.4
Narda[b]	809	64	12.4 - 18.0
DeMornay-Bonardi[c]	DBE-715-2	720	18.0 - 26.5
Microwave Associates[d]	MA518A	5	26.0 - 39.0

[a] The Narda Microwave Corporation, 118-160 Herricks Road, Mineola, New York.

[b] Not used for work on ethyl chloride or chloromethylsilane.

[c] DeMornay-Bonardi Corporation, 780 S. Arroyo Parkway, Pasadena, California.

[d] Microwave Associates Inc., Burlington, Massachusetts.

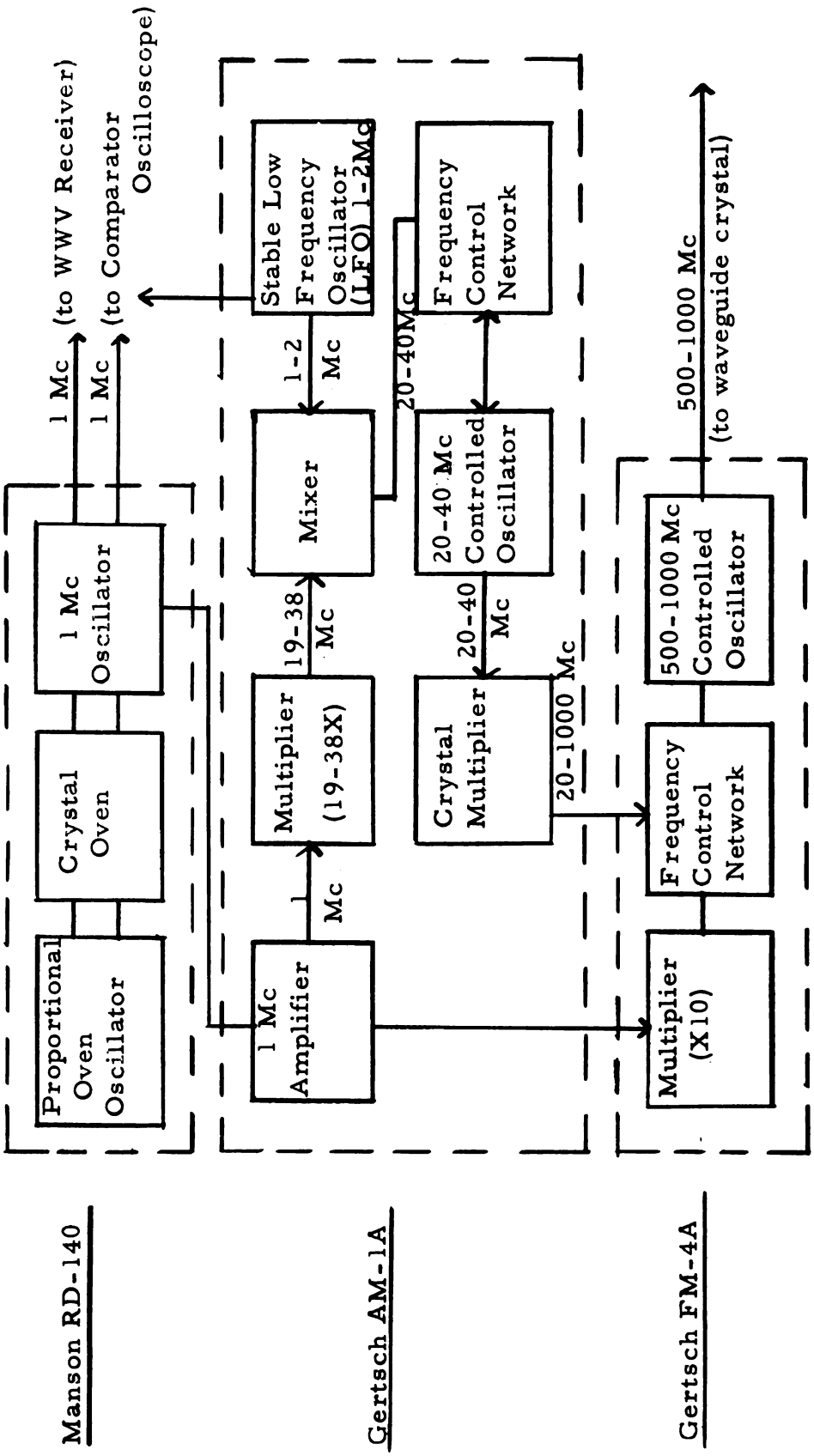

Figure 8. Reference Frequency Generator.

Lissajous figures when beat against the 1 Mc signal. If ν_L is such that a stable Lissajous figure is obtained, then $\nu_L = (p/q)$ where p and q are integers which can be determined from the appearance of the figure. The stability of the LFO is such that ν_L may be set to better than one cycle per second. The Gertsch FM-4A microwave frequency multiplier will measure and generate frequencies 500 Mc to 30,000 Mc. The equation for the output frequency of the FM-4A is

$$\nu_0 = [n(k + \nu_L) \pm 10],$$

where n and k are integers. The stability of the FM-4A is equal to that of the AM-1A.

The frequencies of absorption lines in the microwave spectrum are then measured by the difference in frequency between a harmonic of the accurately known frequency of the FM-4A and the unknown frequency,

$$\nu_{microwave} - m\nu_0 = \nu_{difference},$$

where m is an integer. This difference frequency is measured by means of either the Hallicrafters SX-62-A[1] or Collins 51J-4[2] communications receiver. The frequencies of most lines can be easily measured to $\pm$ 0.05 Mc using these receivers and the uncertainty in the frequencies of sharp lines is believed to be $\pm$ 0.01 Mc.

The Collins receiver is used almost exclusively for frequency measurements since the dial may be read directly to 0.001 Mc. The Hallicrafters receiver may be tuned much more rapidly and is normally used in the initial location of frequency markers and for measuring approximate splittings and line widths. The radio receivers are also

---

[1]The Hallicrafters Company, 4401 W. Fifth Ave., Chicago 24, Illinois.

[2]Collins Radio Company, Cedar Rapids, Iowa.

used for receiving the National Bureau of Standards radio station WWV. The 10th harmonic of the 1 Mc oscillator is compared to the 10 Mc carrier of WWV, whose accuracy at a receiver is generally better than one part in 10^7. If the strength of the 10^{th} harmonic of the oscillator and the incoming WWV signal are approximately comparable and reasonably close in frequency, the background noise will pulsate with a frequency which is one-half the difference in frequency between the two signals. If the 1 Mc oscillator is adjusted so that the pulses occur at a rate of less than one every two seconds the 1 Mc oscillator will be accurate to better than one part in 10^7.

The difference frequencies are generated by means of the system shown schematically in Figure 9.

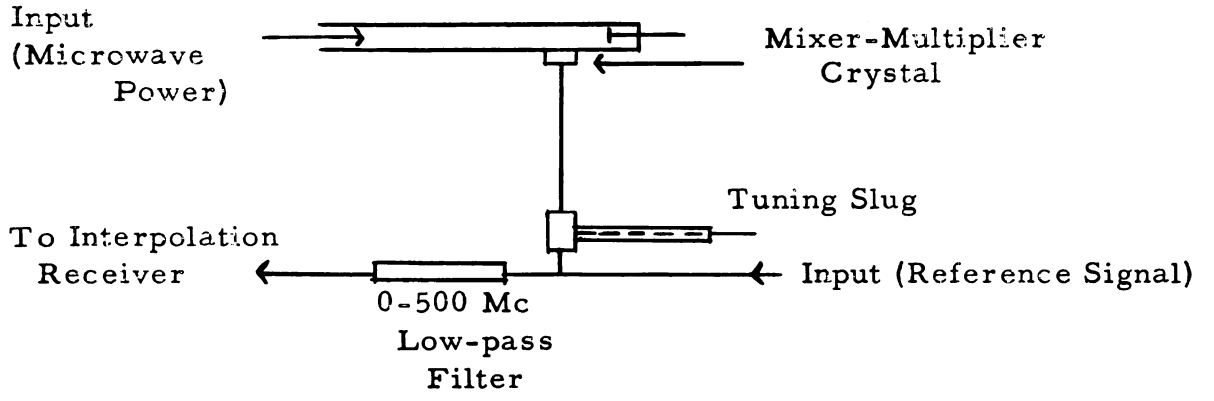

Figure 9. Difference Frequency Generator.

The reference signal is sent directly to the mixer-multiplier crystal where its harmonics are generated and mixed with the microwave signal. The difference frequencies are fed back along the same coaxial cable and the one that is less than 500 Mc passes through the low-pass filter to the receiver.

If the microwave signal is frequency modulated, the beat signal appearing at the input of the receiver will be varied also. For example, if the klystron is varied from 24030 Mc to 24040 Mc and the reference signal is 800 Mc, the beat frequency will vary from 30 Mc to 40 Mc (24030-30(800) = 30; the 30^{th} harmonic of the reference being used). If the receiver is tuned to 36.50 Mc a sound will be heard in the speaker each time the klystron frequency passes 24036.50 Mc. The variation of the klystron frequency is accomplished by the sawtooth voltage placed on the reflector electrode as explained previously. The second trace of the dual-beam oscilloscope is used to display this frequency variation and the beat frequency appears as a sharp "spike" on the trace. The position of the "spike" is then governed by the setting of the interpolation receiver. Both positive and negative beat notes are obtained so that if, in the example mentioned above, the klystron is swept from 23975 Mc to 24025 Mc, the reference frequency is 800 Mc, and the receiver is tuned to 20 Mc, two sounds will be heard in the speaker for each sweep and two markers will appear on the oscilloscope, one at 23980.00 Mc and one at 24020.00 Mc.

Since the 100 kc signal and the frequency markers suffer unequal time delays when being amplified, they may not reach the oscilloscope simultaneously, so that we may have a slight displacement of identical frequencies on the two traces. This is compensated for however, by sweeping the klystron first from high to low frequency and then low to high, making measurements both ways and taking the average of the two measurements.

IV. MOLECULAR STRUCTURE OF ETHYL CHLORIDE

4.1 Introduction

Due to its importance as one of the simplest halogen-substituted hydrocarbons ethyl chloride has been the subject of a number of reports of microwave spectra. The a-type spectra of $CH_3CH_2Cl^{35}$, $CH_3CH_2Cl^{37}$, and $CH_2DCH_2Cl^{35}$ were first reported by Wagner and Dailey (44) who also proposed a structure for the compound and determined the quadrupole coupling parameters. The b-type spectra of the $CH_3CH_2Cl^{35}$ and $CH_3CH_2Cl^{37}$ species were examined by Barchukov et al. (45) who determined the projection of the dipole moment along the a axis in addition to proposing a structure. The potential barrier hindering internal rotation of the methyl group was evaluated by Lide (46) from an analysis of splittings in transitions of the first excited torsional state using the structure proposed by Wagner and Dailey.

Further interest in ethyl chloride at this laboratory stemmed from a desire to provide a basis for comparison of the structure, barrier to internal rotation, and quadrupole parameters with the corresponding quantities in chloromethylsilane (Chapter V), cyclopropyl chloride (Chapter VI), and cyclobutyl chloride. The structure proposed by Wagner and Dailey (44) included a value of 1.5495A for the carbon-carbon bond length which is longer than found in normal hydrocarbons ($\sim$1.53A). Since the barrier to internal rotation in ethyl chloride is considerably larger than that generally accepted for ethane, a long carbon-carbon bond would have been of interest for theories of internal rotation. In order to obtain a complete set of molecular parameters by means of the substitution method proposed by Kraitchman (9), several isotopic species of ethyl chloride were prepared and their spectra examined.

4.2 Preparation of Samples

In addition to the $CH_3CH_2Cl^{35}$, $CH_3CH_2Cl^{37}$, and $CH_2DCH_2Cl^{35}$ (gauche and trans)[1] species which were re-examined, the species $CH_3CD_2Cl^{35}$, $C^{13}H_3CH_2Cl^{35}$, and $CH_3C^{13}H_2Cl^{35}$ were prepared and their spectra examined. These compounds were made following for the most part procedures given in the literature. All preparations were done in a vacuum system, with the purity of the final products determined by examination of their infrared spectra.

$CH_3CH_2Cl^{35}$ and $CH_3CH_2Cl^{37}$

The $CH_3CH_2Cl^{35}$ and $CH_3CH_2Cl^{37}$ spectra were examined using a sample of ethyl chloride obtained from the Eastman Kodak Company (Cl^{37} - 24.6% in natural abundance). The sample was used without further purification.

CH_3CD_2Cl

The CH_3CD_2Cl was prepared by a modification of a published synthesis for labeled ethanol (47). The synthesis begins with the absorption of acetyl chloride vapor by a stirred solution of lithium aluminum deuteride in diethylene glycol diethyl ether, followed by alcoholysis with ethylene glycol monophenyl ether (2-phenoxyethanol). The deuterated ethanol (CH_3CD_2OH) which is evolved is trapped in a bulb cooled by liquid air. The alcohol is distilled over onto frozen phosphorus trichloride and upon warming CH_3CD_2Cl is evolved. The equations representing the reactions are:

$$2CH_3COCl + LiAlD_4 \longrightarrow LiAlCl_2(OCD_2CH_3)_2$$

$$LiAlCl_2(OCD_2CH_3)_2 + 2HO\text{-}(CH_2)_2\text{-}O\text{-}\varphi \longrightarrow$$

$$2CH_3CD_2OH + LiAlCl_2(O\text{-}(CH_2)_2\text{-}O\text{-}\varphi)_2$$

$$3CH_3CD_2OH + PCl_3 \longrightarrow 3CH_2CH_2Cl + H_3PO_3$$

---

[1] Trans and gauche refer to the relative position of the deuterium and chlorine atoms.

CH_2DCH_2Cl (trans and gauche)

The trans and gauche CH_2DCH_2Cl were made by allowing a mixture of ethylene and deuterium chloride to stand for several hours at Dry Ice temperature in the presence of anhydrous aluminum chloride. The deuterium chloride was made by adding phosphorus trichloride dropwise to deuterium oxide (48). The equations involved in the preparation are:

$$PCl_3 + 3D_2O \longrightarrow 3DCl + D_3PO_3$$

$$C_2H_4 + DCl \xrightarrow{AlCl_3} CH_2DCH_2Cl$$

The final sample is an equilibrium mixture of one part trans isomer to two parts gauche isomer.

$C^{13}H_3CH_2Cl$

The basic procedure used in the preparation of this isotope may be divided into two parts, the first is the preparation of sodium acetate from methyl iodide as given by Cox, Turner, and Warne (49), and the second is the preparation of ethanol from sodium acetate as given by Cox and Turner (47). The equations representing the overall preparation are:

$$C^{13}H_3I + KCN \xrightarrow{H_2O} C^{13}H_3CN + KI$$

$$C^{13}H_3CN \xrightarrow[2)\ H_2SO_4]{1)\ NaOH} C^{13}H_3COOH \xrightarrow{NaOH} C^{13}H_3COONa$$

$$2C^{13}H_3COONa + (C_2H_5)_2SO_4 \longrightarrow 2C^{13}H_3COOC_2H_5 + Na_2SO_4$$

$$C^{13}H_3COOC_2H_5 \xrightarrow{LiAlH_4} C^{13}H_3CH_2OH$$

$$C^{13}H_3CH_2OH \xrightarrow{PCl_3} C^{13}H_3CH_2Cl$$

A sealed flask containing labeled methyl iodide (approximately 45% $C^{13}H_3I$), potassium cyanide, and water was shaken until the reaction mixture became homogeneous. The flask was then cracked open and the mixture of water, acetonitrile, and any unchanged methyl iodide was

vacuum distilled into a flask containing a sodium hydroxide solution. This flask was sealed off and heated at 80°C for a period of four hours. Following the addition of silver sulfate the mixture was acidified and steam-distilled. The pH of the distillate was adjusted to 8.8 with sodium hydroxide and labeled sodium acetate obtained by evaporation. The finely powdered sodium acetate was heated with diethyl sulfate and a slow stream of nitrogen gas was used to sweep out the ethyl acetate formed. The preparation of the $C^{13}H_3CH_2Cl$ from the $C^{13}H_3COOC_2H_5$ followed closely the procedure given for the preparation of CH_3CD_2Cl from acetyl chloride, however, using $C^{13}H_3COOC_2H_5$ and $LiAlH_4$ in place of the CH_3COCl and $LiAlD_4$ respectively. A dilution of C-13 occurs in the reduction such that the final sample contained 20-25% of $C^{13}H_3CH_2Cl$.

$CH_3C^{13}H_2Cl$

For the preparation of $CH_3C^{13}H_2Cl$ a sample of CH_3COONa containing approximately 50% $CH_3C^{13}OONa$ was obtained from the Isotope Specialties Company.[1] The procedure for converting the sodium acetate to ethyl chloride follows exactly the last three steps of the previous synthesis. The equations are:

$$2CH_3C^{13}OONa + (C_2H_5)_2SO_4 \longrightarrow 2CH_3C^{13}OOC_2H_5 + Na_2SO_4$$

$$CH_3C^{13}OOC_2H_5 \xrightarrow{LiAlH_4} CH_3C^{13}H_2OH$$

$$CH_3C^{13}H_2OH \xrightarrow{PCl_3} CH_3C^{13}H_2Cl$$

4.3 Microwave Spectra

Once the isotopic species to be used in the structure determination have been prepared the procedure for analyzing the spectrum of each may be outlined as follows:

---

[1]Isotope Specialties Company, 170 W. Providentia, Burbank, California.

a) Computation of the principal moments of inertia of the species based upon an assumed structure. The rotational constants, energy levels, and transition frequencies are then computed.

b) Search of the microwave spectrum of the compound for the predicted absorption lines and careful measurement of the frequencies of absorption lines in the regions of those predicted.

c) Assignment of absorption lines to the energy levels involved and recalculation of the principal moments of inertia based upon the experimentally measured frequencies.

Initial Computation of Moments of Inertia, Rotational Constants and Transition Frequencies

The structure assumed for ethyl chloride was that reported by Wagner and Dailey (44). They gave accurate values for the rotational constants B and C but were unable to determine A to any degree of accuracy since the transitions they studied were insensitive to this constant. The parameters they reported included:

CC	1.5495 ± 0.0005A	HCH	$110^{\circ}00' \pm 30'$
CH	1.101 ± 0.003A	CCCl	$110^{\circ}30' \pm 2'$
CCl	1.7785 ± 0.0003A		

The Russian workers (45) reported values of A for the Cl-35 and Cl-37 species. The moments of inertia and rotational constants for each isotopic species were computed, assuming that isotopic substitution does not affect the position coordinates of an atom. The calculation was performed using "MISTIC" the electronic digital computer at Michigan State University.

The program used is one which transforms from a spherical polar coordinate system with an arbitrarily chosen origin to a center of mass Cartesian coordinate system from which the principal moments of inertia and rotational constants are computed. A more detailed description

of this program may be found in the current literature (50). Preliminary calculations showed that all the species of ethyl chloride considered were near-symmetric prolate rotors (κ = -0.940 to κ = -0.965).

From the rotational constants the desired energy levels and transition frequencies are computed. The dipole moment of ethyl chloride may be resolved into components along the a and b principal axes (see Figure 10) so that both a and b-type transitions should be observed. The value of the component of the dipole moment along the a axis has been measured by the Russian workers (μ_a = 1.745 D $\pm$ 1.2%) (45) but they report no value for the b component. Wagner and Dailey (44) report that the a component would be about four times larger than the b component and that they were unable to find any b-type transitions.

Substitution of the restrictions on J and K into Equation (2-32) and using the Bohr frequency condition, Equation (2-37), gives for R-branch a-type transitions

$$\nu_R = (\frac{B+C}{2})\, 2J + (A - \frac{B+C}{2})[b\Delta C_1 + b^2\Delta C_2 + b^3\Delta C_3 + \cdots]. \quad (4-1)$$

This type of transition depends primarily on the values of B and C and accounts for Wagner and Dailey (44) being unable to obtain an accurate value of A. The other types of transitions in which we are interested are R-branch b-type transitions $J_{OJ} \longrightarrow (J+1)_1, J+1$, for which

$$\nu_R = (\frac{B+C}{2})\, 2J - (A - \frac{B+C}{2}) + (\frac{C-B}{2})[\Delta C_1 + b\Delta C_2 + \cdots], \quad (4-2)$$

and the Q-branch b-type, $J_{OJ} \longrightarrow J_1, J-1$, for which

$$\nu_R = (A - \frac{B+C}{2}) + (\frac{C-B}{2})[\Delta C_1 + b\Delta C_2 + b^2\Delta C_3 + \cdots]. \quad (4-3)$$

The b-type transitions are very sensitive to the value of A as may be seen from the frequency expressions. With these expressions for the transition frequencies a whole series of absorption lines were computed.

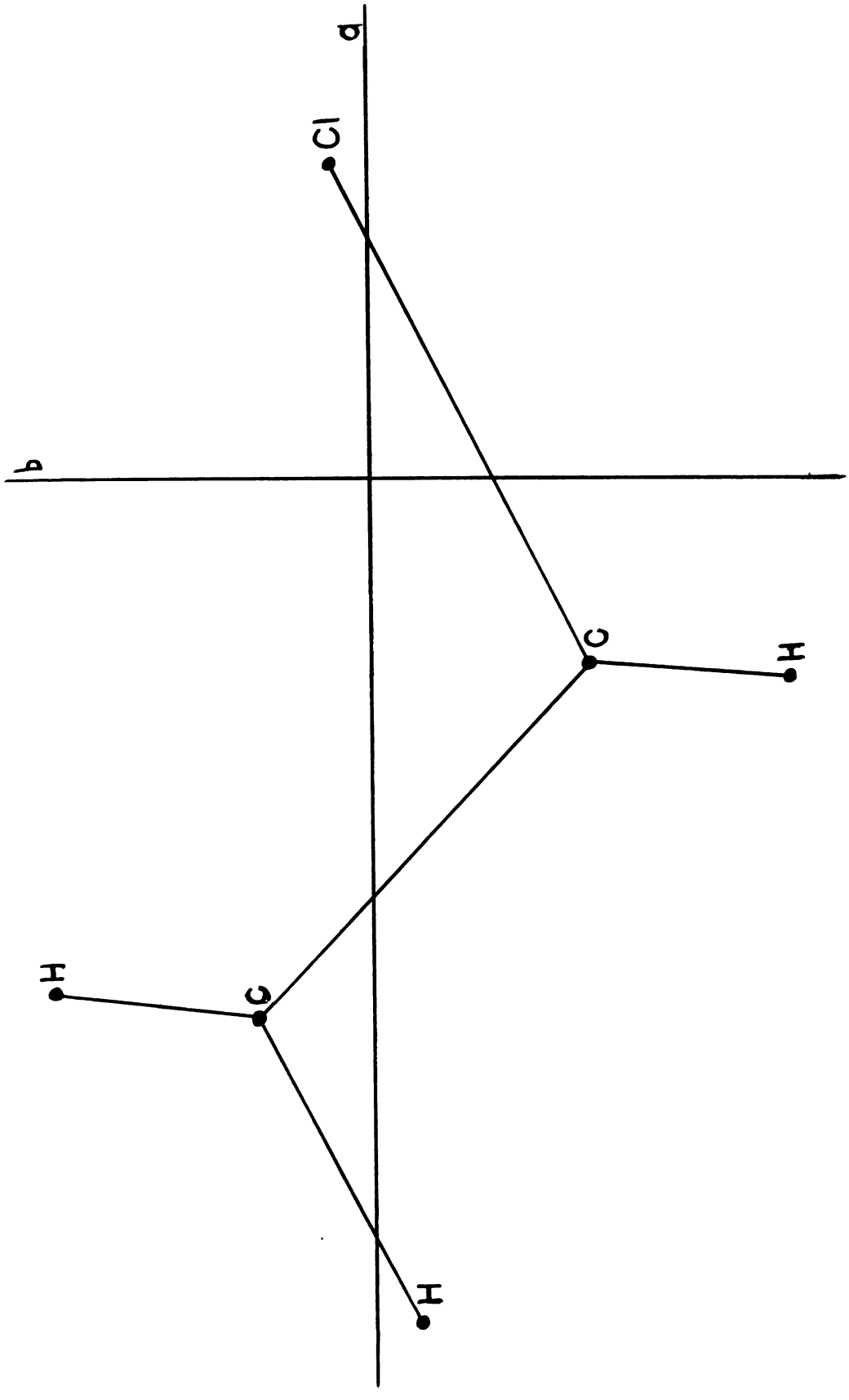

Figure 10. A Projection of Ethyl Chloride in its Plane of Symmetry Showing the Location of the a and b Principal Axes. The c Axis is Perpendicular to the Page.

A perturbation of the energy levels occurs in the case of ethyl chloride due to the quadrupole moment of the chlorine nucleus, so that the single absorption line of a transition, whose frequency (ν_R) is computed as described above, is split into several components (hyperfine structure). From Equation (2-37) and (2-42) we may write for the frequency

$$\nu = \nu_R + \nu_Q \qquad (4\text{-}4)$$

where ν_R (called the hypothetical unsplit frequency) is a function only of A, B, and C while ν_Q is a function of the asymmetry parameter b [Equation (2-33)] and the quadrupole coupling parameters q_m and $q_m \eta$ [Equations (2-46) and (2-47)]. The frequencies ν_R and ν_Q are computed separately since ν_Q is only weakly dependent on the asymmetry parameter b and using only approximate values of A, B, and C one computes highly accurate values of ν_Q. The value of ν_R is obtained from Equations (4-1, 4-2, 4-3) using the assumed values of A, B, and C while the calculation of ν_Q is illustrated in Table V for the Q-branch transition $4_{04} \longrightarrow 4_{13}$ of the parent species ($CH_3CH_2Cl^{35}$). The values of W_Q/h for each level were calculated from Equation (2-48) using the values of q_m and $q_m \eta$ given by Wagner and Dailey (44).[1] The differences, ν_Q, are found for the $F \longrightarrow F'$ transitions of interest. For Q-branch transitions the strongest components are those with $\Delta F = 0$, i.e. $\frac{11}{2} \longrightarrow \frac{11}{2}$, $\frac{9}{2} \longrightarrow \frac{9}{2}$, etc. The relative intensities govern which transitions will predominate as shown in the last line of the table. The pattern predicted for this hyperfine multiplet is shown in the lower half of Table V. Comparison of the predicted appearance may be made with the recorded spectrum of the $4_{04} \longrightarrow 4_{13}$ transition of $CH_2DCH_2Cl^{35}$ (trans) as shown in Figure 6, Chapter III.

---

[1] q_m = -48.85 Mc; $q_m \eta$ = -21.35 Mc; I = $\frac{3}{2}$ for Cl-35 and Cl-37.

Table V. Computation of Hyperfine Structure for the $4_{04} \longrightarrow 4_{13}$ Transition in $CH_3CH_2Cl^{35}$.

	Computation of ν_Q			
F =	$J + \frac{3}{2}$	$J + \frac{1}{2}$	$J - \frac{1}{2}$	$J - \frac{3}{2}$
	$(\frac{11}{2})$	$(\frac{9}{2})$	$(\frac{7}{2})$	$(\frac{5}{2})$
$\frac{W_Q}{h}$ (4_{04})	+4.53MC	-7.92Mc	-3.56Mc	+8.89Mc
$\frac{W_Q}{h}$ (4_{13})	+2.82	-4.93	-2.22	+5.52
$\nu_Q = \frac{\Delta W_Q}{h}$	-1.71	+2.99	+1.34	-3.37
Relative Intensity(a)	31.5	23.6	18.1	14.9

Appearance of the Spectrum

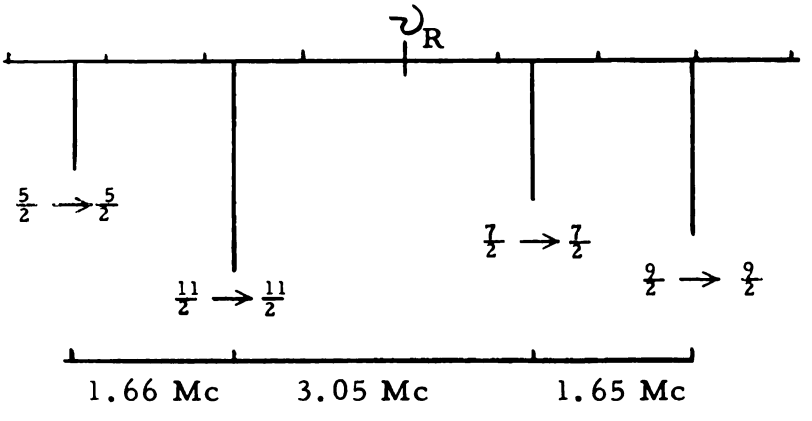

(a) Reference 12, Appendix I.

The calculation shown in Table V is carried out for all of the transitions of interest and accessibility, i.e. one must take into account the regions covered by available klystrons. The calculation of hyperfine splittings may also be carried out using Equation (2-50) with a program designed for use with "MISTIC."

Examination of the Spectra and Assignment of Transitions

The spectra of all the species were examined at Dry Ice temperature using the conventional Hughes-Wilson microwave spectrometer described in Chapter III. Both oscilloscope display and pen-and-ink recording were used. Normally a recording of the region several hundred megacycles on either side of the predicted frequency was made and lines within the region having the predicted quadrupole patterns measured.

Both a-type and b-type transitions were observed for all the isotopic species and with the exception of the R-branch b-type all transitions showed resolvable hyperfine structure. An assignment of transitions was considered to "fit" when at least two R-branch a-type and two Q-branch b-type transitions were consistent to within one tenth of a megacycle with a set of A, B, and C values. The R-branch b-type lines were used as a final confirmation of the assignment in all but two cases. Traces of the $1_{11} \longrightarrow 2_{12}$ transition in $CH_2DCH_2Cl^{35}$ (gauche) and the $4_{04} \longrightarrow 4_{13}$ transition in $CH_2DCH_2Cl^{35}$ (trans) are shown in Figures 6 and 7 in Chapter III. The frequencies of the $1 \longrightarrow 2$ a-type transitions reported by Wagner and Dailey (44) for the species $CH_3CH_2Cl^{35}$, $CH_3CH_2Cl^{37}$, and $CH_2DCH_2Cl^{35}$ were remeasured and found to vary by as much as ± 0.5 Mc from their reported values. Table VI is a list of the frequencies of all the assigned hyperfine component transitions used in the determination of the quadrupole coupling parameters and rotation constants. Table VII is a list of other measured frequencies together with their probable assignment in certain cases. Blanks exist in these tables either because

Table VI. Frequencies (Mc) of the Hyperfine Components in Ethyl Chloride.

	$CH_3CH_2Cl^{35}$	$CH_3CH_2Cl^{37}$	$C^{13}H_3CH_2Cl^{35}$	$CH_3C^{13}H_2Cl^{35}$	$CH_3CD_2Cl^{35}$	$CH_2DCH_2Cl^{35}$(t)	$CH_2DCH_2Cl^{35}$(g)
$0_{00} \rightarrow 1_{01}$							
$\frac{3}{2} \rightarrow \frac{3}{2}$	10446.11	10238.66		10386.51		9726.45	10072.98
$\frac{3}{2} \rightarrow \frac{5}{2}$	10458.46	10248.08		10398.86		9738.77	10084.92
$\frac{3}{2} \rightarrow \frac{1}{2}$	10468.36	10255.97		10408.78		9748.59	10094.21
$1_{11} \rightarrow 2_{12}$							
$\frac{3}{2} \rightarrow \frac{5}{2}$	20371.50	19973.43	19772.27	20235.21	19659.54	19002.3	19643.6
$\frac{5}{2} \rightarrow \frac{5}{2}$	20374.88	19976.16	19775.61	20238.71	19663.44	19005.8	19646.4
$\frac{3}{2} \rightarrow \frac{3}{2}$	20377.89	19978.51	19778.66	20241.57	19665.87	19008.6	19650.0
$\frac{5}{2} \rightarrow \frac{7}{2}$	20383.79	19983.22	19784.42	20247.70	19672.38	19014.6	19655.4
$\frac{1}{2} \rightarrow \frac{1}{2}$	20392.86	19990.44	19793.4	20256.75	19681.83	19023.9	19664.2
$1_{10} \rightarrow 2_{11}$							
$\frac{3}{2} \rightarrow \frac{5}{2}$	21433.79	20996.90	20785.85	21331.72	20820.49	19923.90	20668.28
$\frac{3}{2} \rightarrow \frac{3}{2}$	21436.27	20998.48		21334.11	20823.26	19926.35	20670.34
$\frac{5}{2} \rightarrow \frac{5}{2}$	21442.73	21003.51	20794.83	21340.42	20829.38	19932.95	20677.17
$\frac{5}{2} \rightarrow \frac{7}{2}$	21446.21	21006.28	20798.02	21344.00	20833.26	19936.20	20680.09
$\frac{1}{2} \rightarrow \frac{3}{2}$	21452.27	21011.02	20804.15	21349.93	20839.28	19942.45	20686.34
$\frac{1}{2} \rightarrow \frac{1}{2}$	21455.62	21013.94	20807.44	21353.66	20843.07	19945.95	20689.31

continued

Table VI -- Continued

	$CH_3CH_2Cl^{35}$	$CH_3CH_2Cl^{37}$	$C^{13}H_3CH_2Cl^{35}$	$CH_3C^{13}H_2Cl^{35}$	$CH_3CD_2Cl^{35}$	$CH_2DCH_2Cl^{35}$(t)	$CH_2DCH_2Cl^{35}$(g)
$1_{01} \rightarrow 2_{02}$							
$\frac{1}{2} \rightarrow \frac{3}{2}$	20891.45			20771.41	20223.65		
$\frac{5}{2} \rightarrow \frac{5}{2}$	20892.41			20772.35	20224.63		
$\frac{3}{2} \rightarrow \frac{5}{2}$			20313.27		20237.46		
$\frac{5}{2} \rightarrow \frac{7}{2}$	20904.87		20315.02	20784.91			
$\frac{3}{2} \rightarrow \frac{3}{2}$	20913.68		20322.10	20793.67	20246.72		
$3_{03} \rightarrow 3_{12}$							
$\frac{3}{2} \rightarrow \frac{3}{2}$	27734.22	27726.70	27557.89		20872.9	27830.10	24835.97
$\frac{9}{2} \rightarrow \frac{9}{2}$	27737.02	27728.65	27560.62		20875.6	27832.83	24838.76
$\frac{5}{2} \rightarrow \frac{5}{2}$	27740.18	27730.75	27563.76		20878.7	27835.97	24842.03
$\frac{7}{2} \rightarrow \frac{7}{2}$	27742.94	27733.35	27566.63		20881.6	27838.62	24844.87
$4_{04} \rightarrow 4_{13}$							
$\frac{5}{2} \rightarrow \frac{5}{2}$	28862.92	28810.74	28632.35	28173.62	22140.38	28801.67	
$\frac{11}{2} \rightarrow \frac{11}{2}$	28864.73	28812.06	28634.10	28175.25	22142.19	28803.29	
$\frac{7}{2} \rightarrow \frac{7}{2}$	28867.92	28814.56	28637.11	28178.26	22145.19	28806.52	
$\frac{9}{2} \rightarrow \frac{9}{2}$	28869.63	28815.92	28638.88	28179.95	22147.03	28808.10	

continued

Table VI -- Continued

	$CH_3CH_2Cl^{35}$	$CH_3CH_2Cl^{37}$	$C^{13}H_3CH_2Cl^{35}$	$CH_3C^{13}H_2Cl^{35}$	$CH_3CD_2Cl^{35}$	$CH_2DCH_2Cl^{35}$(t)	$CH_2DCH_2Cl^{35}$(g)
$5_{05} \rightarrow 5_{14}$							
$\frac{7}{2} \rightarrow \frac{7}{2}$		30206.62	30015.11	29682.75	23795.5	30048.54	27342.62
$\frac{13}{2} \rightarrow \frac{13}{2}$		30207.53	30016.32	29683.97	23796.68	30049.65	27343.98
$\frac{9}{2} \rightarrow \frac{9}{2}$		30209.95	30019.42	29686.99	23799.7	30052.73	27347.22
$\frac{11}{2} \rightarrow \frac{11}{2}$		30210.87	30020.68	29688.18	23800.9	30053.86	27348.50
$6_{06} \rightarrow 6_{15}$							
$\frac{9}{2} \rightarrow \frac{9}{2}$							29104.23
$\frac{15}{2} \rightarrow \frac{15}{2}$							29105.22
$\frac{11}{2} \rightarrow \frac{11}{2}$							29108.62
$\frac{13}{2} \rightarrow \frac{13}{2}$							29109.55
$7_{07} \rightarrow 7_{16}$							
$\frac{11}{2} \rightarrow \frac{11}{2}$					28448.6		
$\frac{17}{2} \rightarrow \frac{17}{2}$					28449.4		
$\frac{13}{2} \rightarrow \frac{13}{2}$					28452.5		
$\frac{15}{2} \rightarrow \frac{15}{2}$					28453.3		
$4_{14} \rightarrow 5_{05}$							
Unresolved	28563.29	27382.99		29109.25		24368.57	29433.82

Table VII. Other Measured Frequencies (Mc) in Ethyl Chloride.

Probable Assignment							
$1_{01} \rightarrow 2_{02}$	$C^{13}H_3CH_2Cl^{35}$	20313.27	20315.02	20322.10	20326.92		
$2_{12} \rightarrow 3_{13}$	$C^{13}H_3CH_2Cl^{35}$	29656.62	29665.26	29668.52	29676.07		
$1_{01} \rightarrow 1_{10}$	$CH_3C^{13}H_2Cl^{35}$	25594.39					
$2_{02} \rightarrow 2_{11}$	$CH_3C^{13}H_2Cl^{35}$	26147.5	26150.40	26153.82	26156.49		
$2_{02} \rightarrow 2_{11}$	$CH_2DCH_2Cl^{35}$(g)	24040.68	24037.58	24031.29			
$2_{12} \rightarrow 3_{13}$	$CH_2DCH_2Cl^{35}$(g)	30210.77	30213.68	30219.40	30222.78	30230.9	30239.6
$2_{12} \rightarrow 3_{13}$	$CH_2DCH_2Cl^{35}$(t)	28880.9	28887.7	28890.2	28892.3	28896.8	
$2_{12} \rightarrow 3_{13}$	$CH_3CD_2Cl^{35}$	29485.5	29485.6	29493.3	29496.6	29499.15	29505.15
		27487.81	27489.56	27492.74	27494.32		
		26911.26	26912.37	26914.32	26917.65	26920.98	26923.82
		20786.80	20788.81	20793.72			
		29454.08	29544.1				
		22150.31	22151.01				
		20884.9	20888.2				
		26995.60	26992.78				
		24369.61	20387.36				

a region was inaccessible with present klystrons or because the lines were too weak for accurate measurement. The uncertainty in the absolute frequency measurements of transitions is believed to be no greater than ± 0.05 Mc while the differences in frequencies within multiplets is probably less than ± 0.02 Mc.

The average frequencies of the hyperfine multiplets is used to obtain approximate values of the rotational constants. Differences in the frequencies of the components of a multiplet will depend only on ν_Q, and hence may be used with the approximate values of A, B, and C to compute precise values of q_m and $q_m \eta$. Selected differences within the $0 \rightarrow 1$ and $1 \rightarrow 2$ transitions were used to determine the values of q_m and $q_m \eta$ by means of least squares. The precise values of q_m and $q_m \eta$ were then used to compute ν_R for the various transitions from which precise values of A, B, and C are determined. A comparison of the calculated and observed frequencies obtained after a least squares determination of q_m and $q_m \eta$ is shown in Table VIII for the $CH_3CH_2Cl^{35}$ species. Similar computations were carried out for each isotopic species.

With accurate values of q_m and $q_m \eta$ the hypothetical unsplit frequencies (ν_R) may be computed. These are given in Table IX. From the hypothetical unsplit frequencies the values of A, B, and C are computed. For the determination of B and C the following transitions were used (obtained from Equation (4-1)

$$\begin{aligned} \nu_{0_{00} \rightarrow 1_{01}} &= \nu_0 = B + C \\ \nu_{1_{11} \rightarrow 2_{12}} &= \nu_1 = B + 3C \\ \nu_{1_{10} \rightarrow 2_{11}} &= \nu_2 = 3B + C \,. \end{aligned} \tag{4-5}$$

A least squares analysis shows that in fact

$$\begin{aligned} B &= \tfrac{1}{72} (4\nu_0 - 10\nu_1 + 26\nu_2) \quad \text{and} \\ C &= \tfrac{1}{72} (4\nu_0 + 26\nu_1 - 10\nu_2) \end{aligned} \tag{4-6}$$

Table VIII. Comparison of Calculated and Observed Frequencies of Hyperfine Components in $CH_3CH_2Cl^{35}$.

Transition	F → F'	Calculated Frequency	Observed Frequency
$0_{00} \rightarrow 1_{01}$	3/2 → 3/2	10446.15	10446.11
	3/2 → 5/2	10458.45	10458.46
	3/2 → 1/2	10468.29	10468.37
$1_{11} \rightarrow 2_{12}$	3/2 → 5/2	20371.50	20371.50
	5/2 → 5/2	20374.90	20374.88
	3/2 → 3/2	20377.86	20377.89
	5/2 → 7/2	20383.80	20383.79
	1/2 → 1/2	20392.88	20392.86
$1_{10} \rightarrow 2_{11}$	3/2 → 5/2	21433.83	21433.79
	3/2 → 3/2	21436.25	21436.27
	5/2 → 5/2	21442.73	21442.73
	5/2 → 7/2	21446.13	21446.21
	1/2 → 3/2	21452.28	21452.27
	1/2 → 1/2	21455.68	21455.62
$1_{01} \rightarrow 2_{02}$	1/2 → 3/2	20891.57	20891.45
	5/2 → 5/2	20892.58	20892.41
	3/2 → 5/2	20904.88	} 20904.87
	5/2 → 7/2	20904.94	
	3/2 → 3/2	20913.71	20913.69
$3_{03} \rightarrow 3_{12}$	3/2 → 3/2	27734.23	27734.22
	9/2 → 9/2	27737.01	27737.03
	5/2 → 5/2	27740.18	27740.18
	7/2 → 7/2	17742.95	27742.95
$4_{04} \rightarrow 4_{13}$	5/2 → 5/2	28862.90	28862.92
	11/2 → 11/2	28864.58	28864.73
	7/2 → 7/2	28867.70	28867.92
	9/2 → 9/2	28869.38	28869.63

Table IX. Hypothetical Unsplit Frequencies (Mc) in Ethyl Chloride.

	$CH_3CH_2Cl^{35}$	$CH_3CH_2Cl^{37}$	$C^{13}H_3CH_2Cl^{35}$	$CH_3C^{13}H_2Cl^{35}$	$CH_3CD_2Cl^{35}$	$CH_2DCH_2Cl^{35}$(t)	$CH_2DCH_2Cl^{35}$(g)
$0_{00} - 1_{01}$	10456.00	10246.28		10396.40		9736.29	10082.46
$1_{11} - 2_{12}$	20380.58	19980.66	19781.25	20244.38	19669.02	19011.43	19652.29
$1_{10} - 2_{11}$	21443.38	21004.17	20795.31	21341.22	20830.34	19933.53	20677.47
$1_{01} - 2_{02}$	20903.77			20783.77	20236.43		
$3_{03} - 3_{12}$	27738.99	27730.16	27562.62		20877.60	27834.77	24840.81
$4_{04} - 4_{13}$	28866.49	28813.46	28635.80	28176.95	22143.89	28805.08	
$5_{05} - 5_{14}$		30208.82	20017.99	29685.58	23798.30	30051.30	27345.70
$6_{06} - 6_{15}$							29106.99
$7_{07} - 7_{16}$					28451.00		
$4_{14} - 5_{05}$	28563.29	27382.99		29109.25		24368.57	29433.82

The value of A was then obtained from the frequency of the lowest J Q-branch line observed. The rotational constants, moments of inertia, and second moments are shown in Table X.

The B and C rotational constants for the Cl-35 and Cl-37 species are essentially the same as found by Wagner and Dailey (44) and the A constant in both cases is within 0.5 Mc of that reported by the Russian workers (45). The B and C constants should be nearly free from uncertainty due to centrifugal distortion effects while a small uncertainty from this cause may remain in A. The effect of this uncertainty on the structure determination should be negligible both because the value of A is quite large making the percentage error relatively small, and because differences in corresponding moments of inertia of the various species are used in the coordinate evaluations. The last step is an analysis of the molecular structure based upon these experimentally determined parameters.

4.4 Molecular Structure

The data of the present work combined with those previously reported are sufficient to determine the coordinates of all the atoms in ethyl chloride by the substitution method described in section 2.2. For this purpose the second moments were computed for all the species and are given at the bottom of Table X. The $CH_3CH_2Cl^{35}$ species was chosen as the parent species for use in Equation (2-14). The second moments of the parent species combined with those of $CH_3CH_2Cl^{37}$ determined the coordinates of the Cl atom, those of the two C-13 species determined the coordinates of the two carbon atoms and the trans and gauche deuterium species served to locate the methyl hydrogens. The doubly deuterated species was used with Equations (2-15) and (2-16) to determine the methylene hydrogen coordinates.

Table X. Rotational Constants (Mc), Moments of Inertia (amu A^2),[a] and Second Moments (amu A^2)[b] for Ethyl Chloride.

	$CH_3CH_2Cl^{35}$	$CH_3CH_2Cl^{37}$	$C^{13}H_3CH_2Cl^{35}$	$CH_3C^{13}H_2Cl^{35}$	$CH_3CD_2Cl^{35}$	$CH_2DCH_2Cl^{35}$(t)	$CH_2DCH_2Cl^{35}$(g)
A	31337.35	31285.20	31081.22	30523.34	24140.20	31293.39	28307.27
B	5493.69	5378.99	5325.59	5472.41	5352.75	5098.65	5297.52
C	4962.30	4867.23	4818.56	4923.99	4772.09	4637.60	4784.93
I_a	16.1319	16.1588	16.2648	16.5621	20.9415	16.1546	17.8587
I_b	92.0203	93.9825	94.9250	92.3781	94.4432	99.1500	95.4279
I_c	101.8743	103.8642	104.9133	102.6669	105.9349	109.0070	105.6507
P_{aa}	88.8814	90.8440	91.7868	89.2414	89.7183	96.0012	91.6100
P_{bb}	12.9930	13.0202	13.1266	13.4254	16.2166	13.0058	14.0408
P_{cc}	3.1390	3.1386	3.1382	3.1366	4.7249	3.1488	3.8180

(a) Conversion factor used: 5.05531×10^5 Mc-amu A^2

(b) Computed from Equation (2-17)

For an atom substituted in the plane of symmetry (the ab plane in this case) P_{cc} and P_{cc}' should be the same if the molecule is rigid. However, the zero point motions and hence the effective coordinates of the atoms are always changed by isotopic substitution, causing differences between P_{cc} and P_{cc}' to occur. The values of P_{cc} for the various species of ethyl chloride are shown on the bottom line of Table X. It may be seen that P_{cc} decreases slightly upon substitution of a heavier isotope for the chlorine atom or either carbon atom, whereas there is a much larger increase in P_{cc} upon substitution of deuterium for hydrogen. The reasons for this difference have been described qualitatively for propane (51) and are probably very similar for ethyl chloride.

Examination of Kraitchman's equations (Equation (2-14)) show that if $P_{cc}'-P_{cc}$ is assumed to be zero, the term including this quantity will vanish. Furthermore it is then possible to compute $P_{aa}'-P_{aa}$ and $P_{bb}'-P_{bb}$ using only two of the three experimentally determined moments of inertia. Since $P_{cc}'-P_{cc}$ is not zero, the values of the coordinates obtained will depend upon which two moments of inertia are chosen. That this is true may be seen from the expressions for a_s and b_s

$$|a_s|^2 = \frac{1}{\mu}\ \Delta P_{aa}\left(1 + \frac{\Delta P_{bb}}{P_{bb}-P_{aa}}\right)$$

$$|b_s|^2 = \frac{1}{\mu}\ \Delta P_{bb}\left(1 + \frac{\Delta P_{aa}}{P_{aa}-P_{bb}}\right) \qquad (4\text{-}7)$$

which are obtained from Equation (2-14), dropping the term in ΔP_{cc}. The evaluation of ΔP_{aa} and ΔP_{bb} in terms of moment of inertia differences is now possible for three different cases. If we do not know ΔI_a (the difference in the a moments of inertia for the parent and isotopic species) then it may be shown that

$$\Delta I_a = \Delta I_c - \Delta I_b \quad \text{and} \qquad (4\text{-}8)$$

$$\Delta P_{aa} = \Delta I_b$$

$$\Delta P_{bb} = \Delta I_c - \Delta I_b. \qquad (4\text{-}9)$$

If we do not know ΔI_b, then

$$\Delta P_{aa} = \Delta I_c - \Delta I_a$$

$$\Delta P_{bb} = \Delta I_a \ . \qquad (4\text{-}10)$$

Finally, if we do not know ΔI_c, then

$$\Delta P_{aa} = \Delta I_b$$

$$\Delta P_{bb} = \Delta I_a. \qquad (4\text{-}11)$$

In Table XI the variations of certain of the molecular parameters with choice of moments of inertia is shown.

The values of the CC and CCl distances and the CCCl angle are nearly independent of the choice of moments of inertia. However, the CH(t) distances and CCH(t) angle show large variations reflecting the large difference in P_{cc} shown in Table X for $CH_2DCH_2Cl^{35}$(t) and $CH_3CH_2Cl^{35}$. The large changes in the H(t) parameters are magnified by the small value ($\sim$ 0.1 A) of the b coordinate of H(t). The coordinates listed in Table XII are averages of those used to compute the entries in Table XI. The molecular parameters shown in Table XIII were computed from the coordinates in Table XII with the exception of the methyl group parameters. Because of the small b coordinate of H(t), and because of the large change in inertial defect upon deuterium substitution mentioned above, the methyl group was assumed to have trigonal symmetry about the CC bond with parameters determined by the positions of the out-of-plane hydrogen atoms. Even though examples of "tilted" methyl groups have been described, the molecules most closely resembling ethyl chloride do not appear to have tilted axes (52). The uncertainty in the coordinates of the in-plane hydrogen atom in ethyl chloride is too large for a meaningful analysis of the tilt of the methyl group axis.

Table XI. Variation of Parameters in Ethyl Chloride with Choice of Moments of Inertia.

Parameter	I_a, I_b, I_c	I_b, I_c	I_a, I_c	I_a, I_b
CC	1.5205 A	1.5233 A	1.5175 A	1.5198 A
CCl	1.7888	1.7880	1.7895	1.7861
CH (t)	1.0854	1.0610	1.1017	1.1053
CCCl	111.00°	110.88°	111.12°	108.31°
CCH (t)	109.93°	112.92°	108.12°	108.31°
$\Sigma m_i a_i$	0.1095 amu A	0.1292 amu A	0.0898 amu A	0.1292 amu A
$\Sigma m_i b_i$	0.0433	0.1180	-0.0077	-0.0074
$\Sigma m_i a_i b_i$	-0.0430 amu A^2	-0.2117 amu A^2	0.0625 amu A^2	0.0353 amu A^2

Table XII. Coordinates of the Atoms in the $CH_3CH_2Cl^{35}$ Principal Axis System.

Atom	a	b	c
Cl	1.00635 A	0.11978 A	0
C (methyl)	-1.71313	0.37440	0
C (methylene)	-0.60147	-0.66265	0
H (methylene)	-0.64078	-1.29220	± 0.88759 A
H (t)	-2.68055	-0.12279	0
H (g)	-1.64130	1.00982	± 0.88445
	$\Sigma m_i a_i$ = 0.1144 amu A		
	$\Sigma m_i b_i$ = 0.0366 amu A		
	$\Sigma m_i a_i b_i$ = -0.0390 amu A^2		

Table XIII. Molecular Parameters for Ethyl Chloride.

CC	1.520 ± .003 A	CCCl	$111^{\circ}2' \pm 8'$
CCl	1.788 ± .002 A	HCH (methyl)	$108^{\circ}30' \pm 30'$
CH (methyl)	1.091 ± .010 A	HCH (methylene)	$109^{\circ}12' \pm 30'$
CH (methylene)	1.089 ± .010 A	CCH (methylene)	$111^{\circ}36' \pm 30'$

$CH_3CH_2Cl^{35}$	Experimental	Calculated
I_a	16.1319 amu A^2	16.0519 amu A^2
I_b	92.0202	91.7030
I_c	101.8744	101.4160

The uncertainties reported in Table XIII reflect only an estimate of the inconsistency of the substitution method as applied to ethyl chloride. The precise meaning of the substitution coordinates has been the subject of some discussion (53), but certainly needs further clarification. The tests of internal consistency represented in Tables X and XI have been discussed previously. A further test of consistency is shown in Table XII with the values of the first moments and cross product, all of which should be zero since the a, b, c axes are assumed to be principal axes.

The moments of inertia calculated from the final parameters are slightly smaller than the observed moments which appears to be typical for substitution parameters.

4.5 Discussion of the Structure

Examination of the parameters in Table XIII reveals a number of interesting points. First the carbon-carbon distance in ethyl chloride is not longer than the carbon-carbon distance in saturated hydrocarbons. Comparison of the value found in this investigation with those reported for propane (51) and isobutane (54) shows that in fact it is slightly smaller (1.520A vs. 1.526A). These values have all been determined by the substitution method. In addition, an estimate of what the CC distance in ethane would be by a substitution method has been made by Lide (54) and also gives a value of 1.526 A. The CC distance reported for ethyl fluoride (55), 1.533 A, is somewhat longer than in ethyl chloride. The disagreement in the carbon-carbon bond length of ethyl chloride as reported by Wagner and Dailey (1.5495 A, (44)) appears to be a consequence of attempting to calculate a structure without isotopically substituting all, or nearly all positions within a molecule. Wagner and Dailey substituted neither carbon atom nor the methylene hydrogens,

so that the positions of these atoms would be questionable.

The CCl bond length in Table XIII is slightly longer than in methyl chloride (1.781 A, (56)) and the CCCl included angle is 1.5° larger than tetrahedral. However, the nearness of the chlorine atom (0.1 A) to the a axis prompts one to question the uncertainty in these numbers. Calculations by Laurie (57, 58) indicate that the substitution method tends to give coordinates which are too small when an atom is near an axis. A larger b coordinate would increase the CCl distance 0.004A/0.01A and the CCCl angle 17'/0.01A. In such cases it is common to use the requirement that the first moments and product of inertia vanish to locate the atom. In ethyl chloride over half the mass of the molecule resides at the chlorine nucleus so that the small values of $\Sigma m_i a_i$ and $\Sigma m_i a_i b_i$ shown in Table XII can be made to vanish by changing the b coordinate of the chlorine atom by less than 0.001 A. In addition, chlorine substitution results in an extremely small difference in $P_{cc}'-P_{cc}$, as shown in Table X. This is reflected as a very small variation in the CCl distance and CCCl angle with choice of moments of inertia in Table XI.

The CH distances and HCH angles in the methylene and methyl groups are not unusual. However, the larger than tetrahedral CCH angle together with the large CCCl angle lead to a very small value for the ClCH angle. The uncertainty in the value of this angle may be rather large owing to the large change in inertial defects obtained upon substitution of deuterium for hydrogen. However, all of the coordinates of the methylene hydrogen atoms are large (greater than 0.6 A in absolute value) which should reduce the effect of such changes. The uncertainties listed for the hydrogen atom parameters are based on a 0.01 amu A^2 change in the inertial defects upon deuterium substitution. Even though the combined effects of inaccurate location of the various atoms may be somewhat larger than the listed uncertainties, it seems probable

that the ClCH angle is of the order of 2° or so less than tetrahedral. Table XIV shows a comparison of some of the molecular parameters in ethyl chloride with similar molecules.

4.6 Quadrupole Analysis

The parameters q_m and $q_m\eta$ were determined by least squares as explained in section 2.4. An error analysis showed the splittings to be approximately equally sensitive to q_m and $q_m\eta$. The quadrupole coupling constants χ_{aa}, χ_{bb}, and χ_{cc} were then determined from the values of q_m and $q_m\eta$ together with the relation $\chi_{aa} + \chi_{bb} + \chi_{cc} = 0$.

Table XV gives χ_{aa}, χ_{bb}, and χ_{cc}, the diagonal values of the quadrupole coupling constant tensor in the principal inertial axis system of the molecule. Since ethyl chloride has a plane of symmetry perpendicular to the c axis, the coupling constant χ_{cc} is equal to one of the diagonal values, say χ_{yy}. The relations between the other components are given by Equation (2-54).

Assuming that the direction of the z axis coincides with the C-Cl internuclear line allows the determination of the angle θ_z from the structure, and the parameters computed on this basis are listed in Table XV in the column headed I. Assuming that a principal axis of the tensor lies along the C-Cl bond apparently leads to a non-cylindrical charge distribution about the bond.

If it is assumed that the tensor represents a cylindrical charge distribution, then θ_z and χ_{zz} are determined from Equation (2-57), giving the parameters in the column labeled II in Table XV. The angle θ_z is now 27°, one degree larger than the value determined from the structure. The assumption of a cylindrical charge distribution apparently leads to an angle of 1° between the C-Cl internuclear line and the principal axis of the quadrupole tensor.

Table XIV. Comparison of Ethyl Chloride with Similar Molecules.

Molecule	CC Distance	CCX Angle	CCl Distance
CH_3CH_2Cl[a]	1.520 A	$111^{o}2'$	1.788 A
$CH_3CH_2CH_3$[b]	1.526	$112^{o}24'$	
CH_3CH_2F[c]	1.533	$109^{o}27'$	
CH_3Cl[d]			1.781

[a] This thesis

[b] Reference 51

[c] Reference 55

[d] Reference 56

Table XV. Quadrupole Coupling Constants for Ethyl Chloride.

Isotope	Principal Axes eQq_m (Mc)	η
$CH_3CH_2Cl^{35}$	-49.20 ± 0.10	0.4479 ± 0.0034
$C^{13}H_3CH_2Cl^{35}$	-48.48	0.4641
$CH_3C^{13}H_2Cl^{35}$	-49.51	0.4224
$CH_3CD_2Cl^{35}$	-51.07	0.3957
$CH_2DCH_2Cl^{35}$(t)	-49.32	0.4428
$CH_2DCH_2Cl^{35}$(g)	-47.36	0.5053
$CH_3CH_2Cl^{37}$	-38.65	0.4204
	CCl Bond Axes	
	I[a]	II[b]
χ_{zz}	-68.80 ± 0.15 Mc	-71.24 ± 0.19 Mc
η_{bond}[c]	0.035 ± 0.003	0
θ_z	26°0'	27°0' ± 5'
I	22%	20%

[a] Assuming z axis and C-Cl internuclear line to coincide.

[b] Assuming a cyclindrical charge distribution.

[c] $\eta_{bond} = (\chi_{xx} - \chi_{yy})/\chi_{zz}$

The value of the angle θ_z was also determined from an evaluation of χ_{ab}, the non-zero off-diagonal element in the tensor in the a, b, c axis system. Using data for $CH_3CH_2Cl^{35}$ and $CH_3CD_2Cl^{35}$ and Equation (2-59) the angle θ_z is calculated to be $27^\circ \pm 2^\circ$. Unfortunately the uncertainty is large enough to include both of the previous assumptions.

It is clear that the electrostatic potential in the neighborhood of the chlorine nucleus is approximately cylindrically symmetric in the direction of the C-Cl internuclear line. However, a small amount of asymmetry, or a slightly "bent" bond, or some combination of the two, cannot be ruled out by the present rotational spectra.

The magnitude of the quadrupole coupling constant in the bond direction has been shown (35, 59, 60, 61) to be related to the ionic character of the carbon-chlorine bond by means of Equation (2-60). Assuming $s^2 = 0.15$ and d^2 and II to be negligible the ionicity of the carbon-chlorine bond in ethyl chloride is found to be 20-22% depending upon whether assumption I or II is used as shown in Table XV. This may be compared with 20.8% ionic character in the CCl bond in methyl chloride (35).

4.7 Barrier to Internal Rotation

Lide (46) has determined the height of the potential barrier hindering internal rotation in ethyl chloride by analysis of the fine structure of the $2_{20} \rightarrow 3_{21}$ and $2_{21} \rightarrow 3_{22}$ transitions in the first excited torsional state. The computations required the moment of inertia of the methyl group (I_a) and the angle between the a axis and the CC bond (θ_m). For this purpose the structural parameters of Wagner and Dailey (44) were used. The barrier height has been recomputed using the structure proposed above.

The calculations have been performed using Herschbach's (39) formulation of the theory developed by Wilson and his co-workers (62),

discussed in section 2.5. In this formulation the quantity δ_k referred to by Lide is given to high approximation for ethyl chloride by

$$\delta_k = FaKW_{1E}^{(1)} + Fa^3K^3W_{1E}^{(3)} . \qquad (4\text{-}12)$$

The numerical values of all the parameters needed in the calculation are given in Table XVI.

The barrier height computed using the present structure is 3685 cal/mole. This may be compared to the value 3560 cal/mole given previously (46). The principal reason for the difference is the much smaller moment of inertia of the methyl group used here (3.16 amu A^2 vs. 3.28 amu A^2). It should be pointed out that this value is still subject to revision due to possible differences between the ground state structure used here and the structure in the first excited torsional state for which the barrier dependent frequency differences were recorded.

Table XVI. Internal Rotation in Ethyl Chloride.

δ_k	$= 6.35 \pm 0.20$ Mc[a]
θ_m	$= 42^{\circ}58'$
I_a	$= 3.1613$ amu A^2
r	$= 1 - (I_a \cos^2\theta_m/I_a) - (I_a \sin^2\theta_m/I_b) = 0.87913$
F	$= \hbar^2/2rI = 181.9$ kMc
s	$= 4V_3/9F = 94.43$
V_3	$= 3685 \pm 12$ cal/mole

[a] Reference 46.

V. MOLECULAR STRUCTURE OF CHLOROMETHYLSILANE

5.1 Introduction

The determination of the structures of derivatives of silane and methyl silane has afforded the opportunity for many interesting comparisons with derivatives of methane and ethane. The work reported in this thesis allows direct comparison of one case, ethyl chloride and chloromethylsilane, while further comparisons may be drawn from previously reported work. The work reported here on chloromethylsilane is believed to be the first determination of the molecular structure of a derivative of methylsilane containing halogen substitution in the methyl group.

The assignments of rotational transitions in the species $CH_2Cl^{35}SiH_3$, $CH_2Cl^{37}SiH_3$, $CH_2Cl^{35}SiD_3$, $CD_2Cl^{35}SiH_3$, and $CHDCl^{35}SiH_3$ were made at Harvard University by Dr. R. H. Schwendeman while the assignments for $C^{13}H_2Cl^{35}SiH_3$ and $CH_2Cl^{35}Si^{29}H_3$ were made at Michigan State University by the author. The determination of the structure and the internal rotation analysis was also carried out at Michigan State University.

5.2 Preparation of Samples

The following isotopic species were used in the microwave study of chloromethylsilane

$CH_2Cl^{35}SiH_3$	ground and 1^{st} excited torsional states
$CH_2Cl^{37}SiH_3$	ground state
$CH_2Cl^{35}SiD_3$	ground and 1^{st} excited torsional states
$CD_2Cl^{35}SiH_3$	ground and 1^{st} excited torsional states
$CHDCl^{35}SiH_3$	ground state
$C^{13}H_2Cl^{35}SiH_3$	ground state
$CH_2Cl^{35}Si^{29}H_3$	ground state.

The initial sample of CH_2ClSiH_3 was a gift from Dr. Herbert Kaesz. The preparation of the various isotopic species of chloromethylsilane followed for the most part procedures which are available in the literature. The deuterated samples were prepared at Harvard University by Dr. Schwendeman while the C-13 sample was synthesized in this laboratory. The $CH_2Cl^{37}SiH_3$ and $CH_2Cl^{35}Si^{29}H_3$ species were observed in natural abundance (24.6% and 4.68% respectively).

$C^{13}H_3ClSiH_3$

The equations representing the synthesis are

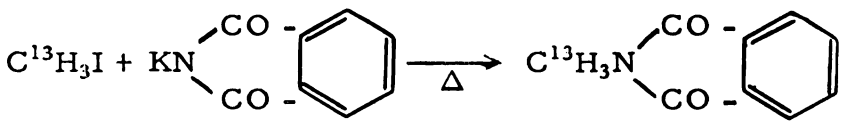

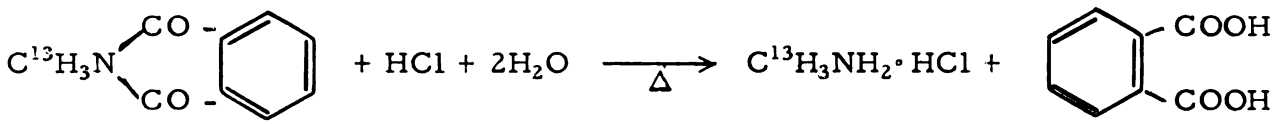

$$C^{13}H_3NH_2 \cdot HCl + H_2NCONH_2 \longrightarrow C^{13}H_3NHCONH_2 + NH_4Cl$$

$$C^{13}H_3NHCONH_2 + NaNO_2 \longrightarrow C^{13}H_3N(NO)CONH_2 + NaOH$$

$$C^{13}H_3N(NO)CONH_2 + KOH \xrightarrow{\text{ether}} C^{13}H_2N_2 + KCNO + 2H_2O$$

$$C^{13}H_2N_2 + SiCl_4 \xrightarrow[\text{powder}]{Cu} C^{13}H_2ClSiCl_3 + N_2$$

$$4C^{13}H_2ClSiCl_3 + 3LiAlH_4 \longrightarrow 4C^{13}H_2ClSiH_3 + 3LiCl + 3AlCl_3$$

The method of Cox and Warne (63) was used directly in the synthesis of N-Methyl-C^{13}-phthalimide. Dry methyl-C^{13}-iodide was vacuum distilled with liquid air cooling into the side arm of a flask which contained potassium phthalimide previously dried by heating under vacuum. The flask was sealed off, then heated at 180°C until no liquid remained in the side arm, which was maintained at room

temperature. The product sublimed to the neck of the flask and was washed out with chloroform after completion of the reaction.

The N-Methyl-C^{13}-phthalimide was refluxed gently for several hours with constant-boiling hydrochloric acid followed by liberation of the methyl-C^{13}-amine with sodium hydroxide in the standard Kjeldahl procedure. The product was trapped in standardized hydrochloric acid.

The method of Arndt (64) was used in the preparation of N-Nitroso-methyl-C^{13}-urea. The methyl-C^{13}-amine hydrochloride was refluxed with urea for several hours followed by the addition of sodium nitrite. This solution was added slowly to a mixture of ice and sulfuric acid cooled in an ice-salt bath. The N-Nitrosomethyl-C^{13}-urea rises to the top as a crystalline foamy precipitate which is filtered, washed with ice water and dried.

Diazomethane-C^{13} was prepared by adding the N-Nitrosomethyl-C^{13}-urea to a mixture of 40% KOH and ether. The deep yellow etheral solution of diazomethane was dried over potassium hydroxide pellets (65).

The solution of diazomethane-C^{13} in diethyl ether was added at -78°C to an ether solution of silicon tetrachloride in the presence of a small amount of copper powder to yield chloromethyl-C^{13}-trichloro-silane (66).

The final step in the synthesis was the reduction of the chloro-methyl-C^{13}-trichlorosilane with a diethylene glycol diethyl ether solution of lithium aluminum hydride to give the desired product, chloromethyl-C^{13}-silane.

$\underline{CH_2ClSiD_3}$

The synthesis follows exactly that of the C-13 sample up to the final step where lithium aluminum deuteride is substituted for the hydride in the reduction of the trichlorosilane compound.

CD_2ClSiH_3 and $CDHClSiH_3$

The preparation was again very similar to that described for the C-13 compound. The difference lies in the use of CD_2N_2 for the preparation of the chloromethyl trichlorosilane. The CD_2N_2 was prepared by converting CD_3COOD to CD_3CONH_2 (67) and then to CD_3NH_2 (68). The deuterated methylamine was then used to prepare deuterated N-Nitrosomethylurea from which the CD_2N_2 was generated with base as described previously. The sample of CD_2ClSiH_3 was found to contain enough $CHDClSiH_3$ to allow its spectrum to be recorded also.

The spectrometers used were both conventional Hughes-Wilson type using 100 kc Stark modulation. The spectrometer used at Michigan State University has been described previously (Chapter III). At Harvard the frequencies of the absorption lines were measured by comparison with the harmonics of a crystal-controlled oscillator operating at 5 Mc which was compared with the 5 Mc carrier of radio station WWV. Since oscilloscope display with a unidirectional sweep circuit was used in all the work at Harvard, the absolute precision in frequency is probably not greater than $\pm$ 0.2 Mc. However, for most of the multiplets the frequency separations should be accurate to $\pm$ 0.05 Mc. Frequency measurements of transitions in the C-13 and Si-29 species, which were studied at Michigan State University, are believed accurate to $\pm$ 0.1 Mc in all cases and $\pm$ 0.05 Mc in favorable cases. The rotational transitions of the C-13 species were measured for the most part using the oscilloscope with bidirectional sweep circuit and are believed accurate to $\pm$ 0.05 Mc in most cases. The Si-29 transitions were measured from a recorder trace using frequency markers every 1 Mc and are probably only accurate to $\pm$ 0.1 Mc.

The spectra were all observed with the sample cell cooled with Dry Ice. Since chloromethylsilane slowly decomposed in the sample cell, occasional changes of sample were necessary.

5.3 Microwave Spectra

Figure 11 is a projection of chloromethylsilane in the plane of symmetry (the ab plane). The molecule is a near prolate symmetric top with the asymmetry parameter κ varying from approximately -0.95 to -0.97 for the various species ($b_p \sim -0.007$). Both a-type and b-type transitions were observed.

Most of the observed lines were of two general classes: the R-branch parallel transitions with $K_{-1} = 0$ or 1; and the Q-branch perpendicular transitions with K_{-1} changing from 0 to 1. The multiplet structure of the parallel transitions was either unresolved or only partially resolved, while under favorable conditions the perpendicular transitions consisted of two pairs of clearly resolved lines, the members of each pair being separated by 0.8 to 1.7 Mc, the centers of gravity of the pairs having a separation of approximately 5 Mc. The measured hyperfine component frequencies of the C-13 and Si-29 species are shown in Table XVII. The hypothetical unsplit frequencies of the species measured at Harvard University as well as the C-13 and Si-29 species measured at Michigan State University are shown in Tables XVIII and XIX.

Rough values of the rotational constants were determined by fitting the hypothetical unsplit frequencies of the observed transitions with lowest J to the rigid rotator expression for the energy levels. Since all the species are near symmetric prolate tops the combinations of rotational constants which prove most convenient as fitting parameters are $\frac{1}{2}(B+C)$, $\frac{1}{2}(C-B)$, and $(A - \frac{B+C}{2})$. If the frequencies of the remaining transitions for a given species were computed using the fitting parameters selected for the lowest J transitions, small discrepancies outside of experimental error appeared between the calculated and observed frequencies. In particular the value of $\frac{1}{2}(B+C)$ required to fit the $J = 3 \rightarrow 4$ a-type transitions was somewhat different from that required to fit the

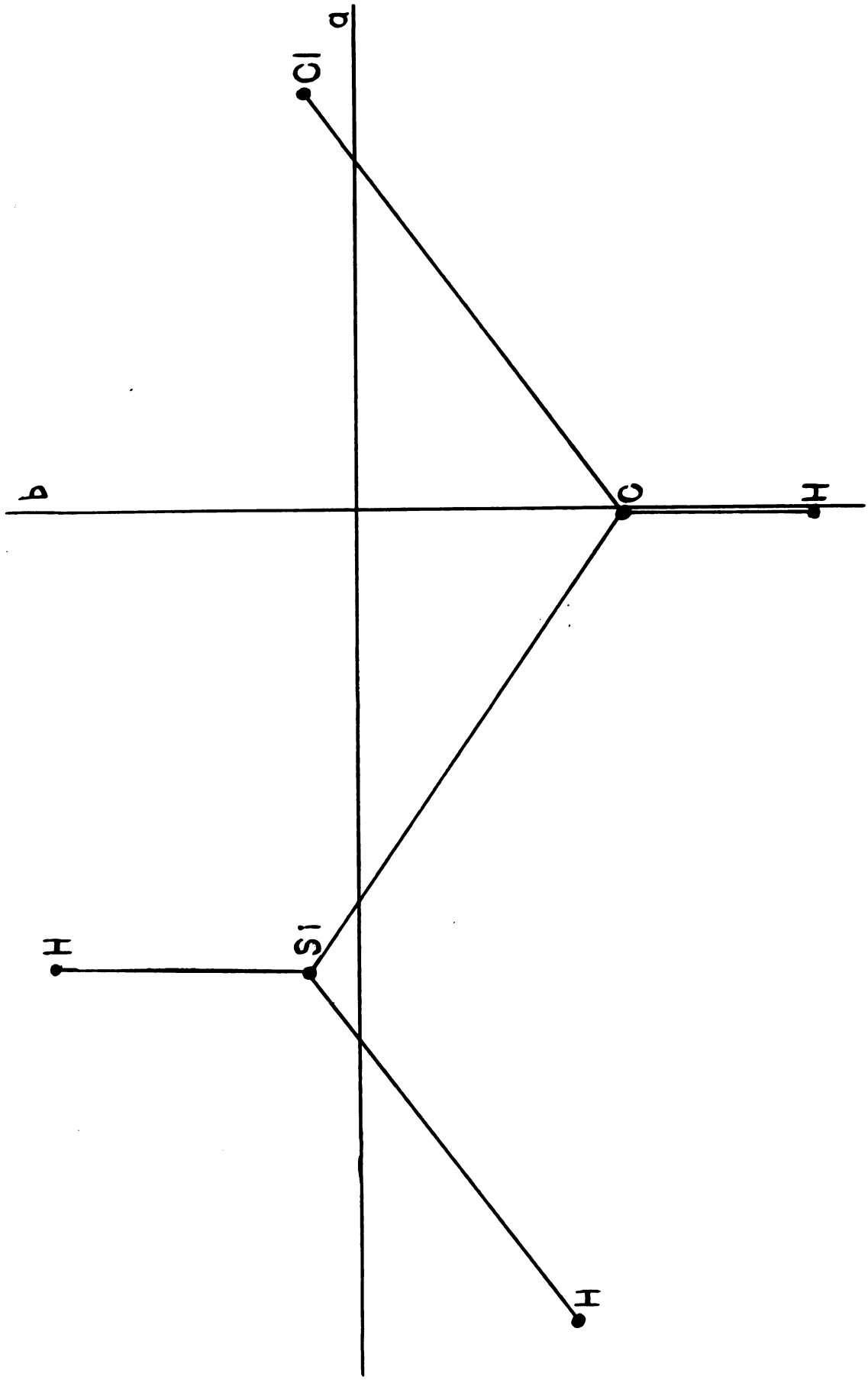

Figure 11. A Projection of Chloromethylsilane in its Plane of Symmetry Showing the Location of the a and b Principal Axes. The c Axis is Perpendicular to the Page.

Table XVII. Frequencies (Mc) of Hyperfine Components in $C^{13}H_2Cl^{35}SiH_3$ and $CH_2Cl^{35}Si^{29}H_3$.

	$C^{13}H_2Cl^{35}SiH_3$	$CH_2Cl^{35}Si^{29}H_3$
$3_{12} \rightarrow 4_{13}$		
$\frac{9}{2} \rightarrow \frac{11}{2}$; $\frac{3}{2} \rightarrow \frac{5}{2}$	25069.3	24718.0
$\frac{7}{2} \rightarrow \frac{9}{2}$; $\frac{5}{2} \rightarrow \frac{7}{2}$	25068.4	
$3_{03} \rightarrow 4_{04}$		
unresolved	24485.55	24179.0
$3_{13} \rightarrow 4_{14}$		
$\frac{9}{2} \rightarrow \frac{11}{2}$; $\frac{7}{2} \rightarrow \frac{9}{2}$	23953.9	
$\frac{5}{2} \rightarrow \frac{7}{2}$; $\frac{3}{2} \rightarrow \frac{5}{2}$	23953.1	
$4_{13} \rightarrow 5_{14}$		
$\frac{11}{2} \rightarrow \frac{13}{2}$; $\frac{5}{2} \rightarrow \frac{7}{2}$	31330.68	30892.78
$\frac{9}{2} \rightarrow \frac{11}{2}$; $\frac{7}{2} \rightarrow \frac{9}{2}$	31329.88	
$4_{04} \rightarrow 5_{05}$		
unresolved	30582.3	30203.92
$4_{14} \rightarrow 5_{15}$		
$\frac{11}{2} \rightarrow \frac{13}{2}$; $\frac{9}{2} \rightarrow \frac{11}{2}$	29936.2	29599.25
$\frac{7}{2} \rightarrow \frac{9}{2}$; $\frac{5}{2} \rightarrow \frac{7}{2}$	29935.7	
$5_{15} \rightarrow 6_{06}$		
$\frac{11}{2} \rightarrow \frac{13}{2}$	20648.29	
$\frac{9}{2} \rightarrow \frac{11}{2}$	20646.97	
$\frac{13}{2} \rightarrow \frac{15}{2}$	20644.81	
$\frac{7}{2} \rightarrow \frac{9}{2}$	20643.52	
$6_{16} \rightarrow 7_{07}$		
$\frac{13}{2} \rightarrow \frac{15}{2}$		26079.28
$\frac{11}{2} \rightarrow \frac{13}{2}$		26078.28
$\frac{15}{2} \rightarrow \frac{17}{2}$		26076.00
$\frac{9}{2} \rightarrow \frac{11}{2}$		26075.08
$8_{08} \rightarrow 8_{17}$		
$\frac{17}{2} \rightarrow \frac{17}{2}$	23549.7	23782.8
$\frac{15}{2} \rightarrow \frac{15}{2}$		
$\frac{19}{2} \rightarrow \frac{19}{2}$	23543.7	23776.2
$\frac{13}{2} \rightarrow \frac{13}{2}$	23542.4	
$9_{09} \rightarrow 9_{18}$		
$\frac{19}{2} \rightarrow \frac{19}{2}$	25084.85	25187.9
$\frac{17}{2} \rightarrow \frac{17}{2}$	25083.90	25187.0
$\frac{21}{2} \rightarrow \frac{21}{2}$	25078.50	25181.6
$\frac{15}{2} \rightarrow \frac{15}{2}$	25077.48	25180.8

continued

Table XVII -- Continued

	$C^{13}H_2Cl^{35}SiH_3$	$CH_2Cl^{35}Si^{29}H_3$
$10_{0,10} \rightarrow 10_{19}$		
$\frac{21}{2} \rightarrow \frac{21}{2}$	26856.0	26798.7
$\frac{19}{2} \rightarrow \frac{19}{2}$	26855.1	26797.7
$\frac{23}{2} \rightarrow \frac{23}{2}$	26849.4	26791.7
$\frac{17}{2} \rightarrow \frac{17}{2}$	26848.5	26790.7
$11_{0,11} \rightarrow 11_{1,10}$		
$\frac{23}{2} \rightarrow \frac{23}{2}$	28877.90	28633.52
$\frac{21}{2} \rightarrow \frac{21}{2}$	28877.25	
$\frac{25}{2} \rightarrow \frac{25}{2}$	28871.18	28626.79
$\frac{19}{2} \rightarrow \frac{19}{2}$	28870.45	

Table XVIII. Hypothetical Unsplit Frequencies (Mc)[a] of Observed Transitions in Ground State Species of Chloromethylsilane.

	$CH_2Cl^{35}SiH_3$	$CH_2Cl^{37}SiH_3$	$C^{13}H_2Cl^{35}SiH_3$	$CH_2ClSi^{29}H_3$	$CD_2Cl^{35}SiH_3$	$CHDCl^{35}SiH_3$	$CH_2Cl^{35}SiD_3$
$3_{03}-4_{04}$	24539.45	23955.17		24179.60	24095.95	24316.27	22508.38
$3_{13}-4_{14}$	24030.18	23466.80	23953.63		23519.83		22091.50
$3_{12}-4_{13}$	25093.48	24485.10	25068.86	24718.01	24752.39		22964.29
$4_{04}-5_{05}$	30652.24	29923.80	30582.35	30203.97			28116.99
$4_{14}-5_{15}$	30032.34		29936.02	29599.32	29389.32	29696.89	27609.21
$4_{13}-5_{14}$	31360.87	30601.08	31330.29	30892.79	30930.22	31156.99	28700.44
$5_{05}-5_{14}$	20761.87					18508.34	
$6_{06}-6_{15}$	21634.98	21511.17				19490.20	
$7_{07}-7_{16}$	22684.78	22511.60			19057.54		18011.15
$8_{08}-8_{17}$	23924.41	23692.14	23546.17	23779.57	20593.01	22089.27	19034.52
$9_{09}-9_{18}$	25368.30		25081.23	25184.38	22399.13	23742.34	20228.29
$10_{0,10}-10_{1,9}$	27031.04	26645.25	26852.29	26794.74	24495.28		21604.26
$11_{0,11}-11_{1,10}$	28927.25	28445.64	28874.24	28630.20			
$12_{0,12}-12_{1,11}$	31070.41				29613.69		

[a] Uncertainty estimated to be ± 0.2 Mc.

Table XIX. Hypothetical Unsplit Frequencies (Mc)[a] of Observed Transitions in First Excited Torsional State Species of Chloromethylsilane.

Transition	$CH_2Cl^{35}SiH_3$	$CH_2Cl^{35}SiD_3$	$CD_2Cl^{35}SiH_3$
$3_{03}-4_{04}$		22435.80	23992.05
$3_{13}-4_{14}$			23429.48
$3_{12}-4_{13}$			24631.06
$4_{04}-5_{05}$	30517.53	28028.14	29954.65
$4_{14}-5_{15}$	29915.57	27534.57	29277.72
$4_{13}-5_{14}$	31203.74	28592.69	30779.07
$7_{07}-7_{16}$	22477.10		
$8_{08}-8_{17}$	23674.57		20397.79
$9_{09}-9_{18}$		20003.13	
$10_{0,10}-10_{1,9}$	26672.38	21330.46	
$11_{0,11}-11_{1,10}$	28501.29	22844.72	
$12_{0,12}-12_{1,11}$			29142.97

[a] Uncertainty estimated to be ± 0.2 Mc.

$J = 4 \rightarrow 5$ transitions. In addition a term in $J^2 (J + 1)^2$ was required to fit the Q-branch b-type transitions. Examination of the expressions given by Polo (69) for the first order approximation to the energy of a non-rigid near symmetric rotator showed that contributions from the centrifugal distortion constants D_J and δ_J[1] would remove the discrepancies. It was found that the values

$$D_J = 4\text{kc and } \delta_J = 0.5 \text{ kc}$$

could be used for all the ground state species. The first excited torsional state species were fit separately using the values

$$D_J = 3\text{kc and } \delta_J = 0.4 \text{ kc}.$$

The rotational constants in Tables XX and XXI were obtained from the hypothetical unsplit frequencies after the above centrifugal distortion corrections were applied.

5.4 Molecular Structure

The moments of inertia of a sufficient variety of isotopic species are available to use the substitution method of Kraitchman (9) to determine the coordinates of every atom in the molecule except the silicon hydrogen atoms. Table XXII lists the values of the second moments for all the isotopic species. The last column of Table XXII provides a comparison of the values of P_{cc}, which should be unaltered for substitution of an atom in the plane of symmetry of a rigid molecule. The coordinates of the chlorine, silicon, and carbon atoms listed in

---

[1]For an asymmetric rotator such as chloromethylsilane a first order treatment shows that the centrifugal distortion correction to the rigid rotator energy is a function of six constants, the D_J, D_{JK}, and D_K mentioned previously (section 2.3) and δ_J, R_5 and R_6. A qualitative description of the nature of these constants is reasonable for only the simplest molecules; consequently they are ordinarily treated as adjustable parameters and varied to fit the discrepancies between the experimental frequencies and those calculated using the rigid rotator expressions for the energy.

Table XX. Rotational Constants (Mc) and Moments of Inertia (amu A^2)[a] for Ground State Species of Chloromethylsilane.

	A	B	C	I_a	I_b	I_c
$CH_2Cl^{35}SiH_3$	21759.21	3204.08	2938.09	23.2330	157.7772	172.0612
$CH_2Cl^{37}SiH_3$	21692.92	3125.14	2870.40	23.3040	161.7625	176.1187
$C^{13}H_2Cl^{35}SiH_3$	21080.42	3204.37	2925.47	23.9811	157.7630	172.8033
$CH_2Cl^{35}Si^{29}H_3$	21726.82	3155.41	2896.53	23.2676	160.2109	174.5299
$CD_2Cl^{35}SiH_3$	17282.73	3172.57	2864.21	29.2506	159.3445	176.4996
$CHDCl^{35}SiH_3$	19250.99	3190.78	2898.44	26.2600	158.4349	174.4149
$CH_2Cl^{35}SiD_3$	17536.11	2925.97	2707.51	28.8280	172.7738	186.7144

[a] Conversion factor used: 5.05531×10^5 Mc-amu A^2

Table XXI. Rotational Constants (Mc) and Moments of Inertia (amu A^2)[a] for First Excited Torsional State Species of Chloromethylsilane.

	$CH_2Cl^{35}SiH_3$	$CH_2Cl^{35}SiD_3$	$CD_2Cl^{35}SiH_3$
A	21666.99	17484.26	17253.46
B	3186.19	2913.42	3155.30
C	2928.36	2701.62	2854.83
I_a	23.3319	28.9135	29.3003
I_b	158.6632	173.5181	160.2165
I_c	172.6328	187.1214	177.0792

[a] Conversion factor used: 5.05531×10^5 Mc-amu A^2

Table XXII. Second Moments (amu A^2)[(a)] for Ground State Species of Chloromethylsilane.

	P_{aa}	P_{bb}	P_{cc}
$CH_2Cl^{35}SiH_3$	153.3027	18.7585	4.4745
$CH_2Cl^{37}SiH_3$	157.2886	18.8301	4.4739
$C^{13}H_2Cl^{35}SiH_3$	153.2926	19.5107	4.4704
$CH_2Cl^{35}Si^{29}H_3$	155.7366	18.7933	4.4743
$CD_2Cl^{35}SiH_3$	153.2968	23.2028	6.0478
$CHDCl^{35}SiH_3$	153.2949	21.1200	5.1400
$CH_2Cl^{35}SiD_3$	165.3301	21.3843	7.4437

[(a)] Computed using Equation (2-17) and the moments of inertia given in Table XX.

Table XXIII are averages of the coordinates obtained using the three possible combinations of two moments of inertia or all three moments of inertia in the Kraitchman equations (previously discussed in section 4.4). The determination of the a coordinate of the carbon atom consistently gave imaginary results which characteristically occurs when an atom lies very close to an axis. This effect is apparently due to the difference in the intramolecular motion in the parent and C-13 substituted molecules. The a coordinate of the carbon atom was therefore set equal to zero in Table XXIII.

The b coordinate of the methylene hydrogen atoms was determined in two ways. Equations (2-14) were used for $CHDCl^{35}SiH_3$ as the substituted molecule or alternatively the moments of inertia of $CD_2Cl^{35}SiH_3$ were used with Equation (2-15). The two procedures give essentially the same results for the b coordinates of the hydrogen atoms. Imaginary results were again obtained for the a coordinates and consequently these were set equal to zero in Table XXIII. The out-of-plane coordinates of the hydrogen atoms were obtained using Equation (2-16). An essentially equivalent value for the out-of-plane coordinates of the methylene hydrogen atoms was obtained from the Kraitchman expression (Equation 2-14) for $|c_i|$ using $CHDCl^{35}SiH_3$ as the substituted molecule.

The in-plane coordinates of the silicon hydrogen atoms were determined by assuming the Si-C line to be the symmetry axis of the silyl group, assuming the H-H distance to be that given by twice the c (out-of-plane) coordinate of either atom, and fitting the difference in moments of inertia of $CH_2Cl^{35}SiD_3$ and $CH_2Cl^{35}SiH_3$.

The bond distances and bond angles obtained from the coordinates in Table XXIII are shown as Structure I in Table XXIV.

When atoms lie too close to an axis to give meaningful values of the coordinates using Kraitchman's equations, it is customary to try to obtain better values of the coordinates by using the requirement that

Table XXIII. Coordinates of the Atoms (A) in the Principal Axis System of $CH_2Cl^{35}SiH_3$.

Atom	a	b	c
Cl	1.4297	0.1943	0
Si	-1.5697	0.1893	0
C	0	-0.8705	0
H(C)	0	-1.5191	±0.8840
H(Si, in plane)	-2.7377	-0.7141	0
H(Si, out of plane)	-1.5607	1.0292	±1.2144

$\Sigma m_i a_i = 0.1742$ amu A

$\Sigma m_i b_i = 0.0645$ amu A

$\Sigma m_i a_i b_i = 0.1340$ amu A^2

Table XXIV. Bond Distances (A) and Bond Angles (degrees) in Chloromethylsilane.

	Structure I[a]	Structure II[b]	"Best" Structure[c]
SiC	1.894	1.884	1.889 ± 0.01
CCl	1.783	1.793	1.788 ± 0.01
CH	1.096	1.096	1.096 ± 0.01
SiH	1.477	1.477	1.477 ± 0.005
SiCCl	109.3	109.3	109.3 ± 0.3
HSiH	110.6	110.6	110.6 ± 0.5
HCH	107.5	107.5	107.5 ± 0.5
SiCH	109.3	109.4	109.3 ± 0.5

[a] Assuming a coordinate of C atom and two methylene H atoms to be zero.

[b] Assuming a coordinate of C atom and two methylene H atoms to be such that $\Sigma m_i a_i = 0$.

[c] Average of structure I and structure II.

the first moments and in-plane product of inertia must vanish. Unfortunately here the a coordinates of both the carbon atom and the methylene hydrogen atoms need to be improved. Moreover the b coordinates of the chlorine and silicon atoms are not very large. Consequently the product of inertia was not used but instead the entire CH_2 triangle was moved enough to reduce the value of $\Sigma m_i a_i$ in Table XXIII to zero. The result of this computation gives the bond distance and bond angles shown as Structure II in Table XXIV.

The principal differences between the two structures given in Table XXIV are the values for the C-Si and C-Cl distances. The SiCCl angle is the same in the two structures and of course the hydrogen parameters are virtually unaffected. The "best" structure in Table XXIV is simply the average of structures I and II. The uncertainties given are an estimate of the combined effect of inconsistencies in the substitution method and the inaccurate location of the near axis atoms. No contribution to the uncertainties has been included for possible differences between substitution parameters and equilibrium values.

5.5 Quadrupole Hyperfine Structure

Analysis of the hyperfine splitting of the Q-branch transitions of $CH_2Cl^{35}SiH_3$ yielded the diagonal values of the quadrupole coupling constant tensor in the principal moment of inertia axis system. The splittings in the R-branch lines were too small to be resolved clearly and consequently were not used. The splittings in the Q-branch transitions are not greatly dependent on $\chi_{aa} = eQ \frac{\partial^2 V}{\partial a^2}$ and consequently the analysis was carried out only for the parent species where a large number of carefully measured Q-branch frequencies were available.

Since the Q-branch multiplets consist of two pairs of closely spaced lines, a single experimental quantity was obtained for each

transition by differencing the average frequency of each pair. If we represent this difference by $\Delta\nu$ we have:

$$\Delta\nu = c_1 \chi_{aa} + c_2 (\chi_{bb} - \chi_{cc}) \qquad (5\text{-}1)$$

where c_1 and c_2 are quantities which depend only on the degree of asymmetry of the molecule and the transition in question. The relevant data for the Q-branch multiplets of $CH_2Cl^{35}SiH_3$ are given in Table XXV. The values of χ_{aa} and $(\chi_{bb} - \chi_{cc})$ were obtained by least squares and also from the slope and intercept respectively of a plot of $\Delta\nu/c_1$ vs. c_1/c_2. The values of $eQq_m = \chi_{aa}$ and $\eta = (\chi_{bb} - \chi_{cc})/\chi_{aa}$ are given in Table XXVI.

The individual coupling constants may be obtained from the parameters chosen and the additional requirement that the sum of the coupling constants is equal to zero. The coupling constants so obtained are the diagonal values of the quadrupole tensor in the principal inertial axis system. No off-diagonal elements are obtained but if an assumption is made concerning the principal axis system of the quadrupole coupling tensor, the diagonal coupling constants may be obtained in this system.

Assuming that the CCl bond direction is a principal axis of the coupling constant tensor allows the determination of θ_z (angle between a and z axes) from the structure. The values of χ_{zz} and $\eta = (\chi_{xx} - \chi_{yy})/\chi_{zz}$ are then computed from Equations (2-55) and appear in the column headed I in Table XXVI (the x axis is perpendicular to the z axis in the plane of symmetry). Assuming that the quadrupole coupling constant tensor is oriented in the direction of the CCl bond requires that the electrostatic potential in the neighborhood of the chlorine nucleus be slightly elliptical about the C-Cl bond.

Alternatively it may be assumed that the coupling constant tensor is cylindrical in which case Equation (2-56) is used to compute the results shown in the column headed II in Table XXVI. It may be seen

Table XXV. Frequencies of Hyperfine Components (Mc)[(a)] in $CH_2Cl^{35}SiH_3$.

Transition	F → F' $J+\frac{3}{2} \rightarrow J+\frac{3}{2}$	$J+\frac{1}{2} \rightarrow J+\frac{1}{2}$	$J-\frac{1}{2} \rightarrow J-\frac{1}{2}$	$J-\frac{3}{2} \rightarrow J-\frac{3}{2}$	Δν(exp)	Δν(calc)
$5_{05} - 5_{14}$	20759.47	20765.66	20763.92	20757.70	6.205	6.201
$6_{06} - 6_{15}$	21632.81	21638.88	21637.41	21631.36	6.060	6.057
$7_{07} - 7_{16}$	22682.47	22688.51	22687.29	22681.16	6.085	6.087
$8_{08} - 8_{17}$	23921.78	23927.90	23926.95	23920.73	6.170	6.184
$9_{09} - 9_{18}$	25365.55	25371.91	25370.91	25364.62	6.325	6.327
$10_{0,10} - 10_{1,9}$	27028.20	27034.75	27033.77	27027.28	6.520	6.501
$11_{0,11} - 11_{1,10}$	28924.30	28931.01	28930.08	28923.43	6.680	6.695
$12_{0,12} - 12_{1,11}$	31067.32	31074.25	31073.42	31066.54	6.905	6.898

(a) Absolute uncertainty estimated to be ± 0.2 Mc.
Uncertainty in Δν estimated to be ± 0.02 Mc.

Table XXVI. Quadrupole Coupling Constants in $CH_2Cl^{35}SiH_3$.

Principal Axes

$eQq_m = -32.51 \pm 0.56$ Mc $\quad\quad \eta = 1.215 \pm 0.021$

Bond Axes

	I[a]	II[b]
χ_{zz}	-68.7 ± 1.6 Mc	-72.0 ± 0.6 Mc
θ_z	36.7°	37.2 ± 0.2°
η_z[c]	0.048 ± 0.016	0
$I + s^2 - d^2$	0.37	0.34
I	0.22	0.19

[a] Assuming θ_z from structure I.

[b] Assuming $\chi_{xx} = \chi_{yy} = \chi_{cc}$.

[c] $\eta_z = (\chi_{xx} - \chi_{yy})/\chi_{zz}$.

that the two values of θ_z in the table differ by 0.5° which is greater than the uncertainty in this angle as determined from the structure.

Using the values of the coupling constants obtained for $CH_2Cl^{35}SiH_3$, the known relation between the Cl-35 and Cl-37 coupling constants (70), and the relative orientations of the principal axes of the various species computed from the structure, it is found that the multiplet splittings of all the species can be predicted within experimental error.

Applying the interpretation of quadrupole coupling constants of terminally bonded atoms by Townes and Dailey (59, 60), the ionicity I of the C-Cl bond is approximately 19-22% depending upon which assumption is used to compute χ_{zz} in Equation (2-60). For this calculation it was assumed that $s^2 = 0.15$ and that d^2 and II are negligible.

5.6 Barrier to Internal Rotation

Rotational transitions in the first excited torsional state of $CH_2Cl^{35}SiH_3$, $CD_2Cl^{35}SiH_3$, and $CH_2Cl^{35}SiD_3$ have been observed and rotational constants assigned (Tables XIX and XXI). Four of the observed transitions in the parent compound show fine structure in addition to that due to quadrupole coupling. These splittings, which are due to internal rotation, have been analyzed according to the method developed by Wilson and his co-workers (62) using the formulation of Herschbach (39). The analysis of these internal rotation splittings was presented in the theory section (2.5). Table XXVII lists the frequencies ν_A, the frequency difference $\nu_A - \nu_E$, and the calculated values of V_3 for the four transitions in $CH_2Cl^{35}SiH_3$. Two sets of numbers are given for two of the transitions and are the result of the partially resolved hyperfine structure due to quadrupole coupling. The interaction between internal rotation and the quadrupole coupling is negligible in this case.

It is also possible to use the average value of V_3 to compute the splittings $\nu_A - \nu_E$. The results of this calculation are given in the

Table XXVII. Internal Rotation in Chloromethylsilane.

Transition	ν_{1A}	$(\nu_{1E}-\nu_{1A})$exp	$(\nu_{1E}-\nu_{1A})$calc	V_3
$10_{2,9}-9_{3,6}$	32235.62 Mc	1.20 Mc	1.21 Mc	2.55 kcal/
	32233.43	1.22		mole
$10_{2,8}-9_{3,7}$	30914.77	0.75	0.86	2.59
$11_{2,10}-10_{3,7}$	26284.7	1.1	1.13	2.53
	26282.6	1.3		
$11_{2,9}-10_{3,8}$	24383.97	0.96	0.94	2.54

I_a = 5.957 amu A^2

θ_m = $34^o2'$

r = $1 - (\cos^2\theta_m I_a/I_a) - (\sin^2\theta_m I_a/I_b) = 0.8129$

F = $\hbar^2/2rI_a$ = 104.4 kMc

Average s = 113.7

$V_3 = 9Fs/4 = 2.55 \pm 0.05$ kcal/mole

next to the last column of Table XXVII. The calculations in Table XXVII required values of the perturbation coefficients at an s value which is higher than that tabulated by Herschbach (39). In order to obtain these values the entries for $72 \leq s \leq 100$ were used to obtain the coefficients of an equation of the form proposed by Swalen (71). The equations are:

$$\log [- (W_{1A}^{(2)} \times 10^6)] = 7.53280 + 1.74940 \log s - 0.904790 \; s^{\frac{1}{2}}$$

$$\log [W_{1E}^{(1)} \times 10^6] = 7.42187 + 1.77560 \log s - 0.907184 \; s^{\frac{1}{2}} \qquad (5\text{-}2)$$

where the W's are the perturbation coefficients discussed by Herschbach (39) and s is given by Equation (2-71). The second order correction to the E level can be obtained by use of the relation $W_{1E}^{(2)} = -\frac{1}{2} W_{1A}^{(2)}$. An extrapolation to s = 113.7 was done by means of these equations.

The potential barrier is determined to be 2.55 ± 0.05 kcal/mole. The estimated uncertainty is believed to be large enough to include the uncertainty in the measurement of the splittings as well as a contribution from uncertainty in the structure. The structural parameters of the ground state were used with the exception of I_a which was obtained from the moments of inertia of the first excited torsional state species of $CH_2Cl^{35}SiH_3$ and $CH_2Cl^{35}SiD_3$. The value of V_3 determined is very sensitive to I_a but not to θ_m, the other structural parameter needed.

5.7 Discussion

The most unusual feature of the proposed structure for chloromethylsilane is the long SiC distance (1.889 A). While the uncertainty in this value is large owing to the insensitivity of the data to the a coordinate of the carbon atom, it seems probable that the SiC distance

is approximately 0.02 A longer than the corresponding distance in methylsilane (1.867 A, (72)). In contrast fluorine substitution on the silicon atom of methylsilane has been shown to decrease the SiC distance (73). A comparison of the structures of ethane (74), ethyl chloride (this thesis), and ethyl fluoride (55) shows that the CC distance is relatively insensitive to halogen substitution. Table XXVIII summarizes the heavy atom geometry and barriers to internal rotation of chloromethylsilane and a number of related molecules.

On the basis of bond distance and quadrupole coupling parameters the CCl bonds in chloromethylsilane and ethyl chloride seem very similar. However, the SiCCl angle in CH_2ClSiH_3 is near tetrahedral, whereas the CCCl angle in CH_3CH_2Cl is 111° (Chapter IV).

The CH and SiH distances appear to be normal. The HCH angle is smaller than expected, particularly since the SiCCl angle is near the tetrahedral value. Small HCH angles in methylene groups have been reported (51), but accompanied by larger than tetrahedral angles between the other two bonds to the carbon. The HSiH angle (110.6°) is approximately 2° larger than in methylsilane (108.3°, (72)), but only slightly larger than in SiH_3F (110.2°, (73)).

The potential barrier hindering internal rotation of the silyl group in chloromethylsilane is approximately 0.9 kcal. higher than the barrier in methylsilane (72), Table XXVIII. A similar increase in the barrier in ethane is noted upon substitution of chlorine for hydrogen (46). Substitution of fluorine for hydrogen in ethane is approximately two-thirds as effective as chlorine substitution in raising the barrier (75). Conversely, fluorination of the silicon atom in methylsilane reduces the barrier (76). These data and those above clearly indicate a striking difference in the behavior of carbon and silicon towards halogen substitution. It will be interesting to see if these trends are corroborated in subsequent structure determinations of similar molecules.

Table XXVIII. Comparison of Chloromethylsilane with Similar Molecules.

	Bond distances (A) and bond angles (degrees).				
	SiC	CC	CCl	SiCCl	CCCl
SiH_3CH_2Cl	1.889		1.788	109.3	
SiH_3CH_3[a]	1.867				
CH_3SiH_2F[b]	1.849				
CH_3CH_2Cl[c]		1.520	1.788		111.0
CH_3CH_3[d]		1.525			
CH_3CH_2F[e]		1.533			

	Barriers to internal rotation (kcal/mole).		
	V_3		V_3
SiH_3CH_2Cl	2.55	CH_3CH_2Cl[g]	3.56
SiH_3CH_3[a]	1.67	CH_3CH_3[h]	2.88
CH_3SiH_2F[f]	1.56	CH_3CH_2F[i]	3.25

[a] Reference 72.
[b] Reference 73.
[c] This thesis.
[d] Reference 74.
[e] Reference 55.
[f] Reference 76.
[g] Reference 46.
[h] K. S. Pitzer, Discussions Faraday Soc. 10, 66 (1951).
[i] Reference 75.

VI. MICROWAVE SPECTRA OF CYCLOPROPYLCHLORIDE

6.1 Introduction

A determination of the structure and the nature of the bonding orbitals in cyclopropyl chloride would be of considerable interest and importance due to its bearing on the theory of "strain" in small-ring compounds. Numerous theoretical treatments (77, 78, 79, 80) of the structure of cyclopropane have been presented and a great deal of controversy appears over the direction of the orbitals in the C-C bonds, the HCH angles, and the ability of the ring to conjugate with unsaturated groups. It is hoped that the determination of the structure of cyclopropyl chloride including an evaluation of the quadrupole coupling constants by microwave spectroscopy will help to resolve some of the controversy.

The study of cyclopropyl chloride is the first in a proposed series of structure determinations on small-ring compounds. The preparative work on the second molecule of the series, cyclobutyl chloride, has already been started. In addition, work on 1, 1-dichlorocyclopropane, cyclobutyl bromide, cyclopentene, and cis-2, 3-epoxybutane is being carried on at other universities.

Prior to the work reported here on cyclopropyl chloride the microwave spectra of the Cl-35 and Cl-37 species had been examined (81) and R-branch a-type transitions assigned. However, no transitions sensitive to the smallest moment of inertia were reported so that the value of the rotational constant A remained largely undetermined. The R-branch a-type transitions of the Cl-35 and Cl-37 species have been remeasured and in addition a series of Q-branch c-type transitions were identified and measured so that all three rotational constants B, C, and A could be calculated accurately. A further check on A and B

was possible when the $0_{00} \rightarrow 1_{10}$ transition, R-branch c-type ($\sim$= A + B) was identified and measured.

An attempt to prepare a deuterated derivative of cyclopropyl chloride failed due to difficulty in the photochlorination of deuterated cyclopropane. A unique method of preparing a C-13 isotope was found (82) but the first attempt (using C-12) was unsuccessful. Further work in the preparation of these isotopes is now underway.

6.2 Preparation of Samples

The initial sample of cyclopropyl chloride was obtained from Dr. Harold Hart and used without further purification. The Cl-37 isotopic species was observed in natural abundance in this sample.

The following equations show the synthesis route which was used in the preparation of deuterated cyclopropane and attempted synthesis of deuterated cyclopropyl chloride. It is felt that the photochlorination step failed mainly because of the small amount ($\sim$ 0.2 cc) of deuterated cyclopropane available. The main products of the photochlorination apparently are polychlorinated derivatives.

$$Br\text{-}CH_2CH_2\text{-}COOH + SOCl_2 \rightarrow Br\text{-}CH_2CH_2\text{-}COCl + SO_2 + HCl$$

$$2Br\text{-}CH_2CH_2\text{-}COCl + LiAlD_4 \xrightarrow{AlCl_3} LiAlCl_2(OCD_2\text{-}CH_2CH_2\text{-}Br)_2$$

$$LiAlCl_2(OCD_2\text{-}CH_2CH_2\text{-}Br)_2 \xrightarrow[H^+]{H_2O} Br\text{-}CH_2CH_2\text{-}CD_2OH$$

$$Br\text{-}CH_2CH_2\text{-}CD_2OH + HBr\,(48\%\ aq.) \longrightarrow Br\text{-}CH_2CH_2\text{-}CD_2Br + H_2O$$

$$Br\text{-}CH_2CH_2\text{-}CD_2Br + Zn \longrightarrow \text{ 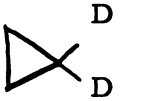 } + ZnBr_2$$

$$2\ \text{  } + Cl_2 \xrightarrow{h\sim} \text{  } + \text{  } + DCl$$

A new method for preparing mono-deuterated cyclopropane utilizing deuterium oxide is now under consideration as a way of obtaining a larger amount of the isotopic species for use in the photochlorination.

A unique preparation of cyclopropane appeared in the recent literature (82) in which diazomethane is added to ethylene in the presence of diethylaluminum iodide as a catalyst. An attempt at this synthesis was made using dimethylaluminum iodide (83) but the only product obtained was a polymeric material, presumably polymethylene formed from the diazomethane. The synthesis appears attractive since a process for synthesizing C-13 diazomethane has already been worked out (section 5.2).

6.3 Microwave Spectra

Figure 12 is a projection of cyclopropyl chloride in the plane of symmetry (the ac plane). The molecule is a near prolate symmetric top with the asymmetry parameter κ equal to approximately -0.97 for the Cl-35 and Cl-37 species. The spectra were observed with the microwave spectrometer described in Chapter III of this thesis.

Using the rotational constants and quadrupole data given by Friend and Dailey (81) calculations indicated that in the region 8-12 kMc there should appear a series of Q-branch c-type transitions for J = 5 to J = 8. Furthermore the quadrupole interaction should split each line into two, giving rise to a series of doublets. However, a long and thorough search of the spectrum from 8-12 kMc showed mainly quartets.

The Q-branch transitions were found only after the quadrupole coupling constants from 1,1-dichlorocyclopropane (84) were used to predict the hyperfine splittings. The new quadrupole constants correctly predicted quartets for these transitions and an assignment was made easily. The values of the observed hyperfine component frequencies for the Q-branch and R-branch c-type transitions appear in Table XXIX along with the calculated and observed hypothetical unsplit frequency. The value of the rotational constant A was determined by fitting the $0 \longrightarrow 1$ transition ($\nu = A + B$) after a good value of B had

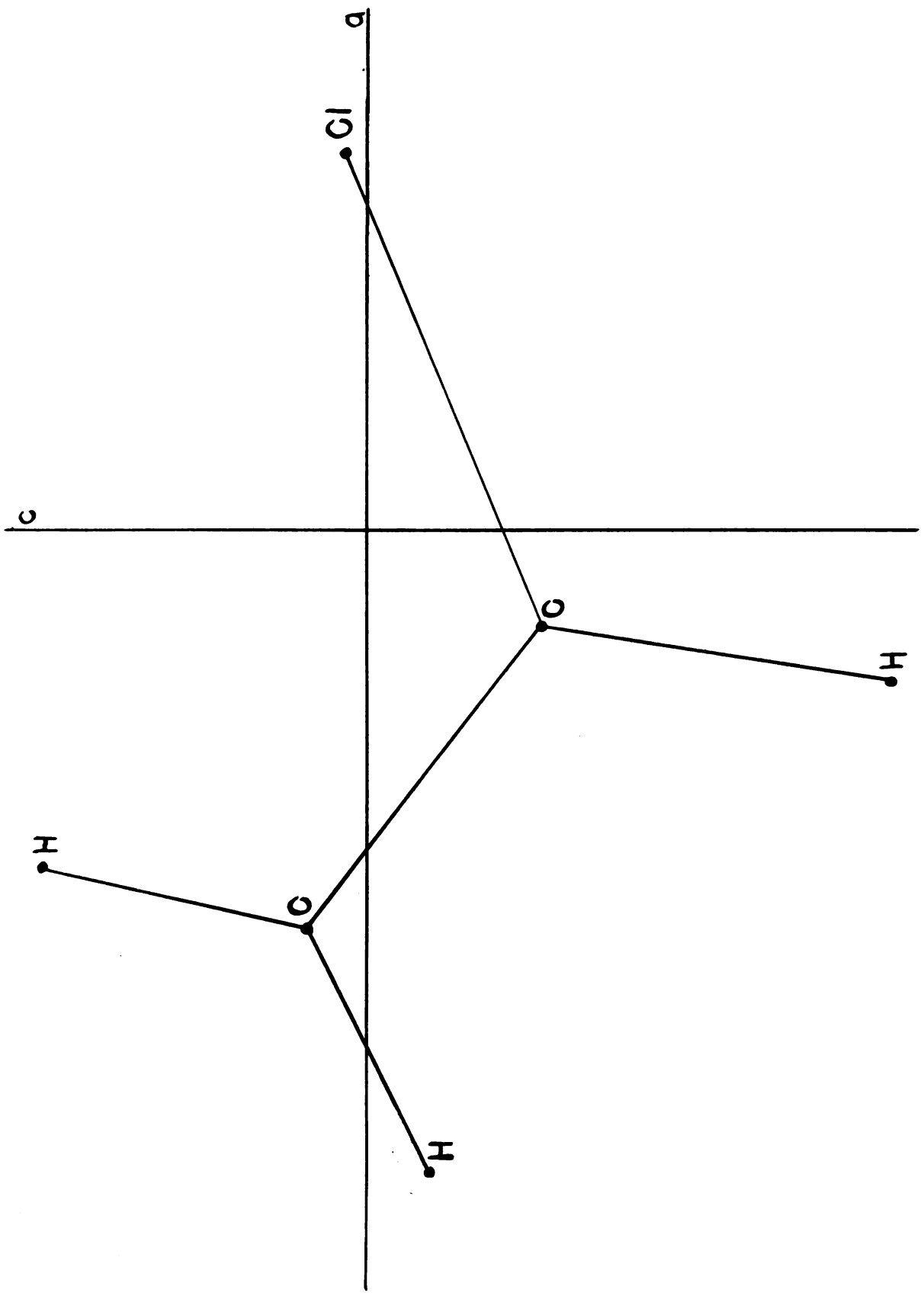

Figure 12. A Projection of Cyclopropyl Chloride in its Plane of Symmetry Showing the Location of the a and c Principal Axes. The b Axis is Perpendicular to the Page.

Table XXIX. Frequencies (Mc) of Hyperfine Components and Hypothetical Unsplit Frequencies of the R-branch and Q-branch c-type Transitions in $C_3H_5Cl^{35}$ and $C_3H_5Cl^{37}$.

Transition	F → F'				Hypothetical Unsplit Frequency	
	$J-\frac{3}{2} \rightarrow J-\frac{3}{2}$	$J+\frac{3}{2} \rightarrow J+\frac{3}{2}$	$J-\frac{1}{2} \rightarrow J-\frac{1}{2}$	$J+\frac{1}{2} \rightarrow J+\frac{1}{2}$	Observed	Calculated[a]
$C_3H_5Cl^{35}$						
$5_{05} \rightarrow 5_{15}$	10779.19	10780.03	10782.40	10783.28	10781.31	10782.27
$6_{06} \rightarrow 6_{16}$	10057.54	10058.14	10060.25	10060.86	10059.25	10060.36
$7_{07} \rightarrow 7_{17}$	9267.84	9268.23	9270.20	9270.59	9269.24	9270.44
$8_{08} \rightarrow 8_{18}$	8432.81	8432.81	8434.88	8434.88	8433.86	8434.67
$C_3H_5Cl^{37}$						
$5_{05} \rightarrow 5_{15}$	10949.30	10949.93	10951.82	10952.45	10950.94	10950.00
$6_{06} \rightarrow 6_{16}$	10255.72	10255.72	10257.95	10257.95	10256.87	10255.58
$7_{07} \rightarrow 7_{17}$	9493.51	9493.51	9495.35	9495.35	9494.46	9492.82
$8_{08} \rightarrow 8_{18}$	8683.32	8683.32	8684.93	8684.93	8684.14	8682.04
	$\frac{3}{2} \rightarrow \frac{1}{2}$	$\frac{3}{2} \rightarrow \frac{5}{2}$	$\frac{3}{2} \rightarrow \frac{3}{2}$			
$C_3H_5Cl^{35}$						
$0_{00} \rightarrow 1_{10}$	20436.6	20440.5	20445.6		20441.57	20441.60
$C_3H_5Cl^{37}$						
$0_{00} \rightarrow 1_{10}$		20338.5	20342.4		20339.27	20339.27

[a] Without centrifugal distortion correction.

been calculated from the R-branch a-type transitions. The $0 \longrightarrow 1$ transition should be almost free of centrifugal distortion effects while the Q-branch lines are of higher J and could be uncertain by a few megacycles due to this effect.

The R-branch a-type transitions reported by Friend and Dailey (81) were remeasured and the frequencies of the hyperfine components appear in Table XXX. Table XXXI is a comparison of the calculated and observed hypothetical unsplit frequencies. Agreement with the published values is within $\pm$ 0.2 Mc for the Cl-35 species and $\pm$ 0.4 Mc for the Cl-37 species. Slightly worse agreement is obtained with some of the individual members of the hyperfine components.

6.4 Molecular Structure

A calculation of the molecular structure of cyclopropyl chloride will not be attempted until more isotopic species have been studied. With only the data presented here on the Cl-35 and Cl-37 species the structure should not differ significantly from that of Friend and Dailey (81). However, using the structure reported by them we have been unable to reproduce their reported calculated rotational constants. Before the substitution method (9) can be used in a structure determination more isotopic species need to be studied.

Table XXXII gives the rotational constants, moments of inertia, and second moments for the Cl-35 and Cl-37 species. From the second moments and also the coordinates of the chlorine atom (a = 1.2861, c = 0.0698), computed using Kraitchman's equations (9), it is seen that the chlorine atom lies very close to the a axis.

6.5 Quadrupole Analysis and Discussion

The quadrupole parameters q_m and $q_m\eta$ were determined from hyperfine splittings using the method of least squares as explained

Table XXX. Frequencies (Mc) of Hyperfine Components of R-Branch a-Type Transitions in $C_3H_5Cl^{35}$ and $C_3H_5Cl^{37}$.

	F → F'							
Transition	(a)	$\frac{7}{2} \rightarrow \frac{7}{2}$	$\frac{3}{2} \rightarrow \frac{5}{2}$	$\frac{5}{2} \rightarrow \frac{7}{2}$	$\frac{7}{2} \rightarrow \frac{9}{2}$	$\frac{1}{2} \rightarrow \frac{3}{2}$	$\frac{5}{2} \rightarrow \frac{5}{2}$	(a)	$\frac{3}{2} \rightarrow \frac{3}{2}$
$C_3H_5Cl^{35}$									
$2_{11} \rightarrow 3_{12}$	22990.75	22994.13	23002.78	23003.30	23006.94	23006.94	23009.35		23015.60
$2_{12} \rightarrow 3_{13}$	22149.30		22154.44	22154.44	22158.03	22158.03	22160.56	22163.39	22163.97
$2_{02} \rightarrow 3_{03}$			22562.14	22565.76	22565.76	22562.14			
$2_{21} \rightarrow 3_{22}$	22572.41		22583.68	22573.64	22587.91	22597.6			
$2_{20} \rightarrow 3_{21}$			22602.66	22592.15	22606.76	22616.37			
$C_3H_5Cl^{37}$									
$2_{11} \rightarrow 3_{12}$			22452.88	22452.88	22455.84	22455.84			
$2_{12} \rightarrow 3_{13}$			21644.74	21644.74	21647.53	21647.53			21651.79
$2_{02} \rightarrow 3_{03}$	22025.61 22030.62		22033.97	22036.61	22036.61	22033.97		22041.99	
$2_{21} \rightarrow 3_{22}$			22053.27	22045.07	22057.11	22062.73			
$2_{20} \rightarrow 3_{21}$			22070.05		22072.81				

$C_3H_5Cl^{35}$	$\frac{7}{2} \rightarrow \frac{9}{2}$	$\frac{5}{2} \rightarrow \frac{7}{2}$	$\frac{9}{2} \rightarrow \frac{11}{2}$	$\frac{3}{2} \rightarrow \frac{5}{2}$	(a)	(a)	(a)
$3_{21} \rightarrow 4_{22}$	30150.98	30153.17	30156.85	30158.85			
$3_{22} \rightarrow 4_{23}$	30104.37	30106.26	30109.98	30112.02			
$3_{03} \rightarrow 4_{04}$			30070.09		30063.41	30065.09	30077.50

(a) Assignment uncertain.

Table XXXI. Hypothetical Unsplit Frequencies (Mc) of the R-Branch a-Type Transitions in $C_3H_5Cl^{35}$ and $C_3H_5Cl^{37}$.

Species	Transition	Hypothetical Unsplit Frequency	
		Observed	Calculated
$C_3H_5Cl^{35}$	$2_{11} \rightarrow 3_{12}$	23005.31	23005.08
	$2_{12} \rightarrow 3_{13}$	22156.42	22156.45
	$2_{02} \rightarrow 3_{03}$	22565.04	22564.90
	$2_{21} \rightarrow 3_{22}$	22583.68	22583.70
	$2_{20} \rightarrow 3_{21}$	22602.45	22602.50
	$3_{22} \rightarrow 4_{23}$	30107.94	30107.95
	$3_{21} \rightarrow 4_{22}$	30154.74	30155.01
$C_3H_5Cl^{37}$	$2_{11} \rightarrow 3_{12}$	22454.72	22454.95
	$2_{12} \rightarrow 3_{13}$	21646.29	21646.06
	$2_{02} \rightarrow 3_{03}$	22036.13	22036.18
	$2_{21} \rightarrow 3_{22}$	22053.40	22053.15
	$2_{20} \rightarrow 3_{21}$	22069.84	22070.12

Table XXXII. Rotational Constants (Mc), Moments of Inertia (amu A^2),[a] and Second Moments[b] for $C_3H_5Cl^{35}$ and $C_3H_5Cl^{37}$.

	$C_3H_5Cl^{35}$	$C_3H_5Cl^{37}$
A	16536.20	16528.92
B	3905.40	3810.35
C	3622.50	3540.70
I_a	30.5712	30.5846
I_b	129.4441	132.6731
I_c	139.5531	142.7771
P_{aa}	119.2130	122.4328
P_{bb}	20.3401	20.3443
P_{cc}	10.2311	10.2403

[a] Conversion factor used: 5.05531×10^5 Mc-amu A^2.

[b] From Equation (2-17).

previously (section 2.4). The $2_{12} \rightarrow 3_{13}$ transition of the Cl-35 species could not be fit with the present quadrupole parameters and consequently was not used in the least squares analysis. The other K = 1 transitions also show rather large deviations ($\sim$ 1 Mc) between calculated and observed frequencies for which no explanation is known. Similar difficulty in fitting K = 1 transitions has been noted in other compounds (e.g. ethyl bromide (85)). The difficulty, which seems certainly to be outside of experimental error, may be due to second-order effects which are not considered here. However, a preliminary estimate of second-order effects using published equations (86) showed a frequency change of only $\pm$ 0.01 Mc.

The quadrupole parameters q_m and $q_m \eta$ were also calculated using Equation (2-48). From Equation (2-48) we may write

$$\Delta\nu = c_1 q_m + c_2 q_m \eta$$

where $\Delta\nu$ is a difference in frequency of two hyperfine components and c_1 and c_2 depend on the degree of asymmetry. A plot of $\Delta\nu/c_1$ vs. c_1/c_2 for the various pairs of hyperfine components will give values of q_m and $q_m\eta$ as intercept and slope respectively. The values obtained for q_m and $q_m\eta$ by this method were in good agreement with the values obtained by least squares. The quadrupole coupling constants χ_{aa}, χ_{bb}, and χ_{cc} were then determined from the values of q_m and $q_m\eta$ together with the relationship

$$\chi_{aa} + \chi_{bb} + \chi_{cc} = 0$$

The values of the quadrupole parameters and coupling constants appear in Table XXXIII.

Without a knowledge of χ_{ac} it is impossible to calculate the direction of the principal axes of χ in the Cl-C-H plane and the value of χ along these axes. However, if it is assumed that the tensor

Table XXXIII. Quadrupole Parameters and Coupling Constants in $C_3H_5Cl^{35}$ and $C_3H_5Cl^{37}$.

	$C_3H_5Cl^{35}$	$C_3H_5Cl^{37}$
eQq_m	-56.639 Mc	-44.373 Mc
$q_m\eta$	16.808	13.009
χ_{aa}	-56.639	-44.373
χ_{bb}	36.724	28.691
χ_{cc}	19.916	15.682

represents a cylindrical charge distribution about the C-Cl bond direction, then the direction (θ_z) of this axis can be calculated. From Equation (2-57), with $\chi_{zz} = -2\chi_{bb}$, θ_z is found to be 23.0°.

Friend and Dailey (81) calculate a value of 23.2° but as mentioned previously we could not reproduce their rotational constants from their reported structure. Using their published values of bond distances and bond angles the value we compute is 22.85°.

A calculation of θ_z was also performed using the CC, CH, and CCl distances and HCH and ClCCl angles reported for 1, 1-dichlorocyclopropane (84) as the structural parameters for cyclopropyl chloride. This gave a value of 22.52° for θ_z.

Finally θ_z was calculated by assuming that the difference between the in-plane and out-of-plane quadrupole coupling constants is the same in cyclopropyl chloride and 1, 1-dichlorocyclopropane. This difference is 2.45 Mc for the dichloro compound and leads to a value of 21.7° for θ_z.

The most that may be concluded from the above series of calculations is that the angle θ_z lies in the range 21.5-23.5°. A further evaluation of the angle will be possible when data for the C-13 (carbon attached to the chlorine) species is available.

It is interesting to note that the coupling constants for 1, 1-dichlorocyclopropane (84) and methylene chloride (87) differ by only about 0.5 Mc and those for cyclopropyl chloride and methyl chloride differ by about 1.3 Mc. The values of the coupling constant in the CCl bond direction are shown in Table XXXIV. The coupling constant χ_{bond} is considerably less ($\sim$5 Mc) in the mono-chloro compounds so that it appears that the ionic character of the CCl bond is greater for the mono-chloro compounds.

Table XXXIV. Values of the Coupling Constant in the Bond Direction for Cyclopropyl Chloride and Some Related Compounds.

Molecule	χ_{bond}
1,1-Dichlorocyclopropane	78.89
Methylene chloride	78.4
Cyclopropyl chloride	73.45
Methyl chloride	74.74

REFERENCES

1. C. E. Williams and N. H. Williams, Phys. Rev. 45, 234 (1934).
2. B. Bleaney and R. P. Penrose, Nature 157, 339 (1946).
3. B. Bleaney and R. P. Penrose, Phys. Rev. 70, 775 (1946).
4. D. K. Coles and W. E. Good, Phys. Rev. 70, 979 (1946).
5. R. H. Hughes and E. B. Wilson, Jr., Phys. Rev. 71, 562 (1947).
6. T. W. Dakin, W. E. Good, and D. K. Coles, Phys. Rev. 70, 560 (1946).
7. D. G. Burkhard and D. M. Dennison, Phys. Rev. 84, 408 (1951).
8. C. H. Townes and B. P. Dailey, J. Chem. Phys. 17, 782 (1949).
9. J. Kraitchman, Am. J. Phys. 21, 17 (1953).
10. C. C. Costain, J. Chem. Phys. 29, 864 (1958).
11. L. Pauling and E. B. Wilson, Jr., Introduction to Quantum Mechanics, New York, McGraw-Hill Book Company, Inc., 1935, p. 275.
12. C. H. Townes and A. L. Schawlow, Microwave Spectroscopy, New York, McGraw-Hill Book Company, Inc., 1955.
13. H. Goldstein, Classical Mechanics, Reading, Massachusetts, Addison-Wesley Publishing Company, Inc., 1950, p. 149.
14. V. W. Laurie, J. Chem. Phys. 28, 704 (1958).
15. Z. I. Slawsky and D. M. Dennison, J. Chem. Phys. 7, 509 (1939).
16. B. S. Ray, Zeits, f. Physik 78, 74 (1932).
17. G. W. King, R. M. Hainer, and P. C. Cross, J. Chem. Phys. 11, 27 (1943).
18. Reference 12, Appendix IV.
19. R. H. Schwendeman, J. Chem. Phys. 27, 986 (1957).
20. E. B. Wilson, Jr., Diss. Far. Soc. 9, 108 (1950).
21. W. E. Good, Phys. Rev. 70, 213 (1946).
22. B. T. Feld, Phys. Rev. 72, 1116 (1947).

23. H. B. G. Casimir, On the Interaction Between Atomic Nuclei and Electrons, Haarlem, Teylers Tweede Genootschop, E. F. Bohn, 1936.

24. J. M. P. Kellogg, I. I. Rabi, N. F. Ramsey, Jr., and J. R. Zaccharias, Phys. Rev. 57, 677 (1940).

25. B. P. Dailey, R. L. Kyhl, M. W. P. Strandberg, J. H. Van Vleck, and E. B. Wilson, Jr., Phys. Rev. 70, 984 (1946).

26. J. H. Van Vleck, Phys. Rev. 71, 468 (1947).

27. D. K. Coles and W. E. Good, Phys. Rev. 70, 979 (1946).

28. J. Bardeen and C. H. Townes, Phys. Rev. 73, 97, 627, 1204 (1948).

29. R. Bersohn, J. Chem. Phys. 18, 1124 (1950).

30. J. K. Bragg, Phys. Rev. 74, 533 (1948).

31. J. K. Bragg and S. Golden, Phys. Rev. 75, 735 (1949).

32. G. Knight and B. T. Feld, Phys. Rev. 74, 354 (1948).

33. Reference 12, Appendix I.

34. K. M. Sinnott, J. Chem. Phys. 34, 851 (1961).

35. B. P. Dailey, J. Chem. Phys. 33, 1641 (1960), and references therein.

36. H. H. Nielson, Phys. Rev. 40, 445 (1932).

37. D. G. Burkhard and D. M. Dennison, Phys. Rev. 84, 408 (1951).

38. D. R. Herschbach, Thesis, Harvard University, 1958.

39. D. R. Herschbach, J. Chem. Phys. 31, 91 (1959).

40. C. C. Lin and J. D. Swalen, Revs. Mod. Phys. 31, 841 (1959).

41. S. Golden and E. B. Wilson, Jr., J. Chem. Phys. 16, 669 (1948).

42. Reference 12, p. 407.

43. L. C. Hedrick, Rev. Sci. Instr. 20, 781 (1949).

44. R. S. Wagner and B. P. Dailey, J. Chem. Phys. 26, 1588 (1957).

45. A. I. Barchukov, T. M. Murina, and A. M. Prokhorov, Opt. i Spekt. 4, 521 (1958).

46. D. R. Lide, Jr., J. Chem. Phys. 30, 37 (1959).

47. J. D. Cox and H. S. Turner, J. Chem. Soc. 3176 (1950).

48. A. J. Tulleners, M. C. Twyn, and H. I, Waterman, Rec. trav. chim. 53, 544 (1934).

49. J. D. Cox, H. S. Turner, and R. J. Warne, J. Chem. Soc. 3167 (1950).

50. R. H. Schwendeman, J. Mol. Spec. 6, 301 (1961).

51. D. R. Lide, Jr., J. Chem. Phys. 33, 1514 (1960).

52. L. Pierce, J. Chem. Phys. 34, 498 (1961).

53. C. C. Costain, J. Chem. Phys. 29, 864 (1958).

54. D. R. Lide, Jr., J. Chem. Phys. 33, 1519 (1960).

55. B. Bak, S. Detoni, L. Hansen-Nygaard, J. T. Nielson, and J. Rastrup-Andersen, Spectrochim. Acta 16, 376 (1960).

56. S. L. Miller, L. C. Aamodt, G. Dousmanis, C. H. Townes, and J. Kraitchman, J. Chem. Phys. 20, 1112 (1952).

57. V. W. Laurie, Symposium on Molecular Structure and Spectroscopy, Ohio State University, 1960.

58. V. W. Laurie, J. Chem. Phys. 34, 291 (1961).

59. C. H. Townes and B. P. Dailey, J. Chem. Phys. 17, 782 (1949).

60. B. P. Dailey and C. H. Townes, J. Chem. Phys. 23, 118 (1955).

61. T. P. Das and E. L. Hahn, Nuclear Quadrupole Resonance Spectroscopy, New York, Academic Press, Inc., 1958.

62. R. W. Kilb, C. C. Lin, and E. B. Wilson, Jr., J. Chem. Phys. 26, 1695 (1957).

63. J. D. Cox and R. J. Warne, J. Chem. Soc., 1896 (1951).

64. Organic Syntheses, Coll. Vol. II, New York, John Wiley and Sons, Inc., 1943, p. 461.

65. Reference 64, p. 165.

66. D. Seyferth and E. G. Rochow, J. Am. Chem. Soc. 77, 907 (1955).

67. A. I. Vogel, Practical Organic Chemistry, London, Longmans, Green, and Co., 1956, p. 402.

68. Reference 67, p. 414.

69. S. R. Polo, Can. J. Phys. 35, 880 (1957).

70. Reference 12, Appendix VII.

71. J. D. Swalen, J. Chem. Phys. 24, 1072 (1956).

72. R. W. Kilb and L. Pierce, J. Chem. Phys. 27, 108 (1957).

73. L. C. Krisher and L. Pierce, J. Chem. Phys. 32, 1619 (1960), and references therein.

74. H. C. Allen, Jr., and E. K. Plyler, J. Chem. Phys. 31, 1062 (1959), and also reference (54).

75. D. R. Herschbach, J. Chem. Phys. 25, 358 (1956), and reference (46).

76. L. Pierce, J. Chem. Phys. 29, 383 (1958).

77. G. H. Duffey, J. Chem. Phys. 14, 342 (1946).

78. C. A. Coulson and W. E. Moffitt, J. Chem. Phys. 15, 151 (1947); Phil. Mag. 40, 1 (1949).

79. A. D. Walsh, Trans. Far. Soc. 45, 179 (1949).

80. A. W. Baker and R. C. Lord, J. Chem. Phys. 23, 1636 (1955).

81. J. P. Friend and B. P. Dailey, J. Chem. Phys. 29, 577 (1958).

82. H. Hoberg, Angew. Chemie 73, No. 3, 114 (1961).

83. A. V. Grosse and J. M. Mavity, J. Org. Chem. 5, 106 (1940).

84. W. H. Flygare, A. Narath, and W. D. Gwinn, J. Chem. Phys. (to be published).

85. R. S. Wagner, B. P. Dailey, and N. Solimene, J. Chem. Phys. 26, 1593 (1957).

86. J. A. Howe, J. Chem. Phys. 34, 1247 (1961).

87. R. J. Meyers and W. D. Gwinn, J. Chem. Phys. 20, 1420 (1952), and W. H. Flygare and W. D. Gwinn, J. Chem. Phys. (to be published).

88. Reference 12, Appendix VI.